Nuclear Physics School 2013, Otranto

Interaction of electroweak probes with the nucleus

Maria B. Barbaro
University of Turin

Outline

- **1. Lepton-nucleus scattering: Introduction and relativistic formalism**
- **2. Inclusive electron scattering at intermediate and high energies: scaling and scaling violations (Meson Exchange Currents)**
- **3. Quasielastic neutrino scattering**
- **4. Parity-violating electron scattering**

Nuclear Physics School 2013, Otranto

1. Lepton-nucleus scattering at intermediate and high energies: Introduction and relativistic formalism

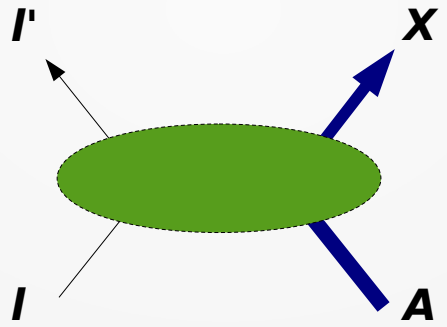

Why using electroweak probes?

- to study the structure of nucleons
- to understand the nuclear dynamics
- to assess the relevant degrees of freedom for describing a nucleus: baryons and mesons or quarks and gluons?
- to study the properties of the probe (neutrino)

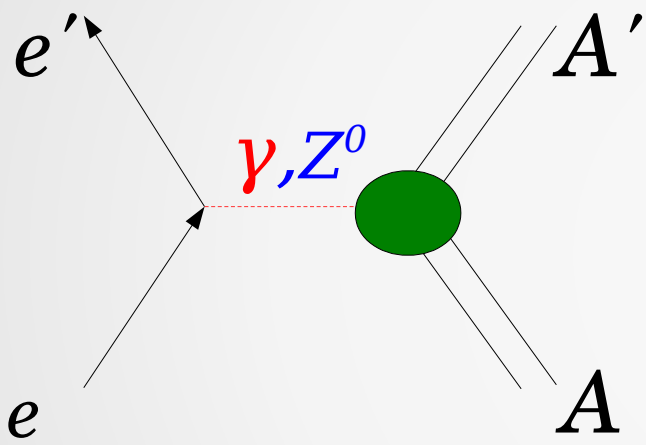

e-A interaction

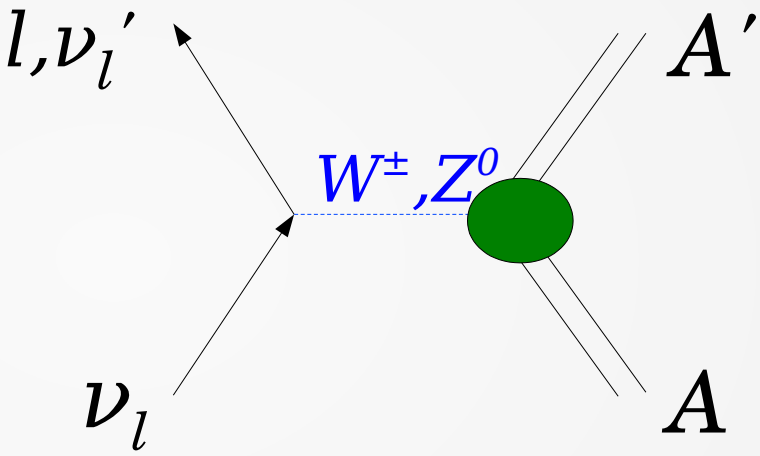

ν-A interaction

- The electroweak interaction is weak: $\alpha = 1/137$ for γ-exchange, Z and W exchange amplitude suppressed by a factor $Q^2/M^2_{Z,W} \simeq 10^{-5}$. Hence:

- perturbative treatment ⇒ only one vector boson exchanged (Born approx.)
- electron scattering: predominantly electromagnetic process ⇒ QED description
- leptonic probes can explore the full nuclear volume without modifying it too much

Why worrying about relativity?

Typical neutrino energies of current experiments are (E_ν ~ 1-few GeV)

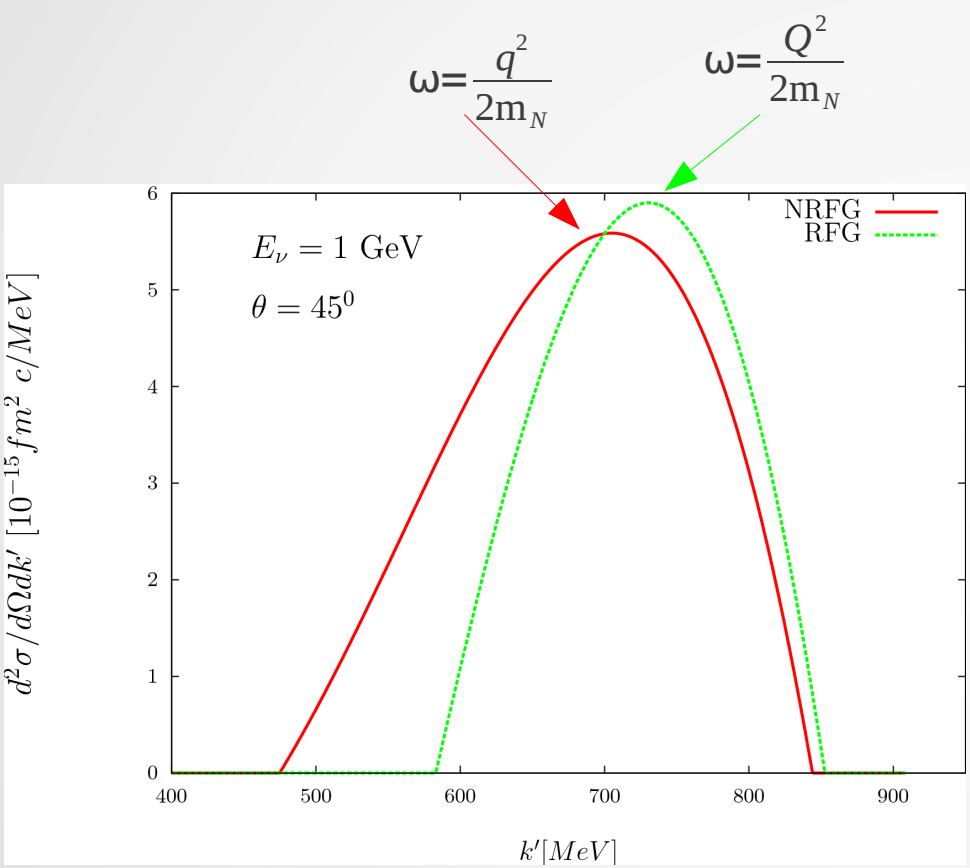

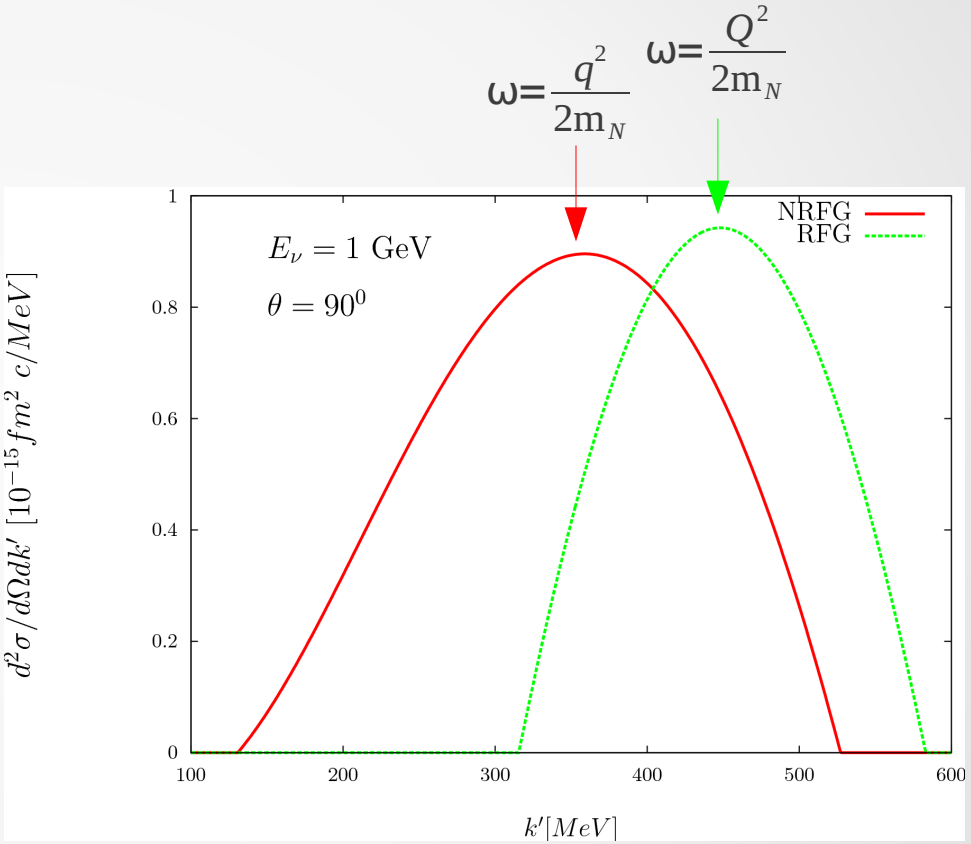

Lepton-nucleus scattering reactions

- INCLUSIVE PROCESSES: A(l, l′)

- only the scattered lepton is detected: A(e, e′), A(ν_μ, μ), A(ν_e, e)

- lepton and/or target can be polarized

- SEMI-INCLUSIVE PROCESSES: A(l, l′N), A(l, l′NN)

- more particles detected in coincidence with the scattered lepton: (e, e′p), (e, e′pp).

- lepton, target and/or final-state nucleons can be polarized

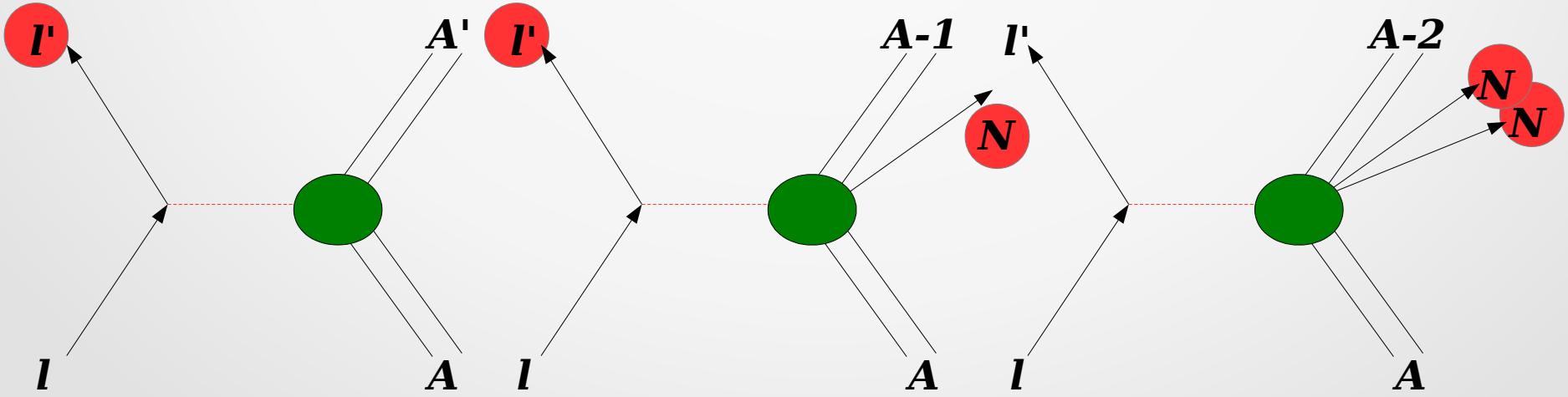

Experimental issues

The cross sections are small ($\sigma_e \sim 10^{-30}cm^2, \sigma_\nu \sim 10^{-39}cm^2$): required to have

- high duty factor capabilities
- high currents
- thick targets

For measuring polarization observables:

- polarized electron beams
- polarized targets
- polarizations of final-state particles: protons, neutrons and deuterons

Intermediate- and high-energy modern facilities:

Electrons	Neutrinos
MAMI/Mainz (1.5 GeV) Jlab/Virginia (6 GeV, now upgrade to 12)	FermiLab/Chicago (~ 1-10 GeV) J-Parc/Japan
both have polarized beams	non monochromatic ν-beams

Inclusive electron scattering spectrum

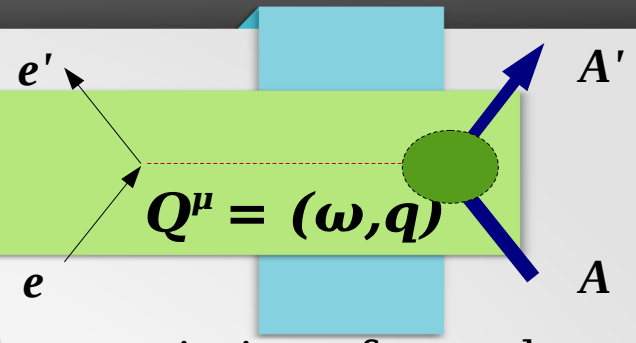

The virtuality of the exchanged photon allows independent variation of q and ω

⇒ $0 \le \omega \le q$

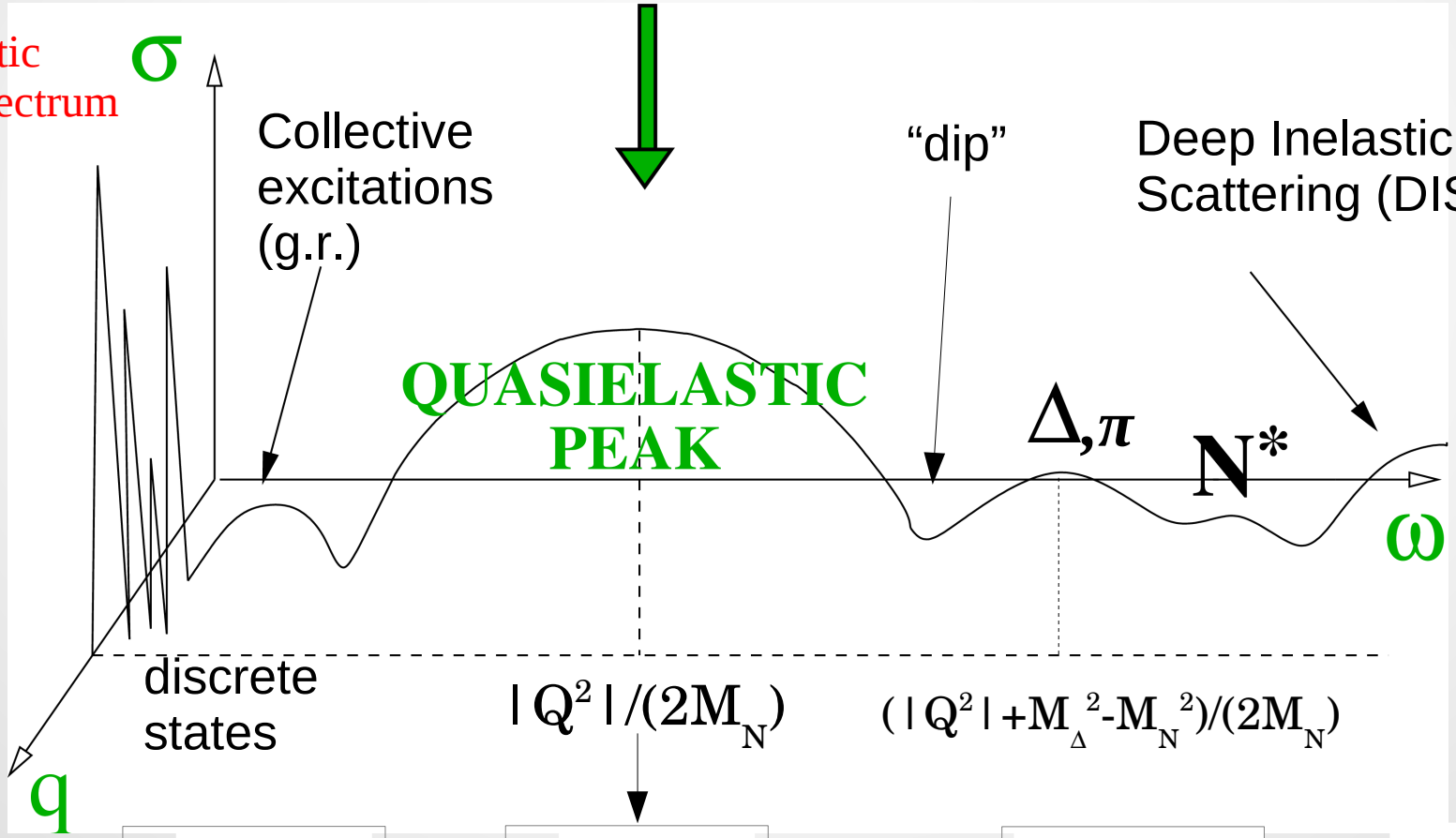

$x_B>1$	$x_B=1$	$0<x_B<1$

$x_B = |Q^2|/2M_N\omega$
Bjorken variable

Data: QE Electron Nucleus Scattering Archive

$^{12}C \quad E_e \; \theta_e$

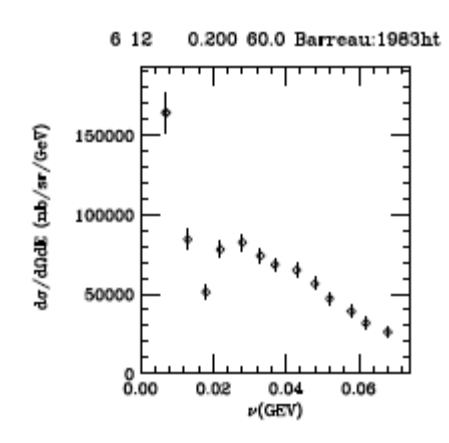

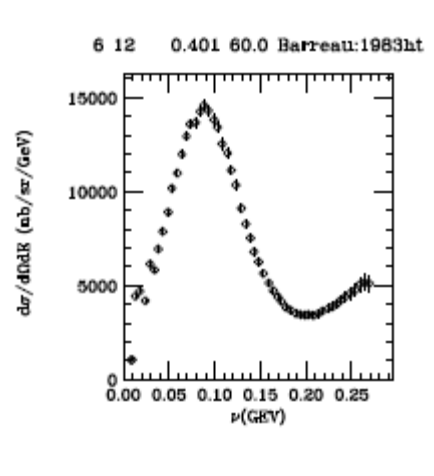

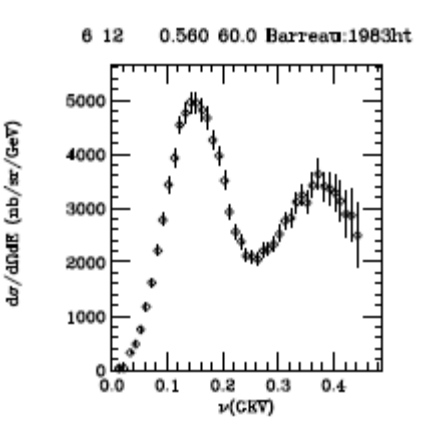

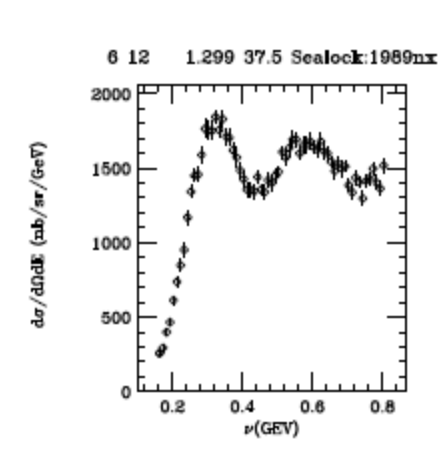

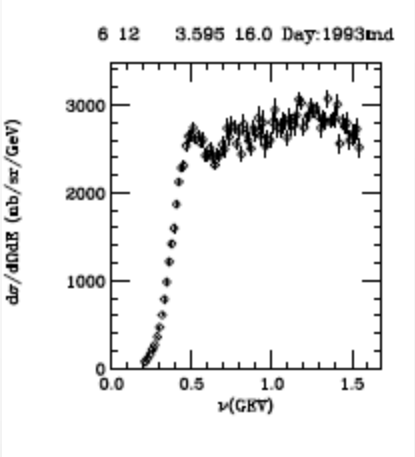

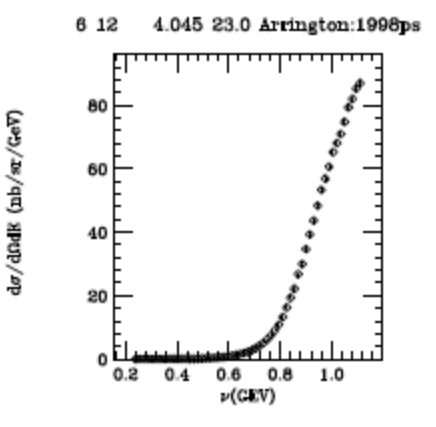

http://faculty.virginia.edu/qes-archive/index.html

O.Benhar, D.Day, I.Sick, Rev. Mod. Phys. 80 (2008)

Relativistic scattering: notations and formalism

Four-vectors $A^\mu = (A_0, \vec{A})$

Bjorken&Drell conventions $g^{00} = 1,\, g^{kk} = -1\ (k = 1,2,3)$

First Born approximation: one virtual boson exchange

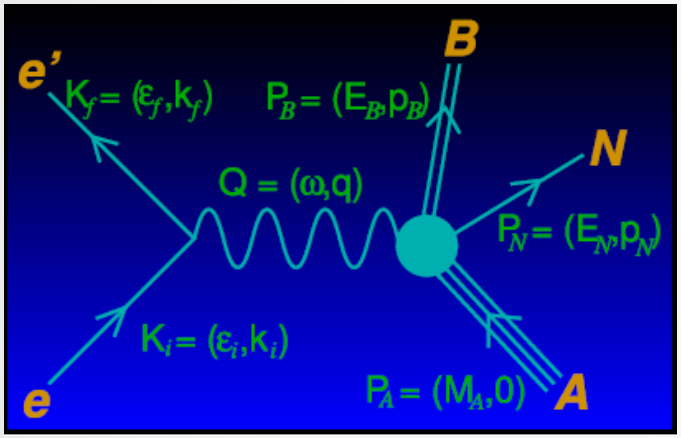

$Q^2 = \omega^2 - q^2 < 0$ space-like virtual boson

$Q^\mu = K^\mu - K'^\mu = P_f^\mu - P_i^\mu$ 4-momentum conservation

$P^2 = M^2$ on-shell condition

$\not{\partial} \equiv \gamma_\mu \partial^\mu$ $\quad \{\gamma^\mu\,,\,\gamma^\nu\} = \gamma^\mu\gamma^\nu + \gamma^\nu\gamma^\mu = 2g^{\mu\nu}\,\mathbb{1}$

$\gamma_5 \equiv i\gamma^0\gamma^1\gamma^2\gamma^3$ $\quad \sigma_{\mu\nu} = \frac{i}{2}\left[\gamma_\mu\,,\,\gamma_\nu\right]$

Dirac equation and Dirac spinors:

$(i\,\not{\partial} - M)\,\Psi = 0$ free particles

$(i\,\not{\partial} - e\,\not{A} - M)\,\Psi = 0$ in presence of e.m. field

$\Psi_{\mathbf{p}}^{(+)}(\mathbf{x},t) = \sqrt{\frac{M}{EV}}\,u(\mathbf{p},s)\,e^{-iP_\mu X^\mu}$ positive energy

$\Psi_{\mathbf{p}}^{(-)}(\mathbf{x},t) = \sqrt{\frac{M}{EV}}\,v(\mathbf{p},s)\,e^{iP_\mu X^\mu}$ negative energy

$(\not{P} - M)\,u(\mathbf{p},s) = 0$

$(\not{P} + M)\,v(\mathbf{p},s) = 0$

$$u(\mathbf{p},s) = \sqrt{\frac{E+M}{2M}}\begin{pmatrix} \chi_s \\ \frac{\boldsymbol{\sigma}\cdot\mathbf{p}}{E+M}\chi_s \end{pmatrix}\,,\quad v(\mathbf{p},s) = \sqrt{\frac{E+M}{2M}}\begin{pmatrix} \frac{\boldsymbol{\sigma}\cdot\mathbf{p}}{E+M}\xi_s \\ \xi_s \end{pmatrix}$$

Dirac spinology

Normalization condition and Dirac adjoint operators: [$\overline{u} \equiv u^\dagger \gamma^0$ & $\overline{\Gamma} \equiv \gamma^0 \Gamma^\dagger \gamma^0$]

$$\overline{u}(\mathrm{p},s)u(\mathrm{p},s) = 1, \quad \overline{v}(\mathrm{p},s)v(\mathrm{p},s) = -1$$

Projection operators:

Energy $\hat{\Lambda}_\pm(\mathrm{p}) = \left(\frac{\pm \not{P}+M}{2M}\right) = \sum_{\pm s} u(\mathrm{p},s)\overline{u}(\mathrm{p},s)$

Spin $\hat{P}(\pm s) = \frac{1}{2}\left(\mathbb{1} \pm \gamma_5 \not{S}\right)$

Four-spin $S^\mu = (s^0, \mathbf{s})$ *satisfies:* $S^2 = S_\mu S^\mu = -1$ *and* $P_\mu S^\mu = 0$

Bilinear covariants and their properties under Lorentz transformations

$\overline{\Psi}\Psi$ (scalar), $\overline{\Psi}\gamma^5\Psi$ (pseudoscalar), $\overline{\Psi}\gamma^\mu\Psi$ (vector), $\overline{\Psi}\gamma^5\gamma^\mu\Psi$ (pseudovector),

Trace theorems:

$$\mathrm{Tr}\,(\not{A}\ \not{B}) = 4A\cdot B, \quad \mathrm{Tr}\,(\gamma^5) = 0, \quad \mathrm{Tr}\,(\gamma^5\ \not{A}\ \not{B}) = 0$$

$$\mathrm{Tr}\,(\not{A}\ \not{B}\ \not{C}\ \not{D}) = 4\left[A\cdot B\ C\cdot D + A\cdot D\ B\cdot C - A\cdot C\ B\cdot D\right]$$

$$\mathrm{Tr}\,(\gamma^5\ \not{A}\ \not{B}\ \not{C}\ \not{D}) = 4i\epsilon_{\alpha\beta\gamma\delta}A^\alpha B^\beta C^\gamma D^\delta$$

(l,l') Inclusive Cross Section

Plane Wave Born Approximation (PWBA), lab system

$$\frac{d\sigma}{d\Omega_e\, d\omega} = K \overline{\Sigma}_{fi} |M_{fi}|^2$$

K kinematic factor

$$M_{fi} = g\, j_\mu \Delta^{\mu\nu} J_\nu$$

invariant amplitude

Coupling constant:
photon ⇒ $g = e$
heavy vector boson X ⇒ $g / M_X \propto \sqrt{G}$

Fermi constant
$1.166 \times 10^{-5}\ GeV^{-2}$

Vector boson propagator:

photon ⇒ $\Delta^{\mu\nu} = \frac{g^{\mu\nu}}{Q^2}$ Feynman's gauge

heavy vector boson X ⇒ $\Delta^{\mu\nu} = \frac{g^{\mu\nu}}{Q^2 - M_X^2} \simeq -\frac{g^{\mu\nu}}{M_X^2}$ $(M_X \simeq 80-90\, GeV/c^2)$

$\overline{\Sigma}_{fi}$ average over initial states and sum over final states

$\overline{\Sigma}_{fi} |M_{fi}|^2$ ⟶ Leptonic and Hadronic tensors

Leptonic and Hadronic Tensors

$\eta_{\mu\nu} = \overline{\sum}_{leptons} j_\mu^* \, j_\nu$ Leptonic tensor

$W^{\mu\nu} = \overline{\sum}_{hadrons} J_{fi}^{\mu *} \, J_{fi}^{\nu}$ Hadronic tensor

j_μ Leptonic current

J_μ Hadronic current

$d\sigma \sim \frac{1}{Q^4} \eta_{\mu\nu}^{em} W_{em}^{\mu\nu}$ Electromagnetic processes (electron scattering)

$d\sigma \sim \frac{1}{M_X^4} \eta_{\mu\nu}^{weak} W_{weak}^{\mu\nu}$ Weak interaction processes (neutrino scattering)

$d\sigma \sim \frac{1}{M_X^2 Q^2} \eta_{\mu\nu}^{em/weak} W_{em/weak}^{\mu\nu}$ Electromagnetic-weak interference (parity-violating electron scattering)

The Leptonic Tensor

$$\eta_{\mu\nu} \equiv \overline{\sum}_{\text{leptons}} j_\mu^* j_\nu$$

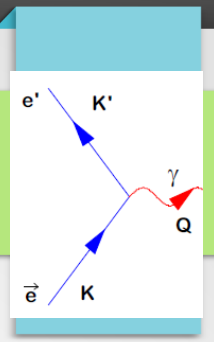

Electromagnetic electron current

$$j_\mu(K',\lambda';K,\lambda) = \bar{u}(K',\lambda')\gamma_\mu u(K,\lambda)$$

Leptonic tensor

$$\eta_{\mu\nu} = \overline{\sum}_{\lambda,\lambda'} [\bar{u}(K,\lambda)\gamma_\mu u(K',\lambda')][\bar{u}(K',\lambda')\gamma_\nu u(K,\lambda)]$$

Unpolarized electrons:

Symmetric under μ ↔ ν

Satisfies current conservation:

$$Q^\mu \eta_{\mu\nu}^{\text{unpol}} = 0$$

$$\begin{aligned} \eta_{\mu\nu}^{\text{unpol}} &= \frac{1}{8m_e^2}\,\text{Tr}\left\{\gamma_\mu(\not{K}'+m_e)\gamma_\nu(\not{K}+m_e)\right\} \\ &= \frac{1}{2m_e^2}\left[K_\mu K'_\nu + K'_\mu K_\nu - g_{\mu\nu}\left(K\cdot K' - m_e^2\right)\right] \end{aligned}$$

Polarized incident electrons:

S^μ $(S^2 = -1 \text{ and } S\cdot K = 0)$

electron spin

$$\begin{aligned} \eta_{\mu\nu} &= \frac{1}{16m_e^2}\,\text{Tr}\left\{\gamma_\mu\left(\not{K}'+m_e\right)\gamma_\nu\left(1+\gamma_5\,\not{S}\right)\left(\not{K}+m_e\right)\right\} \\ &\equiv \frac{1}{2}\left[\eta_{\mu\nu}^{\text{unpol}} + \eta_{\mu\nu}^{\text{pol}}\right] \end{aligned}$$

$$\eta_{\mu\nu}^{\text{pol}} = \frac{1}{2m_e^2}\left(i\epsilon_{\mu\nu\alpha\beta}\, m_e S^\alpha Q^\beta\right)$$

New term, antisymmetric in μ ↔ ν

$Q^\mu \eta_{\mu\nu}^{\text{pol}} = 0$ current conservation

Lepton polarization

- For purely L or T polarized e-

$$\text{longitudinal polarization:} \quad m_e S^\mu = h\epsilon(\beta, \vec{u}_L)$$
$$\text{transverse polarization:} \quad m_e S^\mu = \frac{1}{\gamma} \cdot h\epsilon(0, \vec{u}_\perp) \,,$$

$$\beta = k/\epsilon = \sqrt{1 - (m_e/\epsilon)^2}$$
$$\gamma = 1/\sqrt{1-\beta^2} = \epsilon/m_e$$

- Transverse polarization effects are suppressed by a factor 1/γ relative to longitudinal
- For purely longitudinally polarized electrons and in the ERL ($m_e << \epsilon$)

$$\beta \to 1, \gamma \to \infty \longrightarrow \begin{aligned} K^\mu &\longrightarrow \epsilon(1, \vec{u}_L) \\ (m_e S^\mu)_L &\longrightarrow h\epsilon(1, \vec{u}_L) = hK^\mu \end{aligned}$$

$h = \pm 1$ helicity

- The two leptonic tensors

$$\begin{aligned} 2m_e^2 \eta_{\mu\nu}^{\text{unpol}} &\to K_\mu K'_\nu + K'_\mu K_\nu - g_{\mu\nu} K \cdot K' \equiv \chi_{\mu\nu}^{\text{unpol}} \\ 2m_e^2 \eta_{\mu\nu}^{\text{pol}} &\to -ih\epsilon_{\mu\nu\alpha\beta} K^\alpha K'^\beta \equiv \chi_{\mu\nu}^{\text{pol}} \,, \end{aligned}$$

are comparable in magnitude (both ~ $\epsilon\, \epsilon'$)

- Only longitudinally polarized electrons are relevant for most studies in nuclear and particle physics

The EM Hadronic Tensor

$$W^{\mu\nu} \equiv \overline{\sum}_{\text{hadrons}} J^{\mu *}_{fi} J^{\nu}_{fi}$$

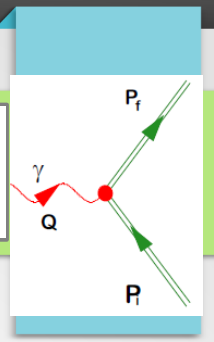

- General structure: the hadronic tensor must be built with P^i_μ , P^f_μ and Q_μ
- The Lorentz scalars in the problem are P^2, Q^2 and $P\cdot Q$
  $P_i^2 = M_i^2 \Rightarrow 2$ independent scalars, for example Q^2 and $P\cdot Q$ (equivalent to q and ω)

$$Q^2 = \omega^2 - q^2$$
$$Q \cdot P_i = \omega M_i$$

- Introduce

$$V_i^\mu \equiv \frac{1}{M_i}\left\{P_i^\mu - \left(\frac{Q\cdot P_i}{Q^2}\right)Q^\mu\right\} \longrightarrow Q\cdot V_i = 0$$

- $W^{\mu\nu}$ must be a second rank Lorentz tensor. The most general form is:

$$W^{\mu\nu} = W_s^{\mu\nu} + W_a^{\mu\nu}$$

$$W_s^{\mu\nu} = X_1 g^{\mu\nu} + X_2 Q^\mu Q^\nu + X_3 V_i^\mu V_i^\nu + X_4\left(Q^\mu V_i^\nu + V_i^\mu Q^\nu\right)$$
$$W_a^{\mu\nu} = iY_1\left(Q^\mu V_i^\nu - V_i^\mu Q^\nu\right) + iY_2\epsilon^{\mu\nu\alpha\beta}Q_\alpha V_{i\beta}\,,$$

symmetric

antisymmetric

$X_\ell\left(Q^2, Q\cdot P_i\right)$

$Y_\ell\left(Q^2, Q\cdot P_i\right)$

structure functions

- Current conservation

$$Q_\mu W_s^{\mu\nu} = 0 = (X_1 + X_2 Q^2)Q^\nu + (X_4 Q^2)V_i^\nu$$
$$Q_\mu W_a^{\mu\nu} = 0 = (Y_1 Q^2)V_i^\nu$$

$$X_1 + X_2 Q^2 = 0$$
$$X_4 = 0$$
$$Y_1 = 0$$

$Y_2 = 0$ since in absence of PV effects the current matrix elements are polar vectors

- Finally

$$W_s^{\mu\nu} = -W_1\left(g^{\mu\nu} - \frac{Q^\mu Q^\nu}{Q^2}\right) + W_2 V_i^\mu V_i^\nu$$
$$W_a^{\mu\nu} = 0\,.$$

$$W_1 \equiv -X_1$$

$$W_2 \equiv X_3$$

EM Response functions

- Contracting the unpolarized leptonic and hadronic tensors:

$$\chi_{\mu\nu}^{\text{unpol}} W_s^{\mu\nu} \sim W_2 + 2W_1 \tan^2 \frac{\theta_e}{2}$$

- The inclusive unpolarized electron scattering c.s. depends upon 2 response functions, which can be separated by varying the scattering angle (Rosenbluth decomposition)

- L/T separation: it is convenient to choose the projections of the current matrix elements to be parallel (L) or perpendicular (T) to the virtual photon direction ***q***:

$$\left(\frac{d\sigma}{d\Omega_e d\omega}\right)^{\text{unpol}} = \sigma_{\text{Mott}} \left\{ v_L R^L + v_T R^T \right\}$$

$$\sigma_{\text{Mott}} = \left\{ \frac{\alpha \cos\frac{\theta_e}{2}}{2\epsilon \sin^2\frac{\theta_e}{2}} \right\}^2$$

$$\begin{aligned} v_L &= \rho^2 \\ v_T &= \frac{1}{2}\rho + \tan^2\frac{\theta_e}{2} \end{aligned}$$

$$(\rho = -Q^2/q^2)$$

$$\begin{aligned} R^L &= (W_2 - \rho W_1)/\rho^2 \\ R^T &= 2W_1 \,. \end{aligned}$$

- The longitudinal and transverse response functions can be constructed directly as components of the hadronic tensor according to:

$$\begin{aligned} R^L(q,\omega) &= \left(\frac{q^2}{Q^2}\right)^2 \left[W^{00} - \frac{\omega}{q}(W^{03} + W^{30}) + \frac{\omega^2}{q^2} W^{33} \right] \\ R^T(q,\omega) &= W^{11} + W^{22} \end{aligned}$$

- They embody the entire dependence on the hadronic structure

The nuclear tensor

- The nuclear tensor

$$W^{\mu\nu} = \overline{\sum_A} \sum_B \sum_X \langle \psi_B, \Phi_X \left| \hat{J}^\mu(\mathbf{q}) \right| \psi_A \rangle^* \langle \psi_B, \Phi_X \left| \hat{J}^\nu(\mathbf{q}) \right| \psi_A \rangle \times \rho(E_B) dE_B \rho(E_X) dE_X \delta(\varepsilon_i - \varepsilon_f + E_A - E_B - E_X)$$

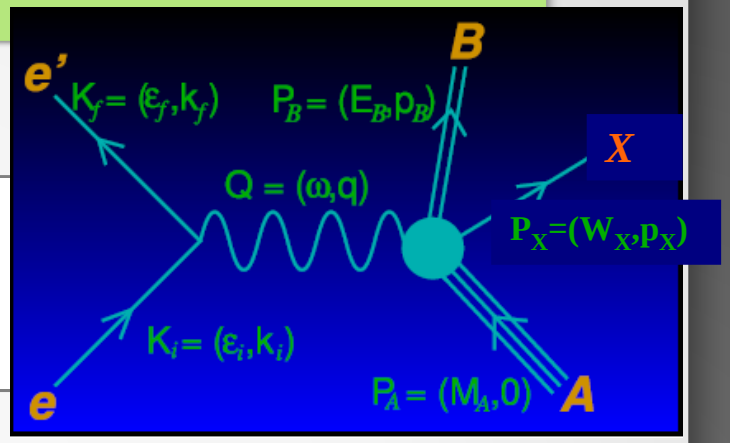

$\hat{J}^\mu(\mathbf{q})$ Fourier transform of the nuclear many-body current operator

$|\psi_A\rangle$ and $|\psi_B\rangle$ eigenstates of the nuclear Hamiltonian

$\rho(E_B)$ and $\rho(E_X)$ distribution functions accounting for the energy-momentum dispersion relation of the final nucleus (B) and hadronic system (X)

$\sum_B \sum_X$ sum over all possible final states that can be reached through the action of J_μ on the g.s.

$W^{\mu\nu}$ is meant to be evaluated at $\mathbf{p}_B + \mathbf{p}_X = \mathbf{q} = \mathbf{k}_i - \mathbf{k}_f$

Equivalent expression for $W^{\mu\nu}$:

$$W^{\mu\nu} = -\frac{1}{\pi} \mathrm{Im}\ (\Pi^{\mu\nu}) = -\frac{1}{\pi} \mathrm{Im} \left(\overline{\sum_i} \langle i | \hat{J}^{\dagger\mu} \hat{G}(\omega + E_i) \hat{J}^\nu | i \rangle \right)$$

Polarization propagator →

$$i\Pi^{\mu\nu}(Q) = \int d^4X e^{iQ\cdot X} \langle i | T[\hat{J}^{\dagger\mu}(X) \hat{J}^\nu(0)] | i \rangle$$

Full propagator of the many-body system

Current conservation and gauge invariance

- Current conservation $Q^\mu J_\mu = 0 \longrightarrow \omega J^0 = q J^3$

  implies relations between the charge (0) and longitudinal (3) components of the hadronic tensor:

$$\begin{aligned} W^{03} &= W^{30} = (\omega/q) W^{00} \\ W^{33} &= (\omega/q)^2 W^{00} \\ &\Rightarrow \quad R^L = W^{00} \end{aligned}$$

$R_L \Rightarrow$ charge distribution

$R_T \Rightarrow$ current distribution

- Gauge invariance must be fulfilled both at the level of the nuclear current matrix elements

$$Q_\mu \langle f | \hat{J}^\mu | i \rangle = 0$$

and at the level of the nuclear tensor and polarization propagators

$$Q_\mu W^{\mu\nu} = 0, \;\; Q_\mu \Pi^{\mu\nu} = 0$$

- Nuclear models must fulfill this fundamental symmetry

Inclusive EM polarized processes

Polarizing the electron and/or the target gives rise to extra response functions:

$$\vec{A}(\vec{e}, e')$$

the geneneral structure of the cross section is

$$d\sigma \sim \Sigma + h\Delta$$

h = electron helicity

with

$$\begin{aligned} \Sigma &= v_L R^L(\theta^*) + v_T R^T(\theta^*) + v_{TL} R^{TL}(\theta^*) \cos\phi^* + v_{TT} R^{TT}(\theta^*) \cos 2\phi^* \\ \Delta &= v_{T'} R^{T'}(\theta^*) + v_{TL'} R^{TL'}(\theta^*) \cos\phi^* \end{aligned}$$

6 response functions

Kinematics

$$e + A \rightarrow e' + B + X$$

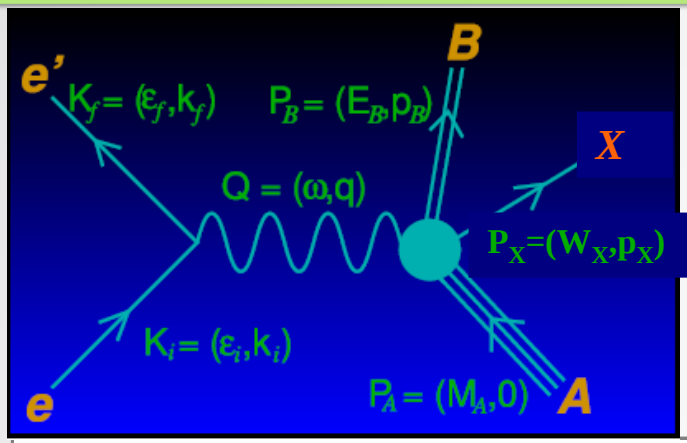

$$P_B^\mu = (E_B, \mathbf{p}_B) = Q^\mu + P_A^\mu - P_X^\mu$$

Missing momentum: $\mathbf{p}_m = \mathbf{p}_B \equiv -\mathbf{p}$

Excitation energy of the residual nucleus in the lab frame:

$$\mathcal{E}(p) \equiv \sqrt{(M_B)^2 + p^2} - \sqrt{(M_B^0)^2 + p^2}$$

$$\begin{aligned} M_A^0 + \omega &= E_X + E_B \qquad \text{energy conservation} \\ &= \sqrt{W_X^2 + p_X^2} + E_B^0 + \mathcal{E} \\ &= \sqrt{W_X^2 + (\mathbf{q}+\mathbf{p})^2} + \sqrt{(M_B^0)^2 + p^2} + \mathcal{E} \end{aligned}$$

W_X final state invariant mass

$\theta = (\boldsymbol{p},\boldsymbol{q})$ angle

$$\mathcal{E} = M_A^0 + \omega - \sqrt{(M_B^0)^2 + p^2} - \sqrt{W_X^2 + q^2 + p^2 + 2pq\cos\theta}$$

$$= \mathcal{E}(q, \omega; p, \cos\theta)$$

$q, \omega, \theta_e, \phi_X, p$ and $\mathcal{E}$

5 independent variables

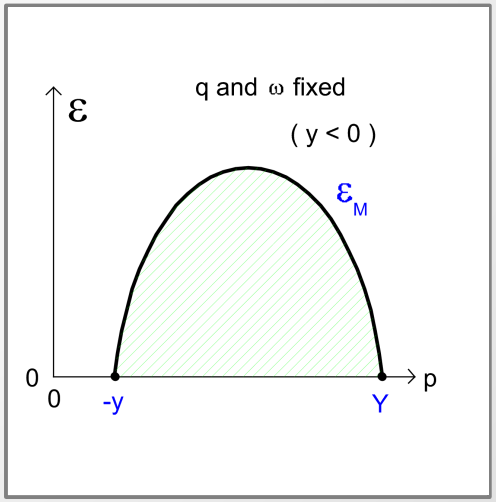

The inclusive nuclear response can be expressed as an integral in the *(ε,p)* plane, corresponding to the possible directions of the final state X:

$$\max[\mathcal{E}(\theta = 0), 0] \leq \mathcal{E} \leq \mathcal{E}(\theta = \pi)$$

Kinematics

The integration limits in p arise from the condition $\mathcal{E}>0$ and turn out to be:

$$y_x = \frac{1}{2W^2}\left[(M_A^0+\omega)\sqrt{(W-M_B^0)^2-W_x^2}\sqrt{(W+M_B^0)^2-W_x^2}-2q\Lambda_x\right]$$

$$Y_x = \frac{1}{2W^2}\left[(M_A^0+\omega)\sqrt{(W-M_B^0)^2-W_x^2}\sqrt{(W+M_B^0)^2-W_x^2}+2q\Lambda_x\right]$$

$- y_X < p < Y_X$

with $W=\sqrt{(M_A^0+\omega)^2-q^2}$ and $\Lambda_x=\frac{1}{2}\left[W^2+(M_B^0)^2-W_x^2\right]$

These expressions simplify in the limit $M_B^0 \to \infty$

$$\mathcal{E} = M_A^0+\omega-\sqrt{(M_B^0)^2+p^2}-\sqrt{W_X^2+q^2+p^2+2pq\cos\theta}$$

$$\mathcal{E}_\infty(\theta) = m_N+\omega-E_S-\sqrt{W_x^2+q^2+p^2+2pq\cos\theta}$$

$$E_S = M_B^0+m_N-M_A^0$$

separation energy

$$y_{x,\infty} = \sqrt{(\omega-E_S+m_N)^2-W_x^2}-q$$

y-scaling variable

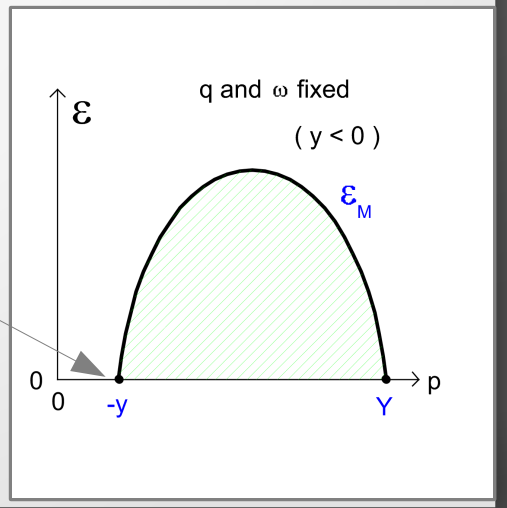

Note that all this is completely general:
- no approximation has been made on the nuclear model
- valid for any final state X

The Quasi Elastic Peak

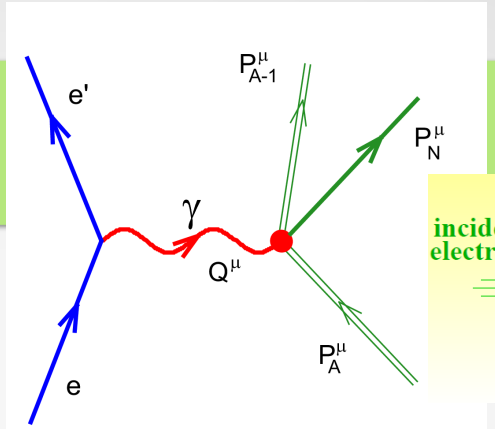

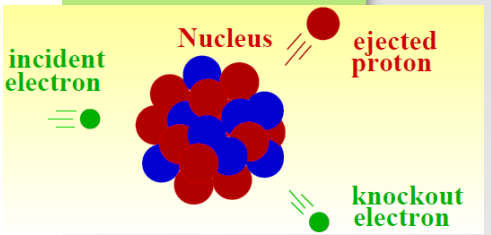

- QE scattering is assumed to be dominated by the ejection of single protons and neutrons (small corrections from ejection of clusters of nucleons)
- If the nucleus were just a collection of protons and neutrons at rest, the c.s. would be a δ-function at the QE condition:

$$\delta(\omega - \omega_{QE}), \qquad \omega_{QE} = \frac{|Q^2|}{2m_N} \qquad \Rightarrow x_B \equiv \frac{|Q^2|}{2m_N \omega} = 1$$

Bjorken scaling variable = 1

- Since the nucleons in the nucleus are moving and interacting, the δ-function becomes a broad peak of width proportional to the Fermi momentum k_F
- The interactions between nucleons in both initial nuclear ground state and final nuclear wave functions cause small shifts away from the QEP
- QE Kinematics: $W_x = m_N$

$$y \cong y_\infty = \sqrt{\tilde{\omega}(2m_N + \tilde{\omega})} - q \qquad \tilde{\omega} \equiv \omega - E_S \qquad \tilde{Q}^2 = \tilde{\omega}^2 - q^2$$

$$y_\infty = 0 \Rightarrow \sqrt{\tilde{\omega}(2m_N + \tilde{\omega})} = q \Rightarrow \tilde{\omega} = |\tilde{Q}^2|/2m_N$$

$$\omega < \omega_{QE} \rightarrow y < 0$$

$$0 \le \mathcal{E}(p) \le \mathcal{E}_M(p) \text{ and } -y \le p \le Y$$

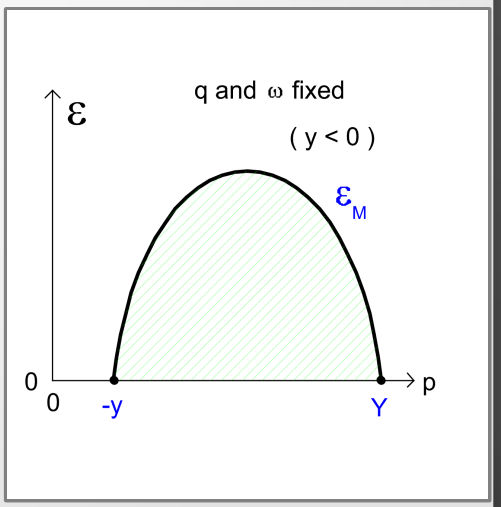

The Quasi Elastic Peak

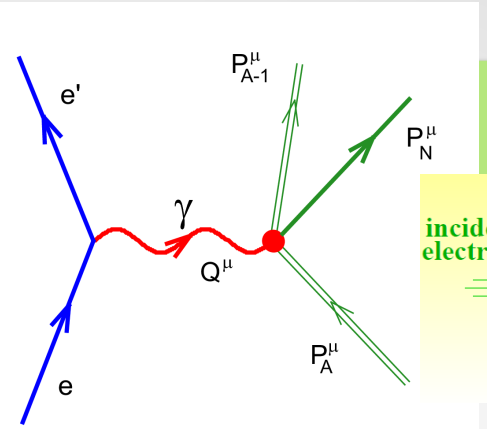

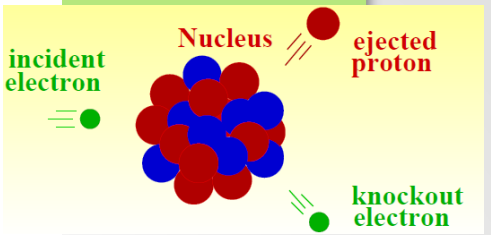

- QE scattering is assumed to be dominated by the ejection of single protons and neutrons (small corrections from ejection of clusters of nucleons)
- If the nucleus were just a collection of protons and neutrons at rest, the c.s. would be a δ-function at the QE condition:

$$\delta(\omega - \omega_{QE}), \qquad \omega_{QE} = \frac{|Q^2|}{2m_N} \qquad \Rightarrow x_B \equiv \frac{|Q^2|}{2m_N \omega} = 1$$

Bjorken scaling variable = 1

- Since the nucleons in the nucleus are moving and interacting, the δ-function becomes a broad peak of width proportional to the Fermi momentum k_F
- The interactions between nucleons in both initial nuclear ground state and final nuclear wave functions cause small shifts away from the QEP
- QE Kinematics: $W_x = m_N$

$$y \cong y_\infty = \sqrt{\tilde{\omega}(2m_N + \tilde{\omega})} - q \qquad \tilde{\omega} \equiv \omega - E_S \qquad \tilde{Q}^2 = \tilde{\omega}^2 - q^2$$

$$y_\infty = 0 \Rightarrow \sqrt{\tilde{\omega}(2m_N + \tilde{\omega})} = q \Rightarrow \tilde{\omega} = |\tilde{Q}^2|/2m_N$$

$$\omega > \omega_{QE} \rightarrow y > 0$$

$$\mathcal{E}_M(-p) \le \mathcal{E}(p) \le \mathcal{E}_M(p) \text{ for } 0 \le p \le y$$
$$0 \le \mathcal{E}(p) \le \mathcal{E}_M(p) \text{ for } y \le p \le Y$$

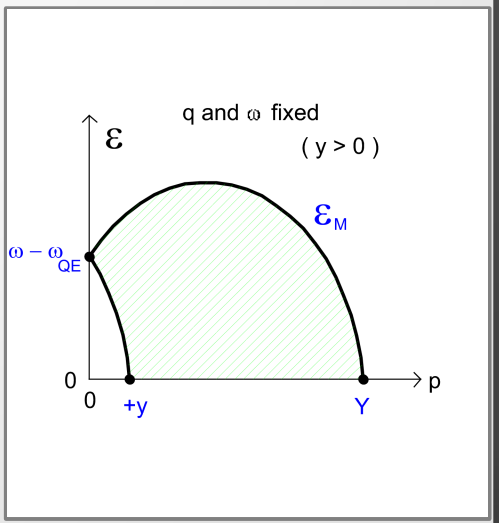

Quasielastic kinematics and y-scaling

(e,e'N) kinematically allowed region

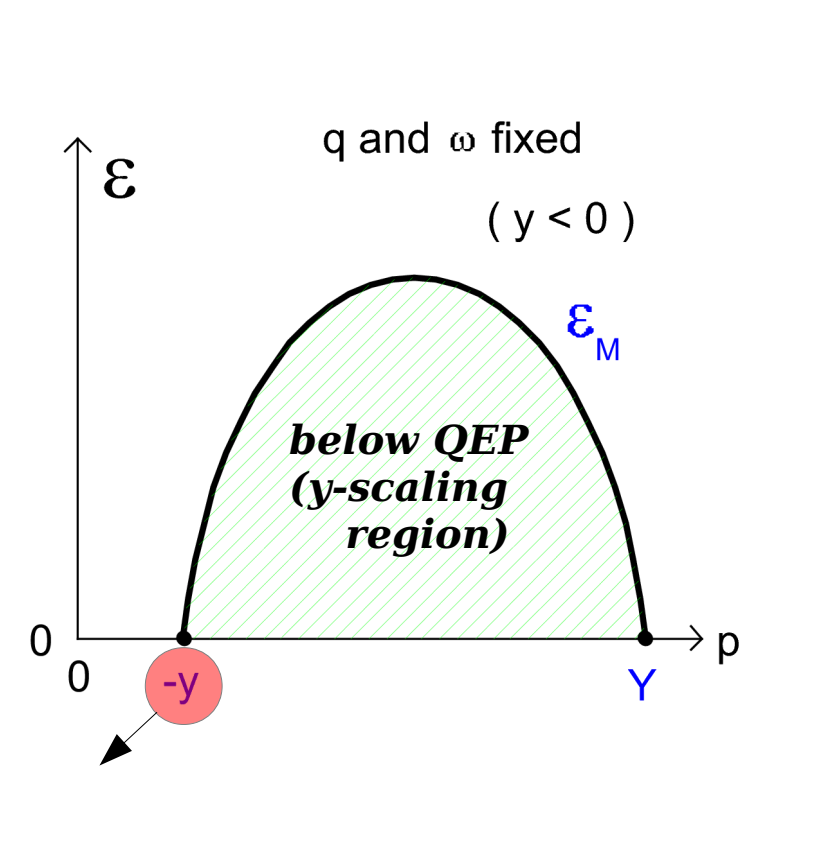

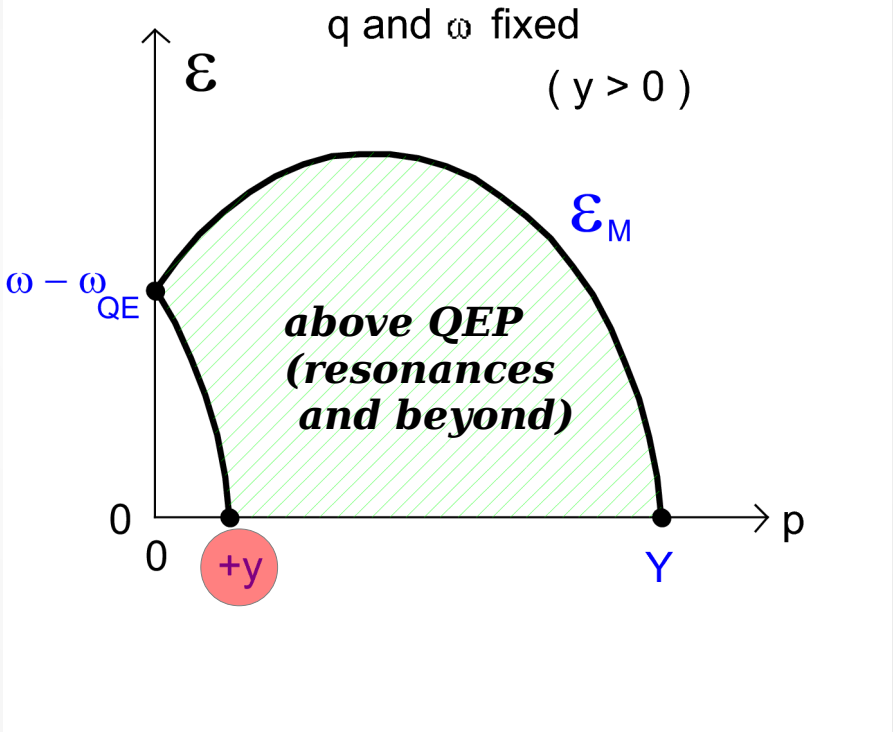

y scaling variable: the lowest value of the missing momentum at the lowest missing energy kinematically allowed for semi-inclusive knockout of nucleons from the nucleus.

$$y \cong y_\infty = \sqrt{\tilde{\omega}(2m_N + \tilde{\omega})} - q$$

$$\tilde{\omega} \equiv \omega - E_S$$

No impulse approximation up to this point: **-p** is the momentum of the recoiling system in the lab frame.

Impulse Approximation

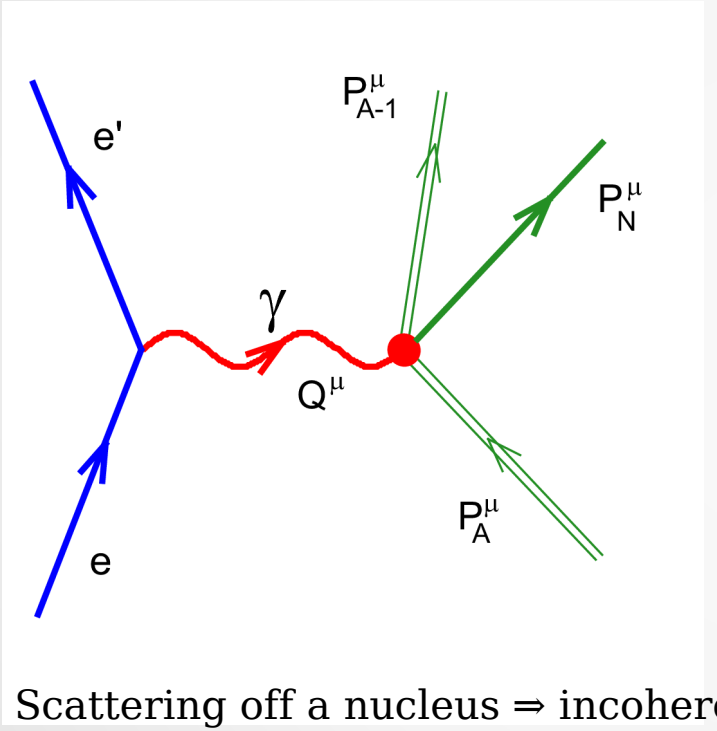

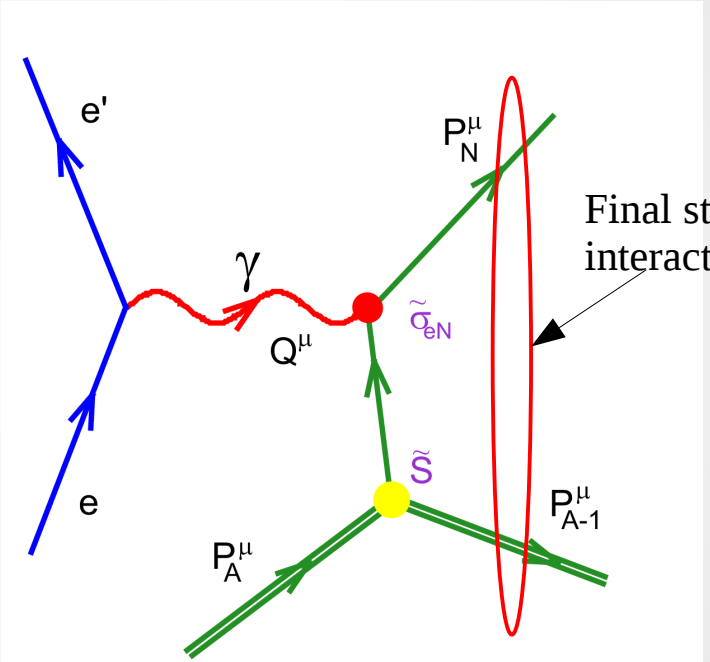

Scattering off a nucleus ⇒ incoherent sum of single-nucleon scattering processes

Nuclear Current ⟹ One-body operator

$$J^{\mu}_{N}(\omega,\vec{q}) = \int d\vec{p}\ \overline{\Psi}_{F}(\vec{p}+\vec{q})\,\hat{J}^{\mu}_{N}\,\Psi_{B}(\vec{p})$$

final nucleon — bound nucleon

The Relativistic Fermi Gas model

- The simplest Relativistic Impulse Approximation (RIA) model fulfilling
  - Lorentz covariance: the hadronic tensor transforms as a Lorentz tensor
  - Gauge invariance: $Q^{\mu}W_{\mu\nu}=0$
- Relativistic version of the Fermi gas model (De Forest and Walecka, 1966)
- The nucleus is viewed as a collection of on-shell nucleons described by Dirac spinors *u(p,s)*
- Nuclear tensor for a generic final hadronic system X :

$$W^{\mu\nu}_{RFG}(\mathbf{q},\omega) = \frac{3\mathcal{N}}{4\pi p_F^3}\int dW_X \int_F d\mathbf{h}\frac{m_N W_X}{\overline{E}_{\mathbf{h}} E_X} w^{\mu\nu}_{inel}(H,Q,E_X)\delta(\omega+\overline{E}_{\mathbf{h}}-E_X)$$

X-system invariant mass

Fermi sphere $\int_F d\mathbf{h} \equiv \int d\mathbf{h} n(\mathbf{h})$, with $n(\mathbf{h}) = \theta(p_F - h)$

$$w^{\mu\nu}_{inel}(H,Q,E_X) = \frac{1}{2}\sum_{s_h}\sum_{X_i}\rho(E_{X_i})\left[\overline{\Phi}_{X_i}\hat{J}^{\mu}u(\mathbf{h},s_h)\right]^*\left[\overline{\Phi}_{X_i}\hat{J}^{\nu}u(\mathbf{h},s_h)\right]$$

single-nucleon tensor

accounts for energy-momentum dispersion relation of the hadronic system X

1-body $h \to X$ current

- Different excitation regions can be explored within the same model:

  - **Quasi-elastic:** the nuclear final state is a particle-hole excitation

$$W^{\mu\nu}_{QE}(\mathbf{q},\omega) = \frac{3\mathcal{N}}{4\pi p_F^3}\int_F d\mathbf{h}\frac{m_N^2}{\overline{E}_{\mathbf{h}}\overline{E}_{\mathbf{p}}} w^{\mu\nu}_{QE}(H,Q)\delta(\omega+\overline{E}_{\mathbf{h}}-\overline{E}_{\mathbf{p}})$$

Nuclear tensor

$$w^{\mu\nu}_{QE} = \frac{1}{2}\sum_{s_h}\sum_{s_p}\left[\overline{u}(\mathbf{p},s_p)\hat{J}^{\mu}u(\mathbf{h},s_h)\right]^{*}\left[\overline{u}(\mathbf{p},s_p)\hat{J}^{\nu}u(\mathbf{h},s_h)\right]$$

Single-nucleon tensor

$$j^{\mu}_{N\to N} = \overline{u}(\mathbf{p})\Gamma^{\mu}u(\mathbf{h}) = \overline{u}(\mathbf{p})\left(F_1\gamma^{\mu}+\frac{i}{2m}F_2\sigma^{\mu\nu}Q_{\nu}\right)u(\mathbf{h}) \quad [G_E\equiv F_1-\tau F_2, G_M\equiv F_1+F_2]$$

EM current

  - **N→Δ transition:** the nuclear final state is a Δ-hole excitation

$$j^{\mu}_{N\to\Delta} = \overline{u^{RS}_{\beta}}(\mathbf{p_\Delta})\left(C_1\Gamma_1^{\mu\beta}+C_2\Gamma_2^{\mu\beta}+C_3\Gamma_3^{\mu\beta}\right)u(\mathbf{h}) \quad [G_E, G_M, G_C]$$

3 form factors:

M1 (magnetic dipole moment) → distribution of the quarks' electric current within N and Δ → dominant

E2 (electric quadrupole moment) and C2 (Coulomb quadrupole moment) → deviation from sphericity of quarks' charge distribution

Recent Jlab measurements of R_{EM} = E2/M1 and R_{SM} = C2/M1 indicate that they are small but non-zero

Higher resonances can be treated in the same framework as long as enough there is enough experimental information on the transtion ff's.
Ex: Roper resonance $N^*(1440)P_{11}$

$$j^{\mu}_{N\to\text{Roper}} = \overline{u}(\mathbf{p}^*,\mathbf{m}^*)\left[\bar{F}_1(\not{Q}Q^{\mu}-Q^2\gamma^{\mu})+i\bar{F}_2\sigma^{\mu\nu}Q_{\nu}\right]u(\mathbf{h})$$

The inelastic hadronic tensor

- The expression for the RFG inelastic hadronic tensor is:

$$W^{\mu\nu}_{RFG}(\kappa,\lambda) = \frac{3\mathcal{N}}{4\pi\eta_F^3}\int d\mu_x \int d\eta \frac{\mu_x}{\bar{\epsilon}\epsilon_x} w^{\mu\nu}_{inel}(\eta,\mu_x;\kappa,\lambda)\delta(2\lambda+\bar{\epsilon}-\epsilon_x)\theta(\eta_F-\eta)$$

$$\kappa^\mu = (\lambda,\boldsymbol{\kappa}) = \left(\frac{\omega}{2m_N},\frac{\mathbf{q}}{2m_N}\right), \quad \tau = \boldsymbol{\kappa}^2-\lambda^2, \quad \eta_F = \frac{p_F}{m_N}, \quad \epsilon_F = \sqrt{1+\eta_F^2}$$

$$\eta^\mu = (\bar{\epsilon},\boldsymbol{\eta}) = \left(\frac{\overline{E}_{\mathbf{h}}}{m_N},\frac{\mathbf{h}}{m_N}\right), \quad \mu_x = \frac{W_x}{m_N}, \quad \epsilon_x = \sqrt{\mu_x^2+(\boldsymbol{\eta}+2\boldsymbol{\kappa})^2},$$

dimensionless variables

$$w^{\mu\nu}_{inel} = -w_1\left(g^{\mu\nu}+\frac{\kappa^\mu\kappa^\nu}{\tau}\right)+w_2\left(\eta^\mu+\kappa^\mu\rho\right)\left(\eta^\nu+\kappa^\nu\rho\right)$$

$$\rho \equiv 1+\frac{1}{4\tau}(\mu_x^2-1)$$

inelasticity parameter
(=1 for quasielastic scattering)

$$\rho = 1/x$$

link between inelasticity and the Bjorken scaling variable corresponding to an on-shell nucleon moving inside the nucleus.
This is different from the “Lab” Bjorken variable, corresponding to a nucleon at rest in the laboratory frame:

$$x_L = \frac{|Q^2|}{2m_N\omega} = \frac{\tau}{\lambda}$$

Phys.Rev.C69 (2004) 035502

The inelastic hadronic tensor

- Using the δ function the **η**-integration can be performed, giving:

$$W^{\mu\nu}_{RFG}(\kappa,\lambda) = \frac{3\mathcal{N}\tau}{2\eta_F^3\kappa}\xi_F \int_{\rho_1(\kappa,\lambda)}^{\rho_2(\kappa,\lambda)} d\rho \left(1-\psi_x^2\right)\theta\left(1-\psi_x^2\right) U^{\mu\nu}(\kappa,\tau,\rho)$$

$\xi_F = \epsilon_F - 1$ Fermi kinetic energy

$$\xi_F \left(1-\psi_x^2\right)\theta\left(1-\psi_x^2\right) U^{\mu\nu}(\kappa,\tau,\rho) = \int_0^{2\pi} \frac{d\Phi}{2\pi} \int_{\epsilon_0(\rho)}^{\epsilon_F} d\bar{\epsilon}\, w^{\mu\nu}_{inel}(\bar{\epsilon},\theta_0,\rho;\kappa,\lambda)$$

from phenomenological fits of s.n. structure functions

$$\psi_x \equiv \text{sign}(\lambda-\tau\rho)\sqrt{\frac{\epsilon_0(\rho)-1}{\epsilon_F-1}}$$

inelastic scaling variable

For each ρ , a "peak" region $-1<\psi_X<1$ can be identified, centered at $\psi_X=0$,

of width $\simeq \frac{2\kappa\eta_F}{\sqrt{4\kappa^2+\mu_X^2}}$, growing with κ

and decreasing with μ_X

$$\rho \equiv 1 + \frac{1}{4\tau}(\mu_x^2 - 1)$$

"single-nucleon" responses

$$U^L = U^{00} = \frac{\kappa^2}{\tau}\left[\left(1+\tau\rho^2\right) w_2(\tau,\rho) - w_1(\tau,\rho) + w_2(\tau,\rho)\mathcal{D}(\kappa,\tau,\rho)\right]$$
$$U^T = U^{11} + U^{22} = 2w_1(\tau,\rho) + w_2(\tau,\rho)\mathcal{D}(\kappa,\tau,\rho)$$

Function arising from Fermi motion and going to zero as $\xi_F \to 0$

They contain medium corrections, which cannot be factorized in a relativistic framework

Phys.Rev.C69 (2004) 035502

The QEP as a special case

$$R_{inel}^{L,T}(\kappa,\tau) = \frac{3\mathcal{N}\tau}{2\eta_F^3\kappa}\xi_F \int_{-1}^{\psi_X^{\max}(\kappa,\lambda)} d\psi_X \left|\frac{\partial\rho}{\partial\psi_X}\right| \left(1-\psi_x^2\right) U^{L,T}(\kappa,\tau,\rho(\psi_X)) ,$$

- Special case:

- Quasi-elastic kinematics: ρ=1 ⇒ (analytic!)

$$W_{QE}^{\mu\nu}(\kappa,\lambda) = \frac{3\mathcal{N}\tau}{2\eta_F^3\kappa}\xi_F \left(1-\psi_x^2\right)\theta\left(1-\psi_x^2\right) U^{\mu\nu}(\kappa,\tau)$$

Parabolic in ψ

ψ scaling variable:
the "reduced" hadronic tensor only depends on ψ

$$\psi_{QE} \equiv \text{sign}(\lambda-\tau)\sqrt{\frac{\epsilon_0-1}{\epsilon_F-1}}$$

$$-1 \le \psi_{QE} \le 1$$

$$\psi_{QE} = 0$$ QEP

$$U^L = U^{00} = \frac{\kappa^2}{\tau}\left[(1+\tau)\,w_2(\tau) - w_1(\tau) + w_2(\tau)\mathcal{D}(\kappa,\tau)\right]$$

$$U^T = U^{11}+U^{22} = 2w_1(\tau) + w_2(\tau)\mathcal{D}(\kappa,\tau)$$

$$R_{QE}^{L,T}(\kappa,\tau) = \frac{3\mathcal{N}\tau}{2\eta_F^3\kappa}\xi_F \left(1-\psi_{QE}^2\right) U^{L,T}(\kappa,\tau)$$

QE response functions

$$\begin{aligned} w_{1,QE}(\tau) &= \tau G_M^2(\tau) \\ w_{2,QE}(\tau) &= \frac{G_E^2(\tau)+\tau G_M^2(\tau)}{1+\tau} \end{aligned}$$

$$\begin{aligned} \mathcal{D}(\kappa,\tau) &= \frac{1}{\epsilon_F-\epsilon_0}\int_{\epsilon_0}^{\epsilon_F} d\bar{\epsilon}\int_0^{2\pi}\frac{d\Phi}{2\pi}\left(\eta\times\hat{\kappa}\right)^2 \\ &= \frac{\tau}{\kappa^2}\left\{\frac{1}{3}\left[\epsilon_F^2+\epsilon_F\epsilon_0+\epsilon_0^2\right]+\lambda\left[\epsilon_F+\epsilon_0\right]+\lambda^2\right\}-(1+\tau) \\ &+ (\rho-1)\frac{\tau}{\kappa^2}\left\{\lambda\left[\epsilon_F+\epsilon_0\right]-2\tau\right\} \\ &= \xi_F\left(1-\psi_{QE}^2\right)\left[1+\xi_F\psi_{QE}^2 - \frac{\lambda}{\kappa}\psi_{QE}\sqrt{\xi_F\left(2+\xi_F\psi_{QE}^2\right)}+\frac{\tau}{3\kappa^2}\xi_F\left(1-\psi_{QE}^2\right)\right] \end{aligned}$$

medium corrections

Some results

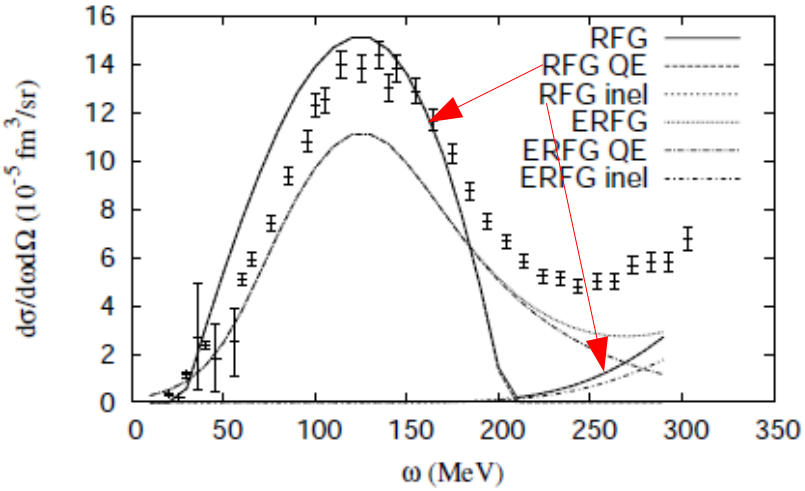

FIG. 2: Inclusive cross section for electron scattering from carbon at $E_{inc} = 500$ MeV and $\theta_e = 60°$ versus the energy transfer. The calculation includes an energy shift $\omega_{shift} = 20$ MeV and the separate QE and inelastic contributions to the cross section are shown. Data are from [41].

MB, J.A.Caballero, T.W.Donnelly, C.Maieron, Phys.Rev.C69 (2004) 035502

Some results

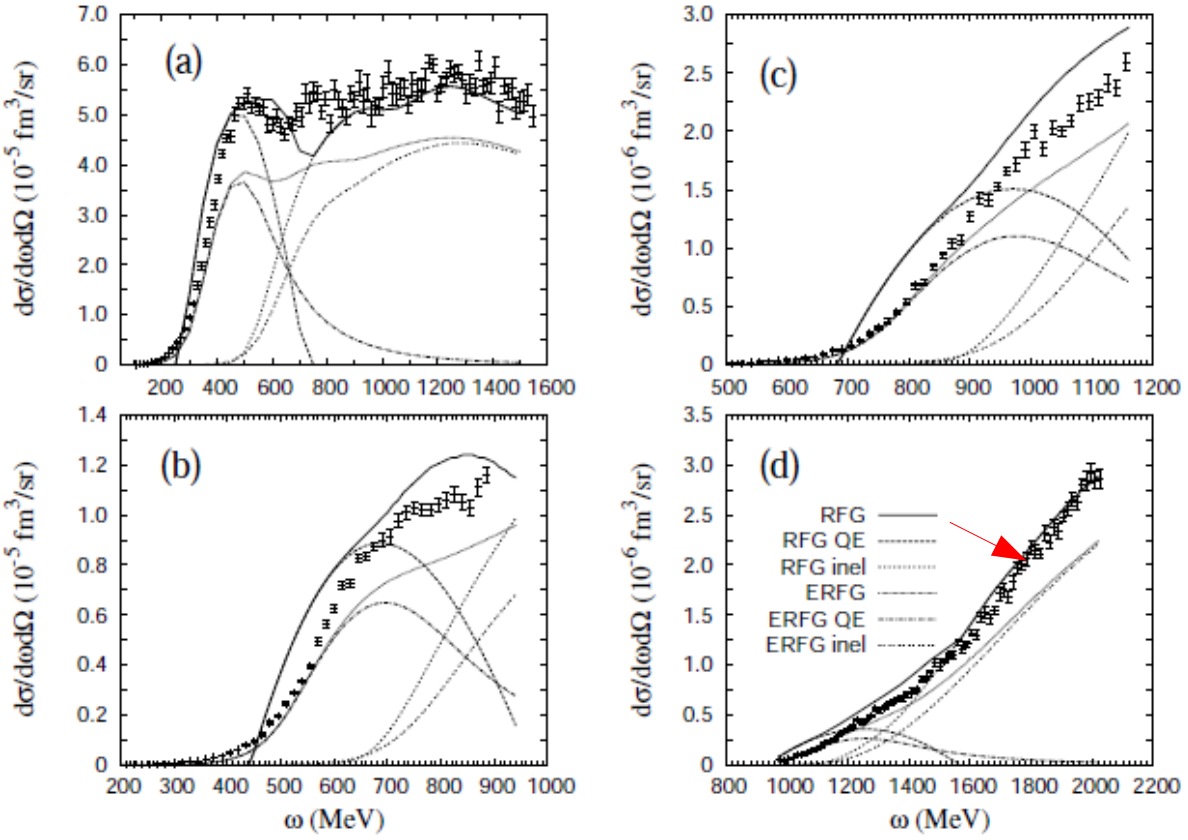

FIG. 4: As for Fig. 2, but at $E_e = 3.595$ GeV and scattering angle $\theta_e = 16°$ (a), 20° (b), 25° (c) and 30° (d). Data are from [39].

MB, J.A.Caballero, T.W.Donnelly, C.Maieron, Phys.Rev.C69 (2004) 035502

Nuclear Physics School 2013, Otranto

2.Inclusive electron scattering at intermediate and high energies:

a) Scaling

b) Meson Exchange Currents (scaling violations)

Inclusive electron scattering spectrum

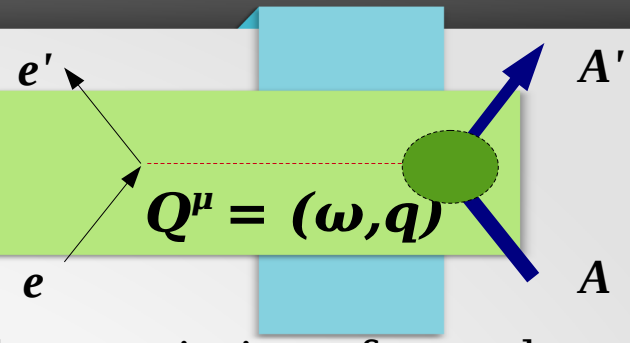

The virtuality of the exchanged photon allows independent variation of q and ω

⇒ $0 \le \omega \le q$

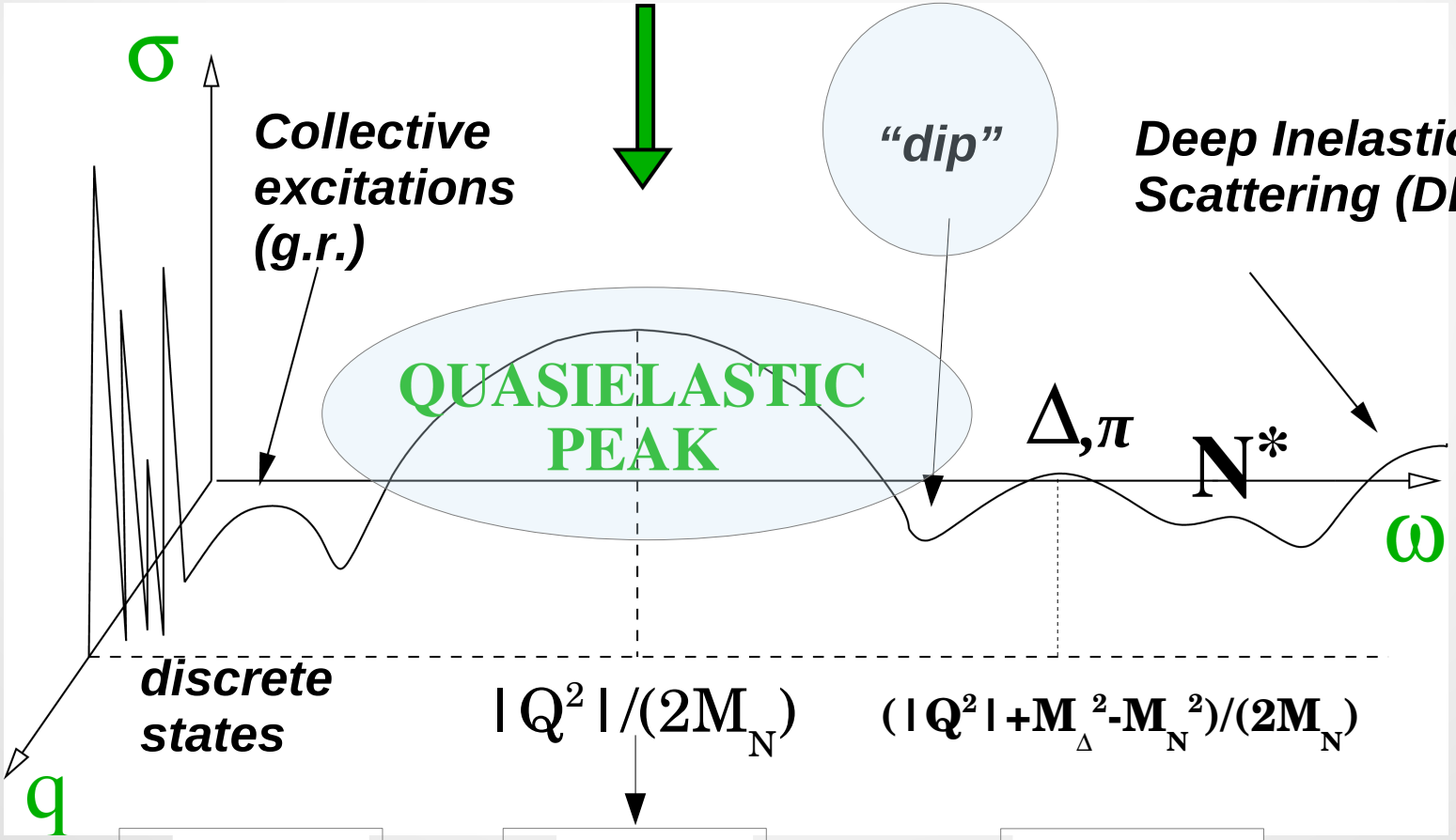

Scaling

- Scaling occurs in very diverse fields of physics (solid state, molecular, atomic, nuclear, particle...), with a wide energy range implied (eV-GeV).
- It usually involves processes where weakly interacting probes (e.g. leptons, neutrons) scatter from composite systems (e.g. atoms, nuclei, nucleons).
- The response of a many-body system to an external probe is said to scale when it no longer depends upon two variables (e.g. q and ω) but only on a particular combination of them, called scaling variable.
- Bjorken x-scaling (Bjorken, 1968), in lepton-nucleon DIS: the nucleon's structure functions F1 and F2 depend on the scaling variable

$$x = \frac{Q^2}{2m_N\omega}$$

and are (almost) independent of Q^2, indicating that the process is an incoherent scattering from pointlike constituents of the nucleon (partons, quarks)

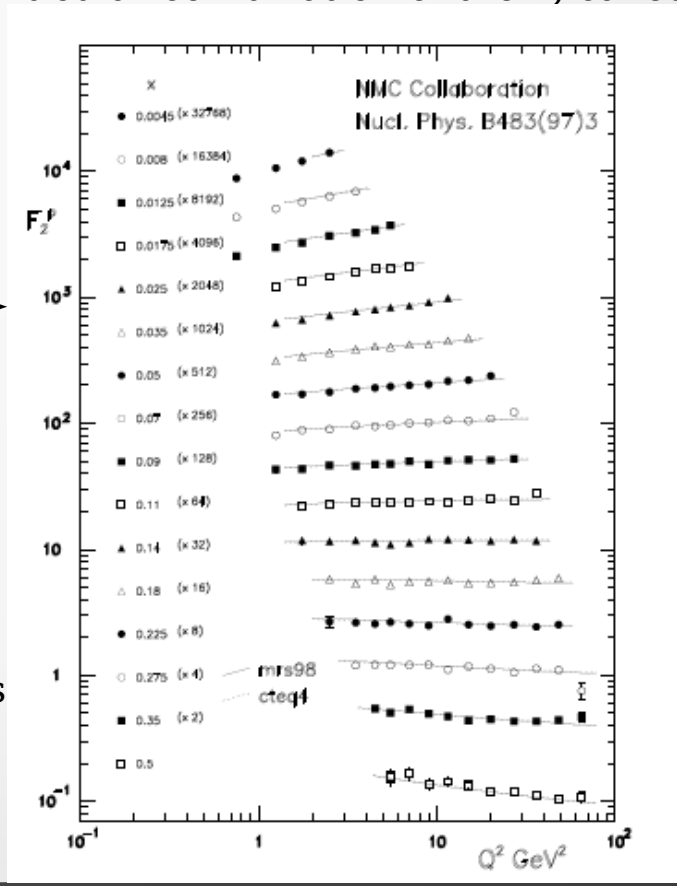

- Nuclear y-scaling (West, 1975), in lepton-nucleus QES: the (e,e') quasielastic reduced cross section depends only on one specific combination of (q,ω) as long as the process can be interpreted as incoherent scattering from the constituent of the nucleus (nucleons).

Y-scaling in the Plane Wave Impulse Approximation

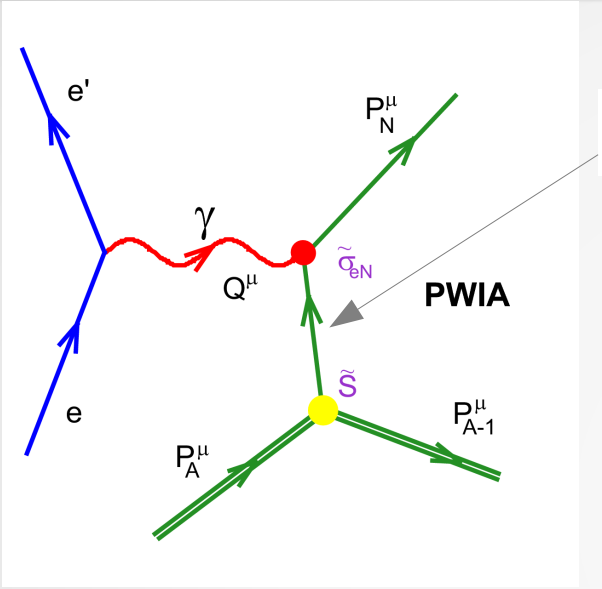

$$E(p,\mathcal{E}) = M_A^0 - \sqrt{(M_{A-1}^0)^2 + p^2} - \mathcal{E}$$

energy of the struck nucleon

$$\frac{d^3\sigma}{d\Omega_e d\omega d\mathrm{p}_N} = K\tilde{\sigma}_{eN}\tilde{S}(p,\mathcal{E})$$

Factorization of (e,e'N) c.s.

half-off-shell single-nucleon c.s.

nuclear spectral function (probability that a nucleon of momentum p and energy E is found in the nuclear g.s.)

The QE (e,e') c.s. is the integral of the (e,e'N) c.s. in the kinematically allowed region of the (p,ε) plane

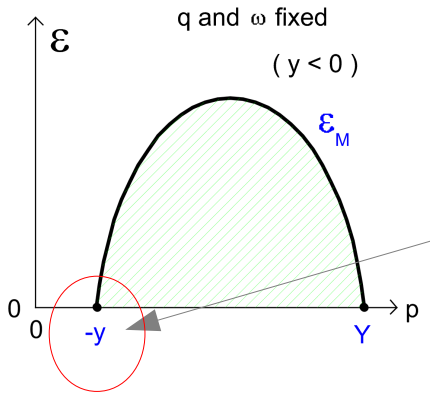

We would like to remove the eN c.s. from the integral in order to isolate the nuclear physics of QE scattering, but it depends upon p and ε.
Assumption: the most important contribution to the integral come from the smallest p and ε

$$F(q,y) \equiv \frac{d^2\sigma/d\Omega_e d\omega}{\tilde{\sigma}_{eN}(q,y;p=-y,\mathcal{E}=0)}.$$

reduced cross section
or
Scaling Function

The scaling function

$$F(q,y) \equiv \frac{d^2\sigma/d\Omega_e d\omega}{\widetilde{\sigma}_{eN}(q,y;p=-y,\mathcal{E}=0)}.$$

- The definition of F(q,y) is just a different representation of the QE inclusive c.s. (no approximation).
- On the other hand, assuming factorization into an eN and spectral function is indeed an approximation (PWIA or DWIA) . It implies that

$$F(q,y) = 2\pi \int_{-y}^{Y} p\, dp\, \widetilde{n}(q,y;p),$$

involving the integral

$$\widetilde{n}(q,y;p) = \int_{0}^{\mathcal{E}_M} d\mathcal{E}\, \widetilde{S}(p,\mathcal{E})$$

If $\mathcal{E}_M$ were ∞ it would be the nuclear momentum distribution

- *y-scaling* occurs if, at high enough values of *q*,

$$F(q,y) \overset{q\to\infty}{\longrightarrow} F(y) \equiv F(\infty,y)$$

the reduced cross section becomes only a function of *y*.

Scaling of I kind

The reduced response, plotted against y for different kinematics, is independent of q:

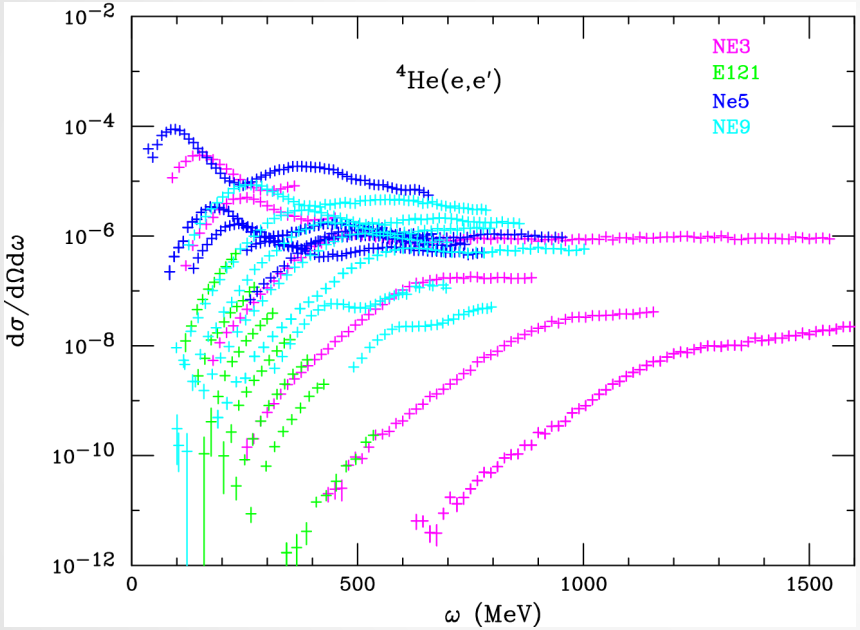

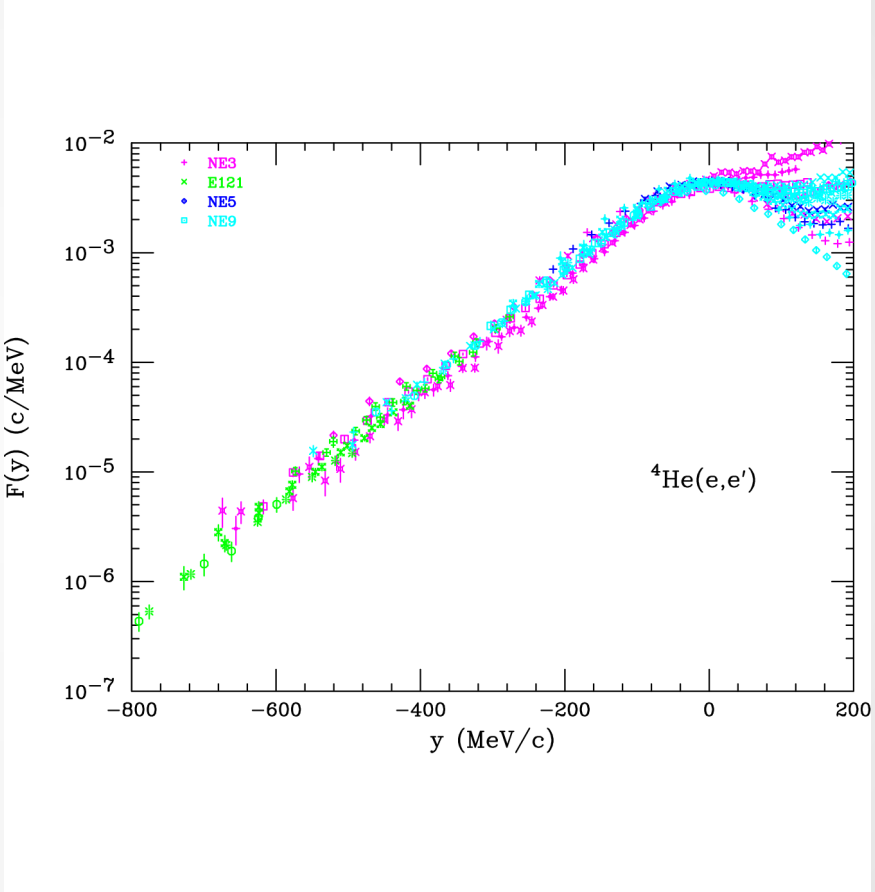

Day, McCarthy, Donnelly, Sick, Annu. Rev. Nucl. Part. Sci. 40 (1990)

Scaling in the RFG

Nuclear tensor:

$$W^{\mu\nu}_{RFG} \sim \int d\mathbf{p} \int d\mathbf{p}_N \delta[\mathbf{q} - (\mathbf{p}_N - \mathbf{p})]\delta[\omega - (E_N - E)] \times n(p)[1 - n(p_N)]w^{\mu\nu}_{nucleon},$$

Momentum distribution:

$$n(p) = \theta(k_F - |\mathbf{p}|)$$

Spectral function:

$$\tilde{S}^{RFG}(p, \mathcal{E}) = \frac{3\mathcal{N}}{8\pi k_F^3}\theta(k_F - p)\delta[\mathcal{E}(p) - \mathcal{E}^{RFG}(p)]$$

$$\mathcal{E}^{RFG}(p) = \sqrt{k_F^2 + m_N^2} - \sqrt{p^2 + m_N^2}$$

y-scaling variable:

$$y_{RFG} = m_N \left(\lambda\sqrt{1 + \frac{1}{\tau}} - \kappa\right)$$

$$\xi_F\psi^2 = \sqrt{1 + (y_{RFG}/m_N)^2} - 1$$

ψ-scaling variable:

$$\psi \equiv \text{sign}(\lambda - \tau)\sqrt{\frac{\epsilon_0 - 1}{\epsilon_F - 1}}$$

dimensionless $(-1 \leq \psi \leq 1)$

Scaling function:

$$F_{RFG}(\kappa, \psi) \cong \frac{\left[d^2\sigma/d\Omega_e d\omega\right]_{RFG}}{\sigma_M[\frac{\kappa}{2\tau}v_L\tilde{G}_E^2 + \frac{\tau}{\kappa}v_T\tilde{G}_M^2]},$$

$$\longrightarrow \quad F_{RFG} = \frac{3}{4k_F}(1 - \psi^2)\theta(1 - \psi^2)[1 + \mathcal{O}(\eta_F^2)].$$

The RFG exactly scales in the variable ψ and the scaling function is a parabola

Scaling of II kind

Let us introduce a dimensionless version of the scaling function

$$f \equiv k_F \times F$$

"superscaling function"

as suggested by the RFG:

$$f_{RFG}(\psi) = \frac{3}{4}(1-\psi^2)\theta(1-\psi^2)\left[1+(\eta_F\psi/2)^2+\cdots\right]$$

Scaling of II kind:
f independent of k_F (nuclear species)

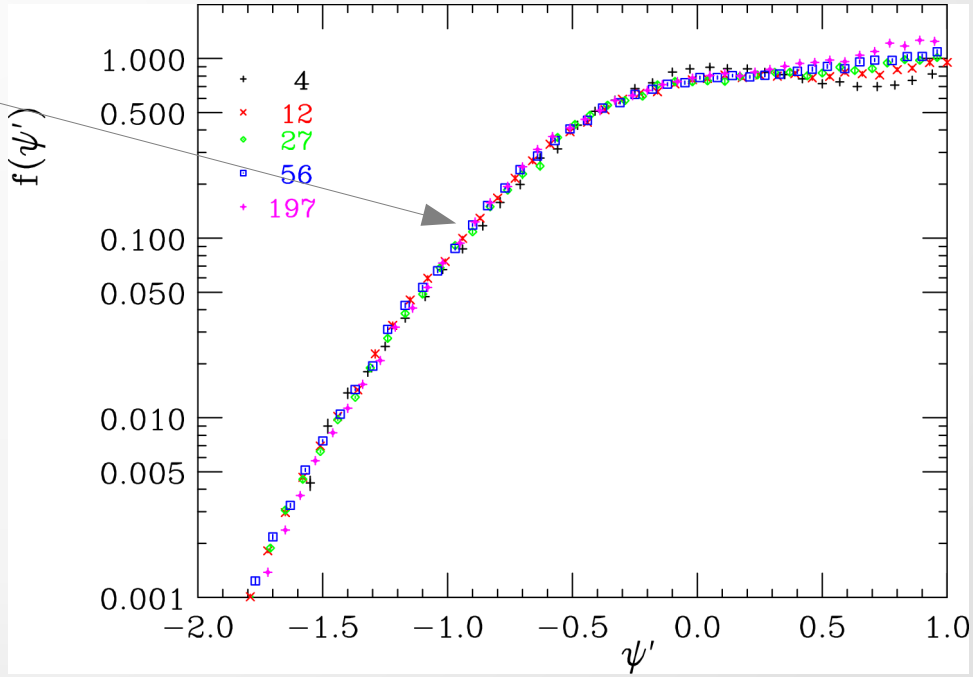

Scaling of the First Kind $\Longleftrightarrow$ *Independence of q*

Scaling of the Second Kind $\Longleftrightarrow$ *Independence of* k_F *or* A

Superscaling $\Longleftrightarrow$ *Both* 1^{st}*- and* 2^{nd}*-Kind Scaling.*

Donnelly, Sick, Phys.Rev.Lett. 82 (1999); Phys.Rev. C60 (1999)

Scaling of 0 kind: L and T channels

$$G_L(\kappa,\lambda) = \frac{\kappa}{2\tau}\tilde{G}_E^2 + \mathcal{O}[\eta_F^2]$$
$$G_T(\kappa,\lambda) = \frac{\tau}{\kappa}\tilde{G}_M^2 + \mathcal{O}[\eta_F^2].$$

$$F_L = \frac{R_L}{G_L}, \qquad F_T = \frac{R_T}{G_T}.$$

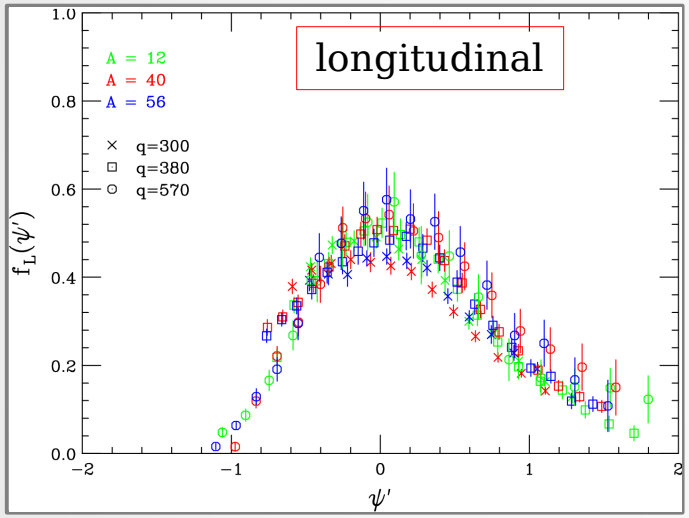

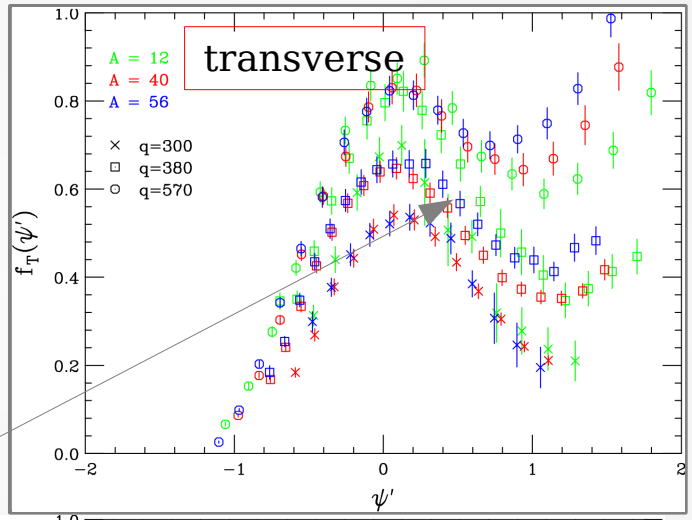

Scaling violations mainly reside in the transverse channel.

The RFG model predicts

$$f_L = f_T = f$$

"scaling of 0th kind"

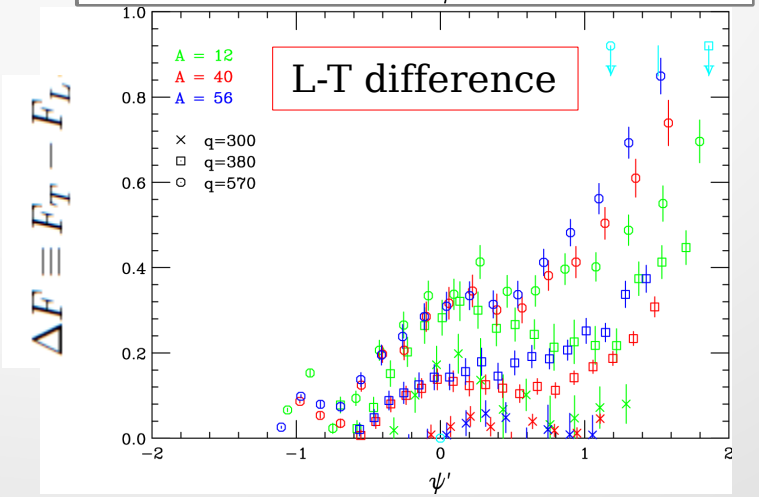

The phenomenological SuperScaling function

Based on the scaling analyses, a phenomenological longitudinal super-scaling function has been extracted from (e,e') world data at high momentum transfer [J.Jourdan, Nucl.Phys.A603, (1996)]

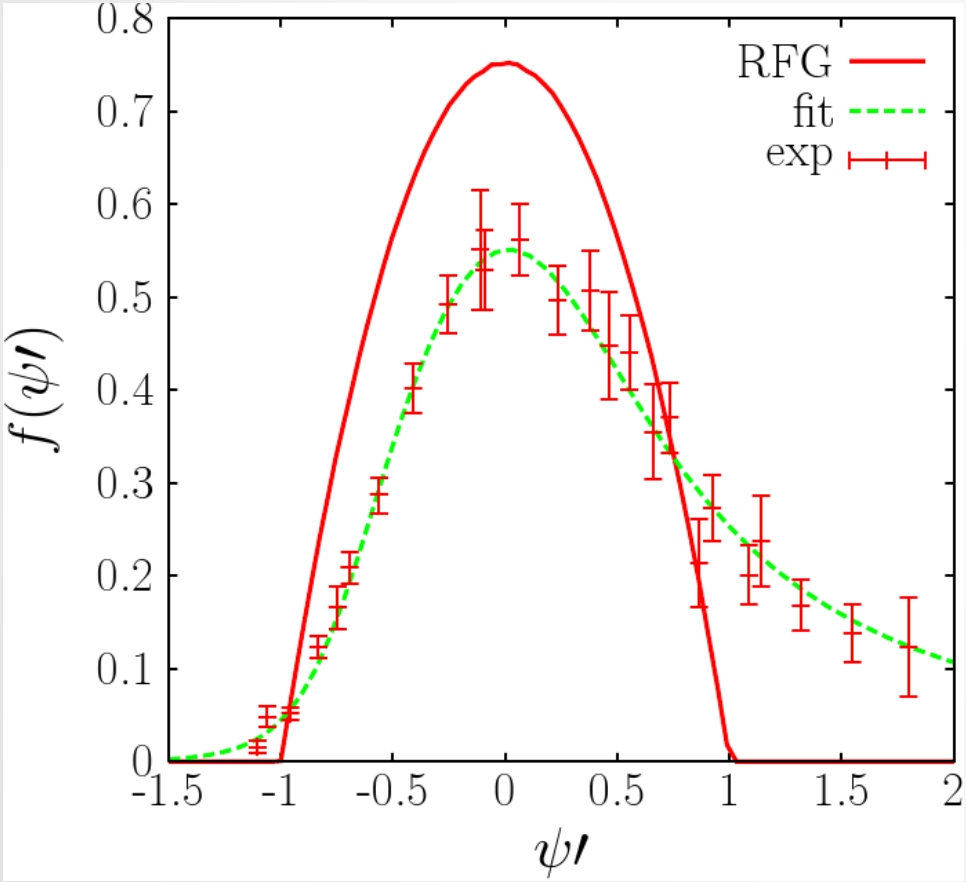

- Asymmetric shape around the QEP position
- 4-parameters fit for a large variety of kinematics and nuclei
- It represents a strong constraint on nuclear models
- The RFG predicts a parabolic super-scaling function: poor representation of data.

Relativistic Impulse Approximation approaches

- RIA: Scattering off a nucleus ⇒Incoherent sum of single-nucleon scattering processes

  Nuclear current ⇒ One-body operator

  1) Relativistic Mean Field Model - RMF

  2) Semi-relativistic Shell Model - RSM

  3) Relativistic Green's Function - RGF

$$J^{\mu}_{N}(\omega,q)=\int d\vec{p}\,\overline{\Psi}_{F}(\vec{p}+\vec{q})\,J^{\mu}_{N}\,\Psi_{B}(\vec{p})$$

  In the RMF approach

  Ψ_B: bound nucleon w.f. ⇒ Relativistic Mean Field (strong S and V potentials)

  Ψ_F: ejected nucleon w.f. ⇒ Final State Interaction, treated in different approaches:

  RPWIA: relativistic plane wave (no FSI)

  rROP: real relativistic optical potential

  RMF: uses the same RMF employed for the initial state

The scaling function in RIA

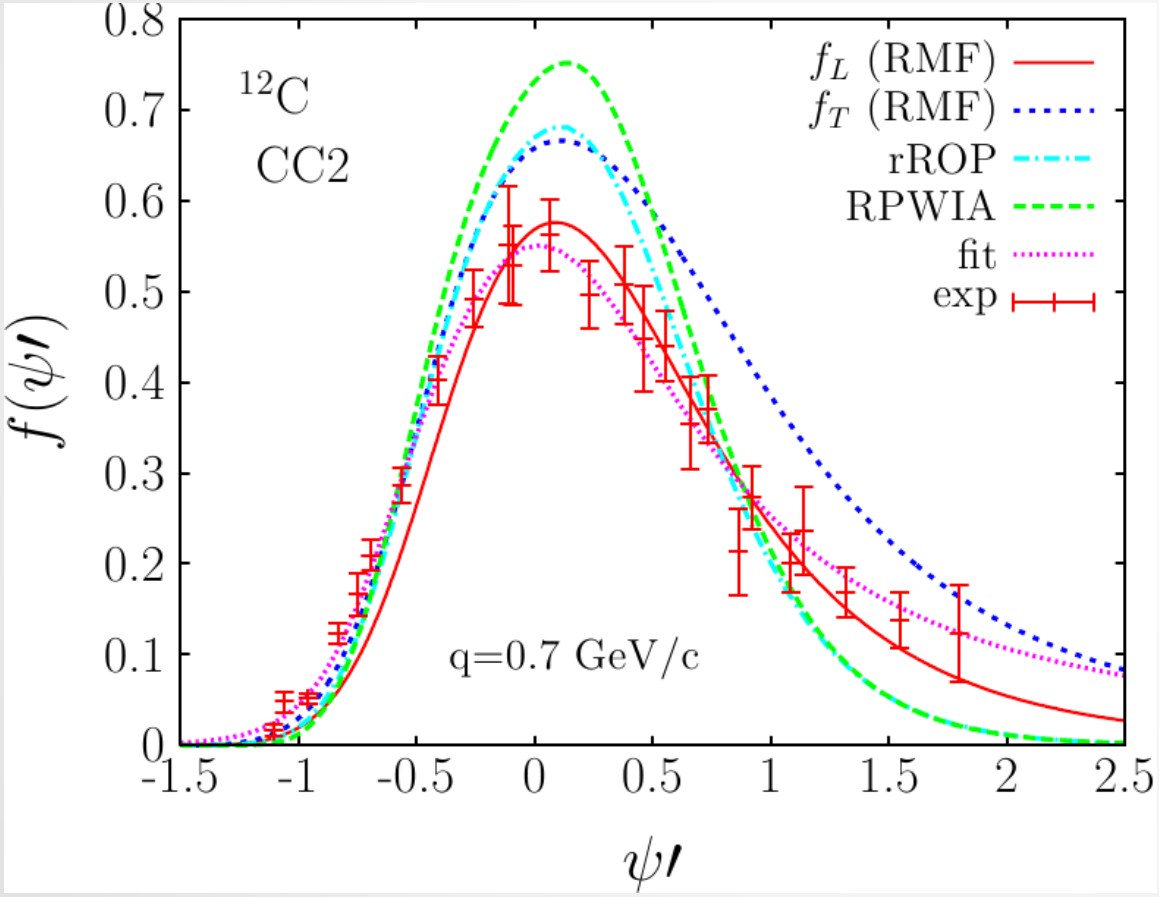

- The Relativistic Mean Field (RMF) model succesfully reproduces the longitudinal scaling function
- RMF predicts $f_T > f_L$ by ~ 20%, in qualitative agreement with the experimental evidence from the (few) separated L/T data
- The Relativistic Plane Wave Impuse Approximation and the rROP give a too high and symmetric scaling fucntion, with $f_T = f_L$

Extension of Scaling analysis to the Δ region

- How to devise a scaling procedure valid in the Δ resonance region?

- 1. Subtract from the data the QE contribution obtained in the super-scaling hypothesis:

$$\left[\frac{d^2\sigma}{d\omega\, d\Omega}\right]_{'\Delta'} = \left[\frac{d^2\sigma}{d\omega\, d\Omega}\right]_{\text{exp}} - \left[\frac{d^2\sigma}{d\omega\, d\Omega}\right]_{QE}$$

- 2. Divide by the elementary N→Δ cross section

$$F_{'\Delta'} = \frac{\left[\frac{d^2\sigma}{d\omega\, d\Omega}\right]_{'\Delta'}}{\sigma_M\left(v_L G_L^{\Delta} + v_T G_T^{\Delta}\right)}$$

- 3. Multiply by the Fermi momentum:

$$f_{'\Delta'} = k_F F_{'\Delta'}$$

- 4. Plot against the appropriate scaling function:

$$\psi_{\Delta} = \psi(q\rho, \omega\rho)$$

$$\rho = 1 + \frac{1}{4\tau}\left(m_{\Delta}^2/m_N^2 - 1\right) \quad \text{inelasticity}$$

Scaling in the Δ region

- How to devise a scaling procedure valid in the Δ resonance region?

- 1. Subtract from the data the QE contribution obtained in the super-scaling hypothesis:

$$\left[\frac{d^2\sigma}{d\omega\, d\Omega}\right]_{\psi'_\Delta} = \left[\frac{d^2\sigma}{d\omega\, d\Omega}\right]_{\text{exp}} - \left[\frac{d^2\sigma}{d\omega\, d\Omega}\right]_{QE}$$

- 2. Divide by the elementary N→Δ cross section

$$F_{\psi'_\Delta} = \frac{\left[\frac{d^2\sigma}{d\omega\, d\Omega}\right]_{\psi'_\Delta}}{\sigma_M\left(v_L G_L^\Delta + v_T G_T^\Delta\right)}$$

- 3. Multiply by the Fermi momentum:

$$f_{\psi'_\Delta} = k_F F_{\psi'_\Delta}$$

- 4. Plot against the appropriate scaling function:

$$\psi_\Delta = \psi(q\rho, \omega\rho)$$

$$\rho = 1 + \frac{1}{4\tau}\left(m_\Delta^2/m_N^2 - 1\right) \quad \text{inelasticity}$$

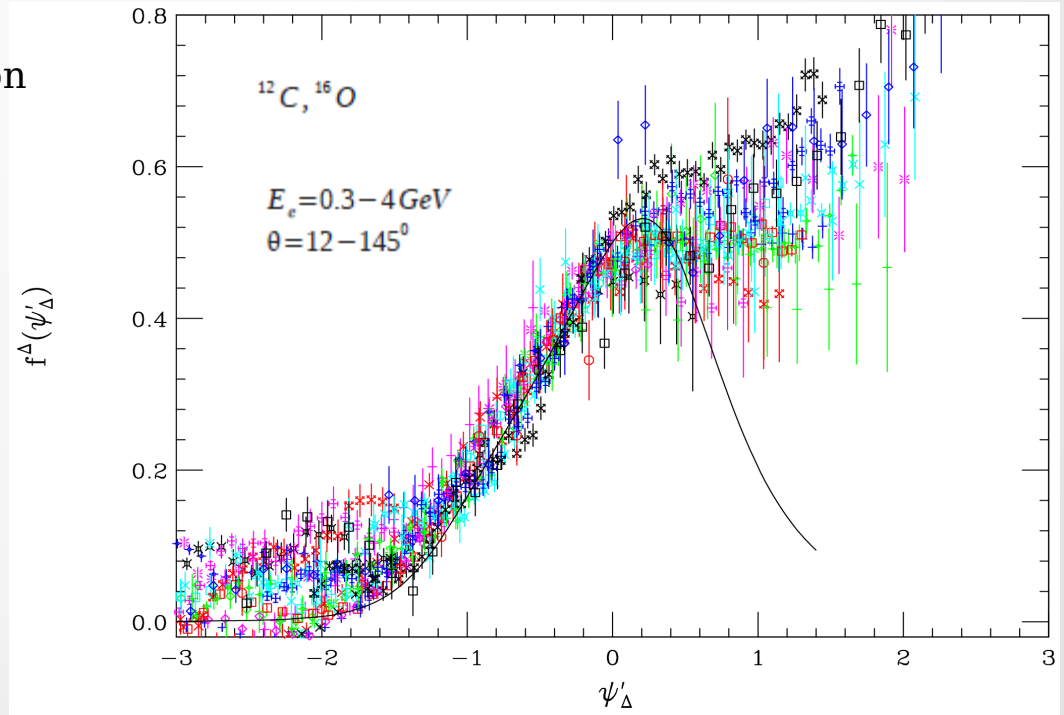

J.E. Amaro, MBB, J.A. Caballero, T.W. Donnelly, A. Molinari, I. Sick, Phys. Rev. C 71, 015501 (2005)

Scaling in the Δ region

- How to devise a scaling procedure valid in the Δ resonance region?

- 1. Subtract from the data the QE contribution obtained in the super-scaling hypothesis:

$$\left[\frac{d^2\sigma}{d\omega\, d\Omega}\right]_{\psi'_\Delta} = \left[\frac{d^2\sigma}{d\omega\, d\Omega}\right]_{\rm exp} - \left[\frac{d^2\sigma}{d\omega\, d\Omega}\right]_{QE}$$

- 2. Divide by the elementary N→Δ cross section

$$F_{\psi'_\Delta} = \frac{\left[\frac{d^2\sigma}{d\omega\, d\Omega}\right]_{\psi'_\Delta}}{\sigma_M\left(v_L G_L^\Delta + v_T G_T^\Delta\right)}$$

- 3. Multiply by the Fermi momentum:

$$f_{\psi'_\Delta} = k_F F_{\psi'_\Delta}$$

- 4. Plot against the appropriate scaling function:

$$\psi_\Delta = \psi(q\rho, \omega\rho)$$

$$\rho = 1 + \frac{1}{4\tau}\left(m_\Delta^2/m_N^2 - 1\right) \quad \text{inelasticity}$$

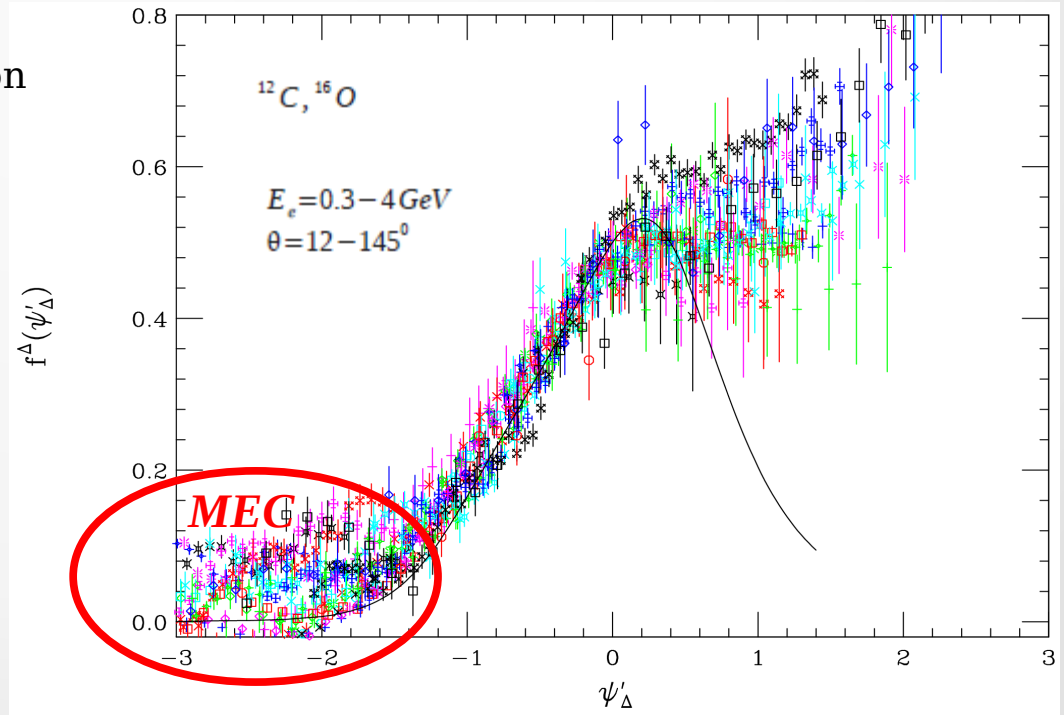

J.E. Amaro, MBB, J.A. Caballero, T.W. Donnelly, A. Molinari, I. Sick, Phys. Rev. C 71, 015501 (2005)

Test of scaling functions

With these 2 scaling functions we can now reconstruct the (e,e') cross sections and compare with data for different kinematics and nuclei:

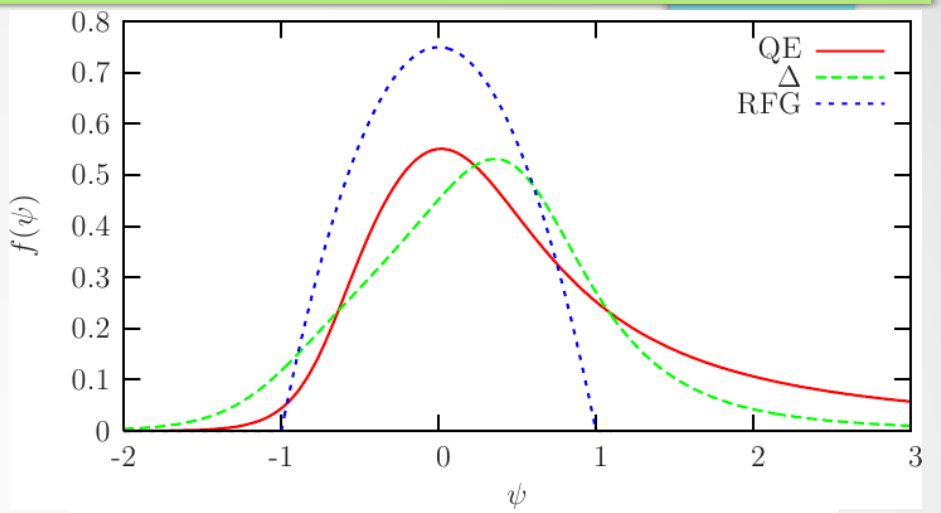

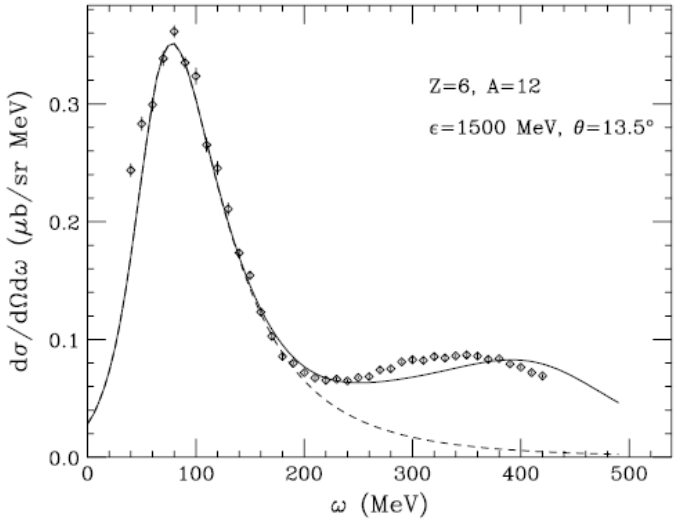

FIG. 3. Experimental (e, e') cross section for ^{12}C at an incident electron energy of 1.5 GeV and a scattering angle of 13.5 degrees, together with the calculated result obtained using f^{QE} and f^{Δ}. The dashed curve is the QE contribution and the solid curve is the total including the Δ.

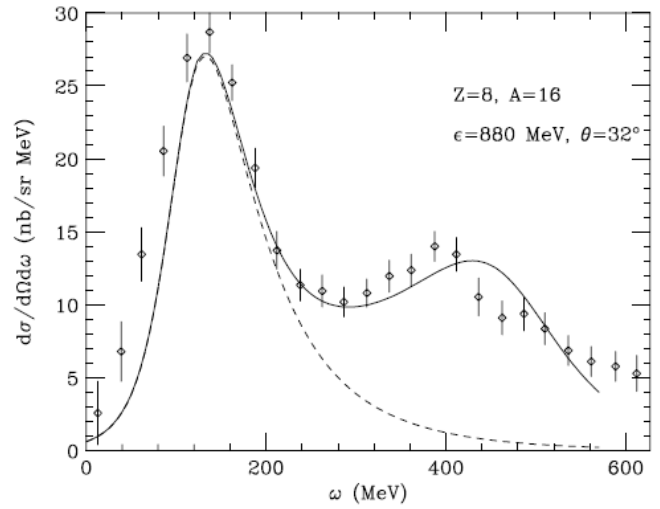

FIG. 5. Experimental (e, e') cross section as in Figs. 3 and 4, but now for ^{16}O at an incident electron energy of 0.88 GeV and a scattering angle of 32 degrees.

Test of scaling functions

With these 2 scaling functions we can now reconstruct the (e,e') cross sections and compare with data for different kinematics and nuclei:

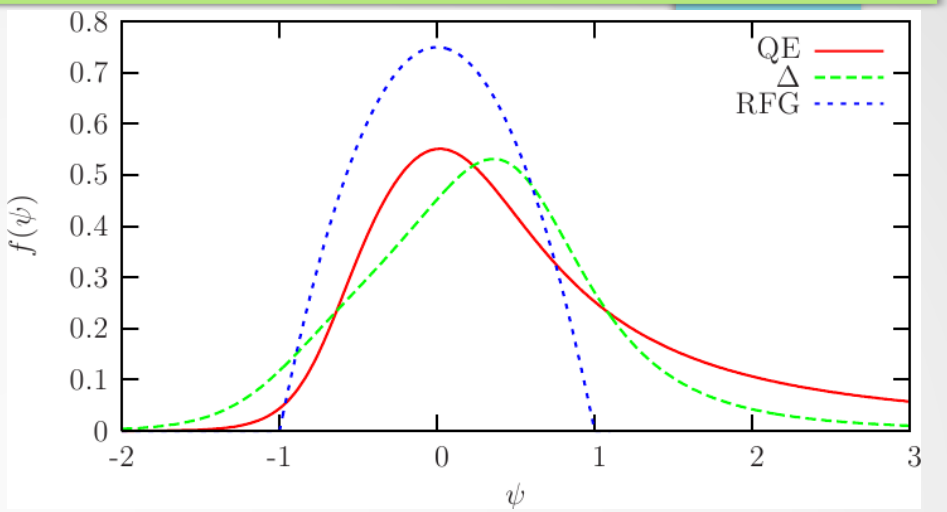

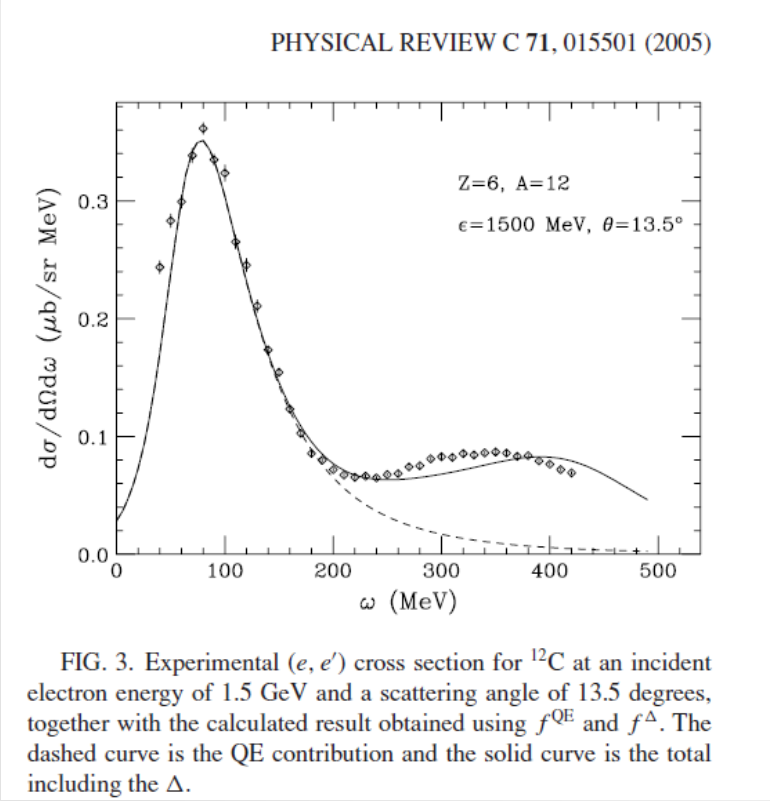

FIG. 3. Experimental (e, e') cross section for ^{12}C at an incident electron energy of 1.5 GeV and a scattering angle of 13.5 degrees, together with the calculated result obtained using f^{QE} and f^{Δ}. The dashed curve is the QE contribution and the solid curve is the total including the Δ.

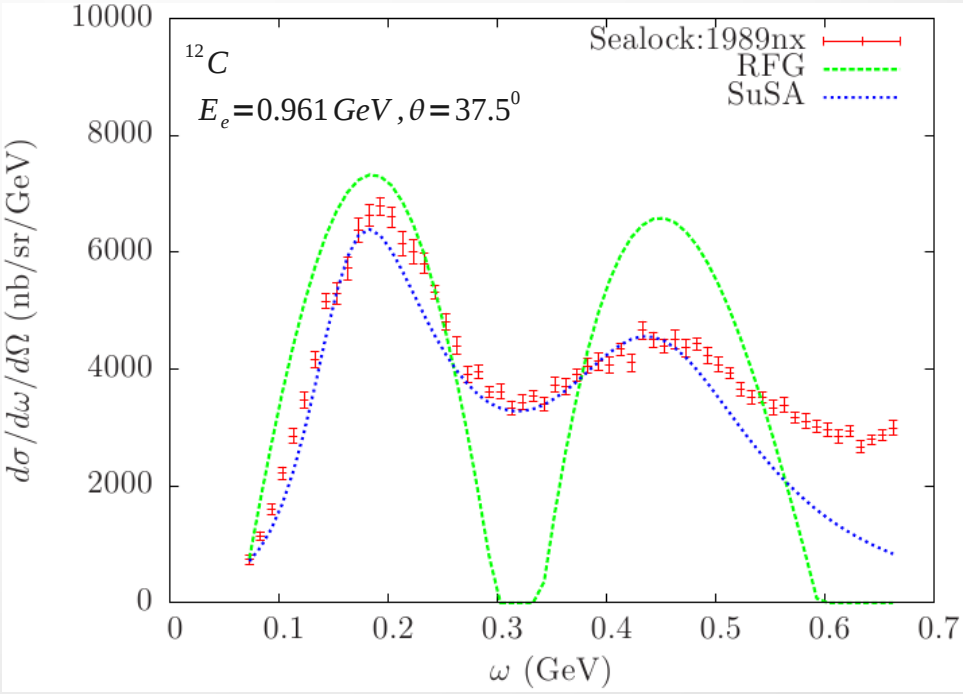

Meson Exchange Currents

Feynman diagrams:

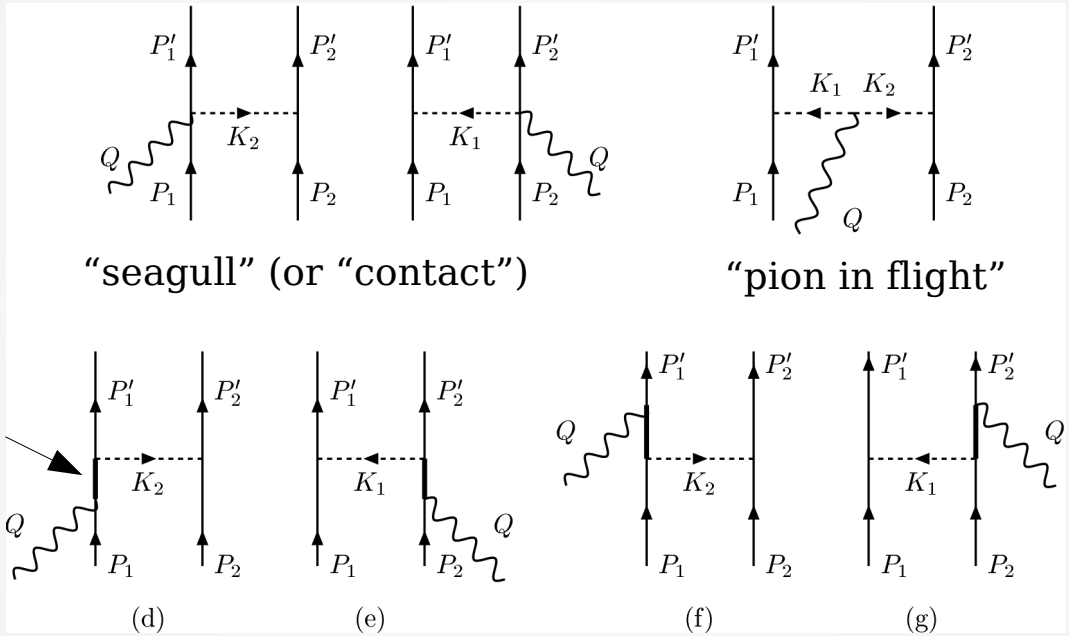

“correlation” and “Δ-MEC” diagrams

Two-body current matrix elements

Pseudovector πNN Lagrangean

$$\mathcal{L}_{\pi NN} = -\frac{f}{m_\pi}\overline{\psi}\gamma_5\gamma^\mu(\partial_\mu\phi_a)\tau_a\psi$$

$$j^\mu_s = \frac{f^2}{m_\pi^2} i\epsilon_{3ab}\overline{u}(\mathbf{p}_1')\tau_a\gamma_5 \not{K}_1 u(\mathbf{p}_1)\frac{F_1^V}{K_1^2-m_\pi^2}\overline{u}(\mathbf{p}_2')\tau_b\gamma_5\gamma^\mu u(\mathbf{p}_2) + (1\leftrightarrow 2)$$

$$j^\mu_p = \frac{f^2}{m_\pi^2}\frac{i\epsilon_{3ab}F_\pi(K_1-K_2)^\mu}{(K_1^2-m_\pi^2)(K_2^2-m_\pi^2)}\overline{u}(\mathbf{p}_1')\tau_a\gamma_5 \not{K}_1 u(\mathbf{p}_1)\overline{u}(\mathbf{p}_2')\tau_b\gamma_5 \not{K}_2 u(\mathbf{p}_2)$$

$$j^\mu_{cor} = \frac{f^2}{m_\pi^2}\overline{u}(\mathbf{p}_1')\tau_a\gamma_5 \not{K}_1 u(\mathbf{p}_1)\frac{1}{K_1^2-m_\pi^2}$$
$$\times\overline{u}(\mathbf{p}_2')\left[\tau_a\gamma_5 \not{K}_1 S_F(P_2+Q)\Gamma^\mu(Q) + \Gamma^\mu(Q)S_F(P_2'-Q)\tau_a\gamma_5 \not{K}_1\right]u(\mathbf{p}_2)$$
$$+(1\leftrightarrow 2)$$

$$S_F(P) = \frac{\not{P}+m}{P^2-m^2}$$ nucleon propagator

$$\Gamma^\mu(Q) = F_1\gamma^\mu + \frac{i}{2m}F_2\sigma^{\mu\nu}Q_\nu$$ electromagnetic nucleon vertex

Gauge invariance

The total two-body current is conserved: $Q_\mu \left(j^\mu_s + j^\mu_p + j^\mu_{cor}\right) = Q_\mu j^\mu_\Delta = 0$

Proof

$$
\begin{aligned}
Q_\mu j^\mu_s(\mathrm{p}'_1,\mathrm{p}'_2,\mathrm{p}_1,\mathrm{p}_2) &= -2m\frac{f^2}{m_\pi^2} i\epsilon_{3ab}\overline{u}(\mathrm{p}'_1)\tau_a\gamma_5 u(\mathrm{p}_1)\frac{F_1^V}{K_1^2-m_\pi^2} \\
&\times\ \overline{u}(\mathrm{p}'_2)\tau_b\gamma_5\ \not{Q} u(\mathrm{p}_2) + (1\leftrightarrow 2) \qquad \text{seagull} \\
Q_\mu j^\mu_p(\mathrm{p}'_1,\mathrm{p}'_2,\mathrm{p}_1,\mathrm{p}_2) &= 4m^2\frac{f^2}{m_\pi^2} i\epsilon_{3ab}F_\pi \frac{(K_1-K_2)\cdot Q}{(K_1^2-m_\pi^2)(K_2^2-m_\pi^2)} \\
&\times\ \overline{u}(\mathrm{p}'_1)\tau_a\gamma_5 u(\mathrm{p}_1)\overline{u}(\mathrm{p}'_2)\tau_b\gamma_5 u(\mathrm{p}_2)\,. \qquad \text{pion in flight} \\
Q_\mu j^\mu_{cor}(\mathrm{p}'_1,\mathrm{p}'_2,\mathrm{p}_1,\mathrm{p}_2) &= 2m\frac{f^2}{m_\pi^2} i\epsilon_{3ab}\overline{u}(\mathrm{p}'_1)\tau_a\gamma_5 u(\mathrm{p}_1)\frac{F_1^V}{K_1^2-m_\pi^2} \\
&\times\ \overline{u}(\mathrm{p}'_2)\tau_b\gamma_5(\not{Q}+2m)u(\mathrm{p}_2) + (1\leftrightarrow 2)\,. \qquad \text{correlations}
\end{aligned}
$$

$$
Q_\mu \left[j^\mu_{cor}(\mathrm{p}'_1,\mathrm{p}'_2,\mathrm{p}_1,\mathrm{p}_2) + j^\mu_s(\mathrm{p}'_1,\mathrm{p}'_2,\mathrm{p}_1,\mathrm{p}_2)\right] = 0 \quad \Leftrightarrow \quad F_\pi = F_1^V
$$

The divergence of the correlation current exactly cancels the pion-in-flight and seagull contributions providing $F_\pi = F_1^V$: correlations are needed to preserve gauge invariance

MEC and associated correlations can be consistently introduced in the RFG basis, where no correlations (except Pauli) exist in the unperturbed wave function.

The Δ-MEC current

The Δ-MEC current is derived from the γNΔ Lagrangian and Δ propagator:

[V. Pascalutsa, O. Scholten, Nucl. Phys. A 591 (1995) 658]

$$\mathcal{L}_{\gamma N\Delta} = \mathcal{L}^1_{\gamma N\Delta} + \mathcal{L}^2_{\gamma N\Delta} + \mathcal{L}^3_{\gamma N\Delta}$$

$$G^{\Delta}_{\beta\rho}(P) = G^{RS}_{\beta\rho}(P) + G^{A}_{\beta\rho}(P)$$

$$\begin{aligned}
\mathcal{L}^1_{\gamma N\Delta} &= \frac{ieG_1}{2m_N}\bar{\psi}^{\alpha}\Theta_{\alpha\mu}(z_1,A)\gamma_\nu\gamma_5 T_3^{\dagger} N F^{\nu\mu} + \text{h.c.} \\
\mathcal{L}^2_{\gamma N\Delta} &= \frac{eG_2}{(2m_N)^2}\bar{\psi}^{\alpha}\Theta_{\alpha\mu}(z_2,A)\gamma_5 T_3^{\dagger}(\partial_\nu N) F^{\nu\mu} + \text{h.c.} \\
\mathcal{L}^3_{\gamma N\Delta} &= -\frac{eG_3}{(2m_N)^2}\bar{\psi}^{\alpha}\Theta_{\alpha\mu}(z_3,A)\gamma_5 T_3^{\dagger} N \partial_\nu F^{\nu\mu} + \text{h.c.}\,,
\end{aligned}$$

$$\Theta_{\mu\nu}(z,A) = g_{\mu\nu} + \left[z + \frac{1}{2}(1+4z)A\right]\gamma_\mu\gamma_\nu$$

z=off-shell parameter
A=arbitrary parameter related to the "contact" invariance of the Lagrangian

Rarita-Schwinger (spin 3/2) propagator:

$$G^{RS}_{\beta\rho}(P) = -\frac{\not{P}+m_\Delta}{P^2-m_\Delta^2}\left[g_{\beta\rho} - \frac{1}{3}\gamma_\beta\gamma_\rho - \frac{2}{3}\frac{P_\beta P_\rho}{m_\Delta^2} - \frac{\gamma_\beta P_\rho - \gamma_\rho P_\beta}{3m_\Delta}\right]$$

A-dependent term:

$$G^{A}_{\beta\rho}(P) = -\frac{1}{3m_\Delta^2}\frac{A+1}{(2A+1)^2}\left[(2A+1)(\gamma_\beta P_\rho + P_\beta\gamma_\rho) - \frac{A+1}{2}\gamma_\beta(\not{P}+2m_\Delta)\gamma_\rho + m_\Delta\gamma_\beta\gamma_\rho\right]$$

$$A=-1 \Longrightarrow G = G^{RS}$$

$$j^{\mu}_{\Delta} = \frac{f_{\pi N\Delta} f}{m_\pi^2}\frac{K_{2\alpha}}{K_2^2 - m_\pi^2} Q_\nu \bar{u}(\mathbf{p_1'})\left[X_a^{\alpha\mu\nu}(P_1',P_1) - X_a^{\alpha\nu\mu}(P_1',P_1)\right]u(\mathbf{p_1})$$
$$\times \bar{u}(\mathbf{p_2'})\gamma_5 \not{K}_2 \tau_a u(\mathbf{p_2}) + (1 \leftrightarrow 2)$$

The current is conserved:

$$Q_\mu j^{\mu}_{\Delta} = 0$$

One particle – one hole diagrams

Matrix elements

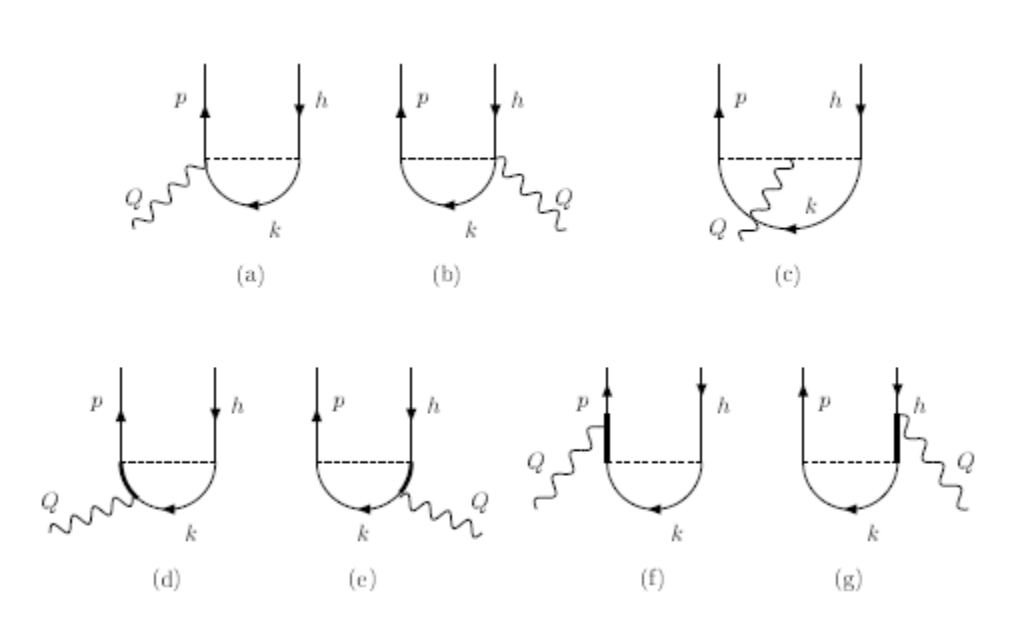

Polarization propagator

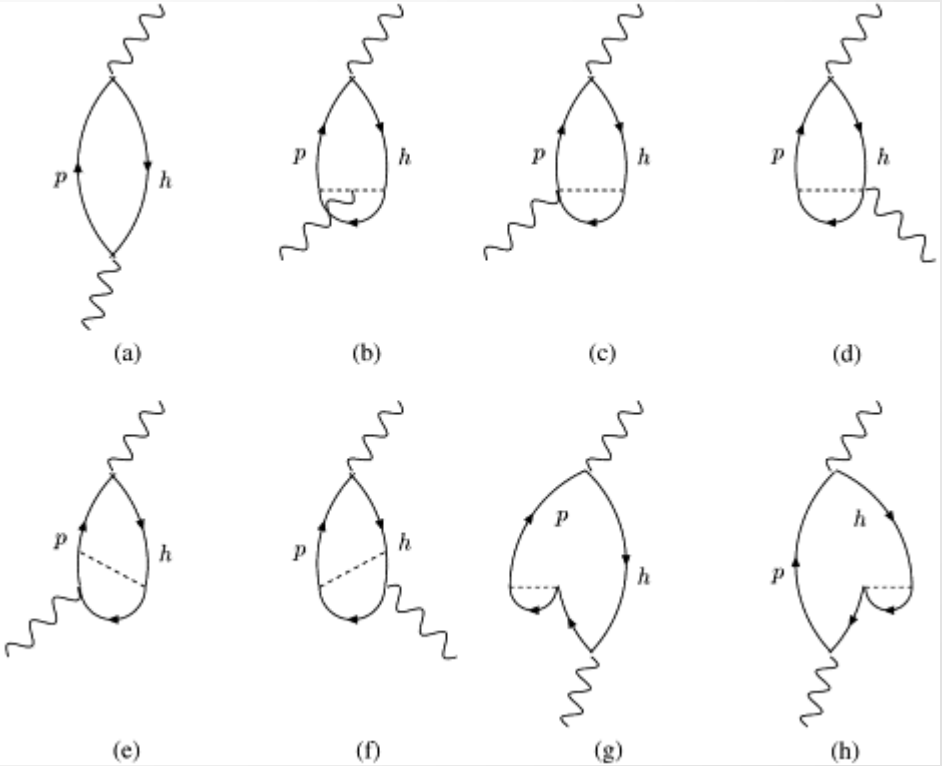

Two particle – two holes diagrams: “direct”

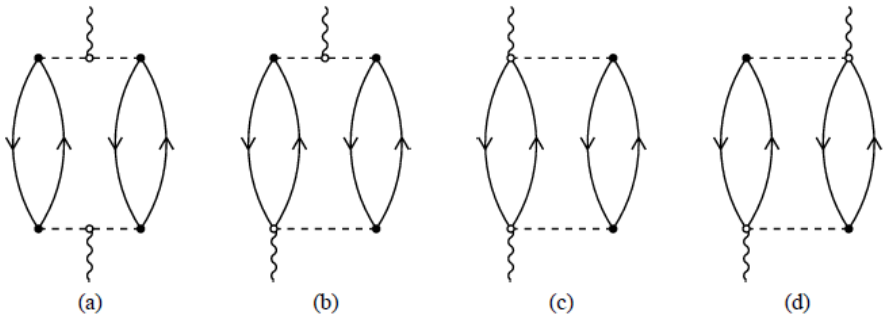

Fig. 2. The direct pionic contributions to the MEC 2p–2h response function.

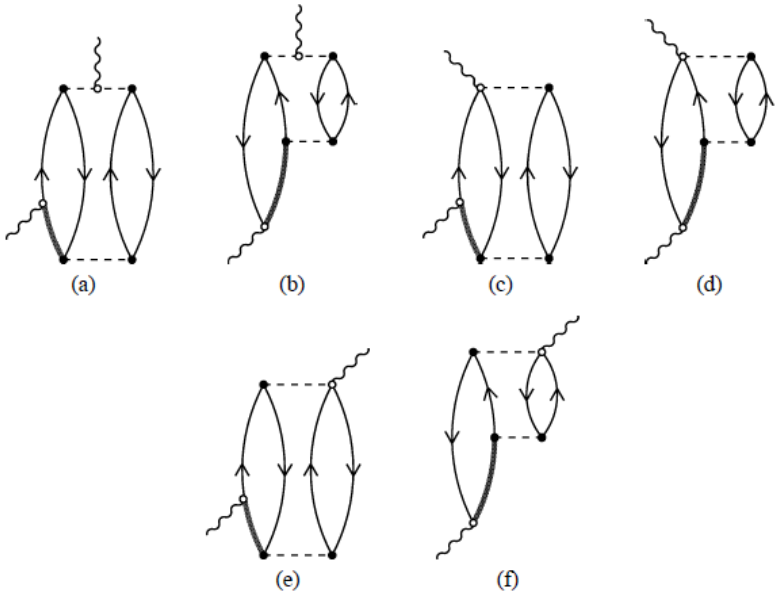

Fig. 3. The direct pionic/Δ interference contributions to the MEC 2p–2h response function.

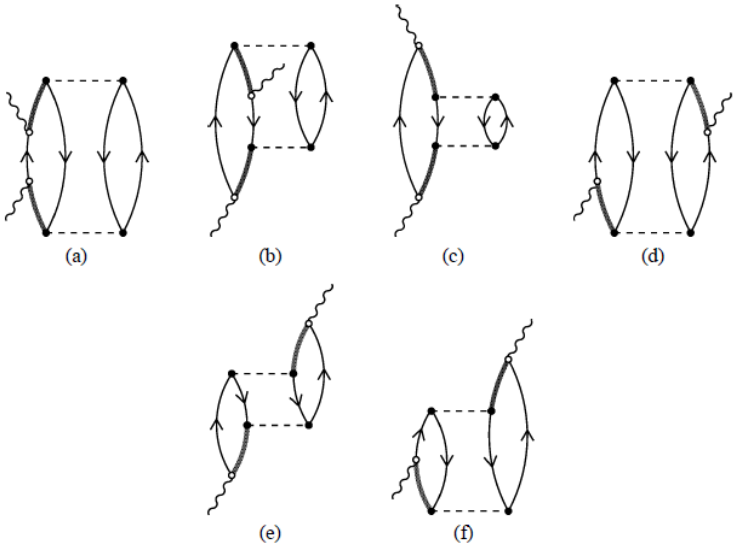

Fig. 4. The direct Δ contributions to the MEC 2p–2h response function.

A. De Pace et al. / Nuclear Physics A 726 (2003) 303–326

Two particle – two hole diagrams: “exchange”

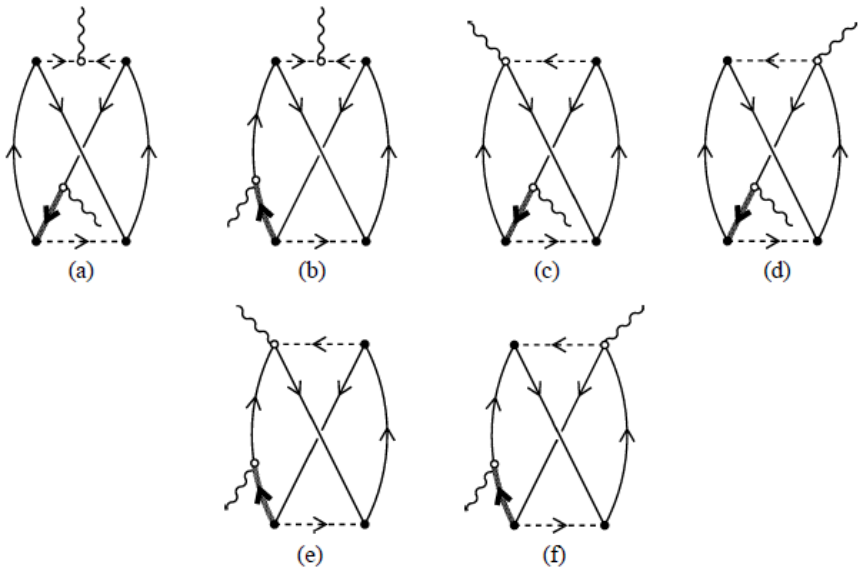

Fig. 5. The exchange pionic/Δ interference contributions to the MEC 2p–2h response function.

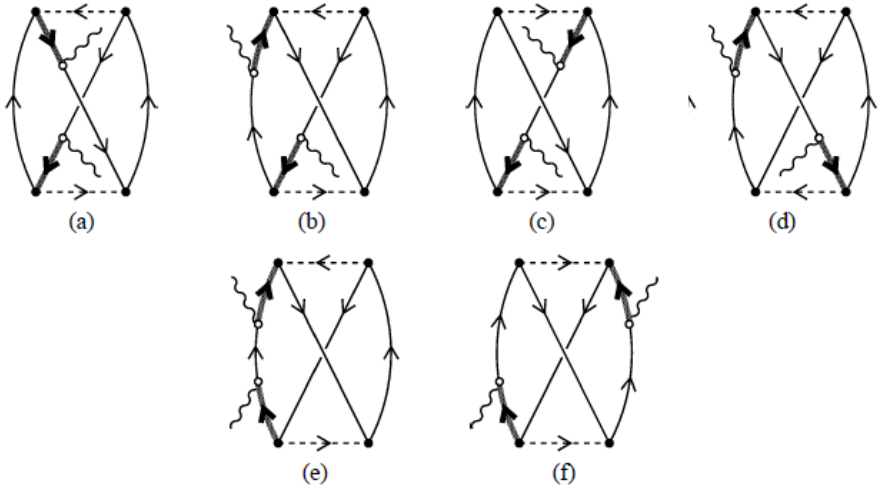

Fig. 6. The exchange Δ contributions to the MEC 2p–2h response function.

A. De Pace et al. / Nuclear Physics A 726 (2003) 303–326

Effects of 1p-1h MEC and correlations in the QEP

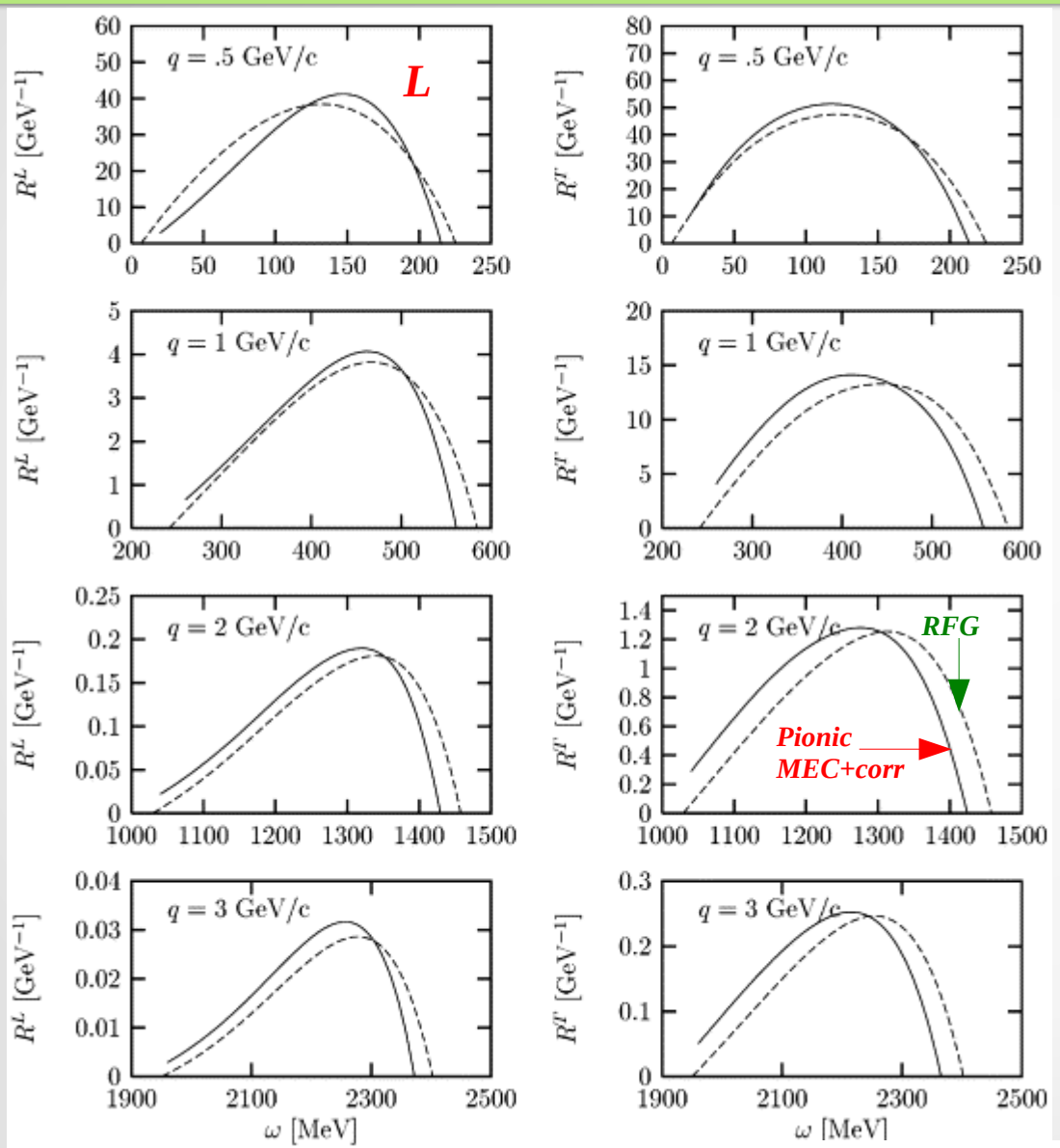

Purely pionic MEC+corr

J.E. Amaro et al. / Physics Reports 368 (2002) 317–407

Effects of 1p-1h MEC and correlations in the QEP

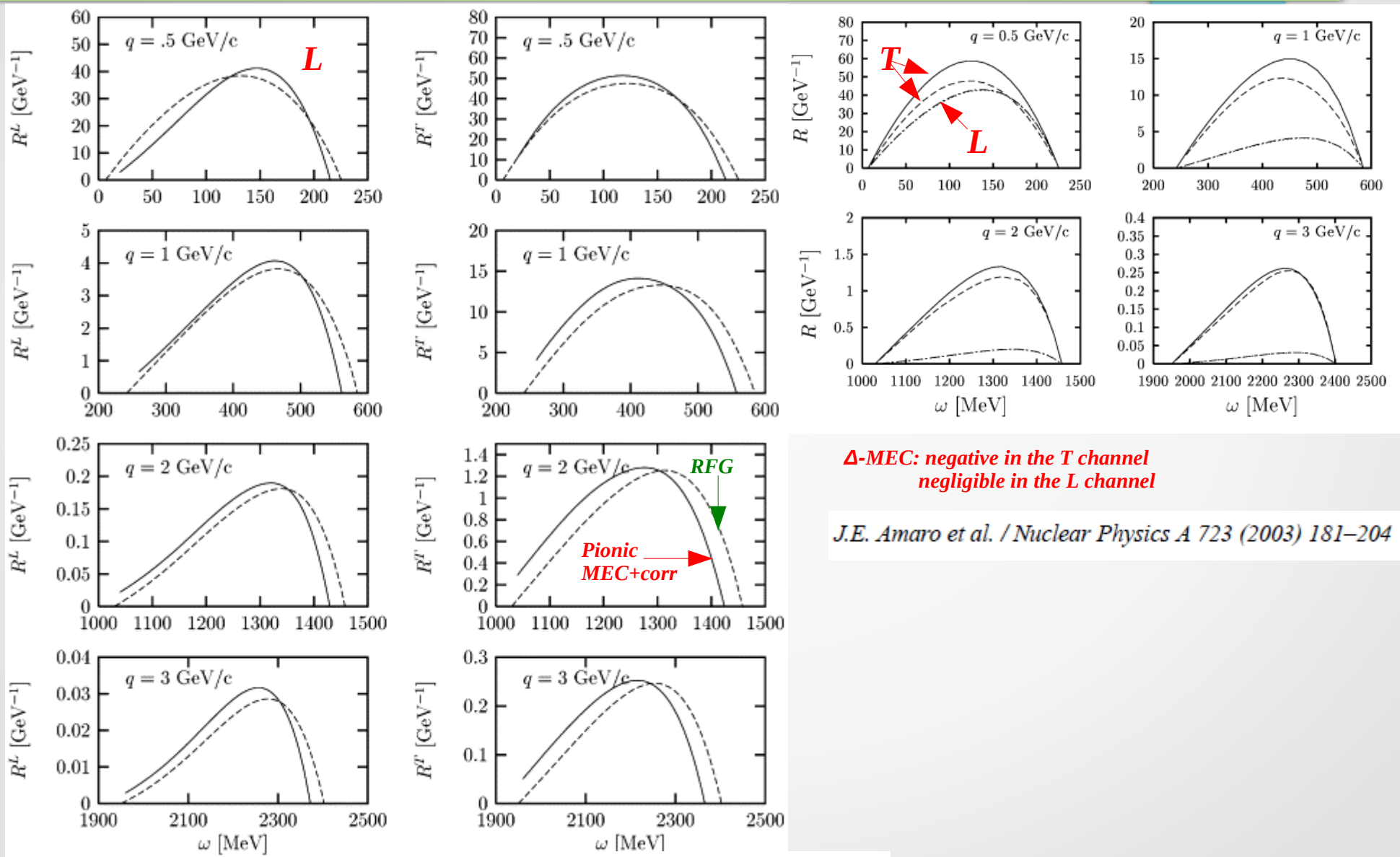

Δ-MEC: negative in the T channel
negligible in the L channel

J.E. Amaro et al. / Nuclear Physics A 723 (2003) 181–204

Purely pionic MEC+corr

J.E. Amaro et al. / Physics Reports 368 (2002) 317–407

The role of MEC in SuperScaling: 1p-1h

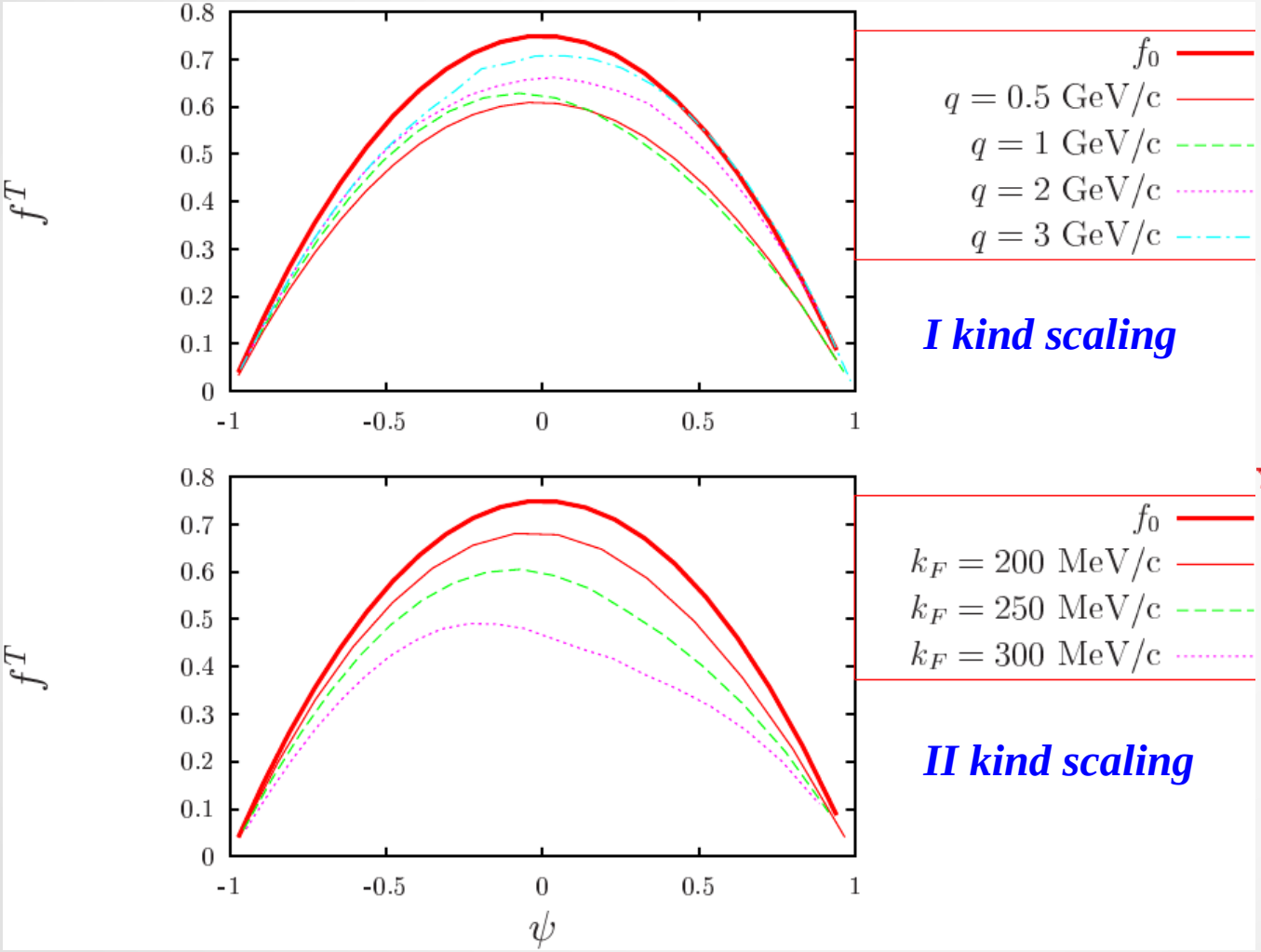

Amaro et al., NPA723, 181 (2003)

- The response is calculated on the RFG basis and is mainly transverse (small L contribution)
- The Δ-MEC give the dominant contribution
- The net contribution to the cross section is negative
- Correlation diagrams needed to preserve gauge invariance give a positive contribution which roughly compensate MEC: the net contribution is small (few %)
- Both kinds of scaling are violated

The role of MEC in Superscaling: 2p-2h $\psi'>0$

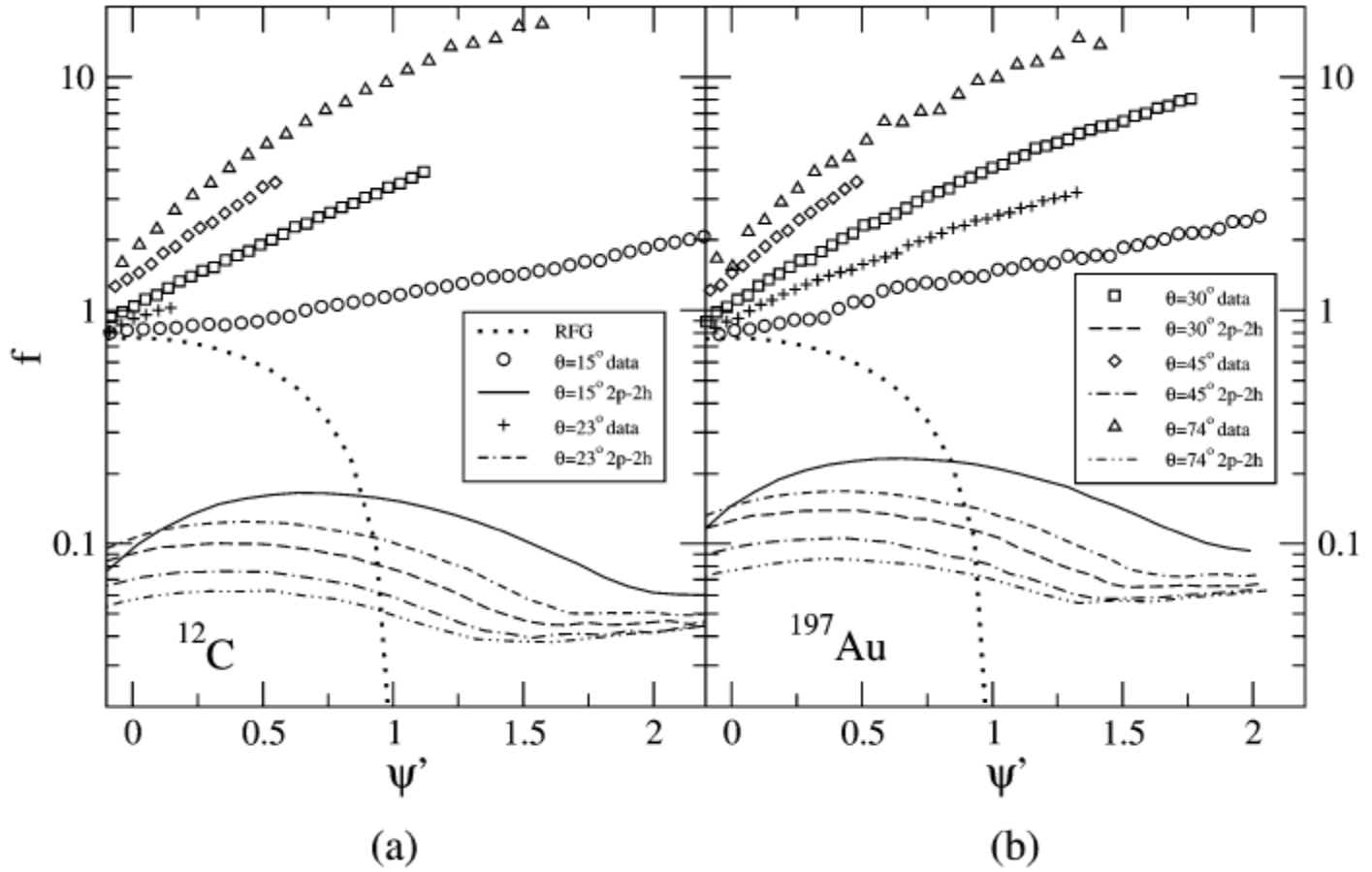

Fig. 10. As for Fig. 9, but now showing comparisons with data from JLab [39].

A. De Pace et al. / Nuclear Physics A 741 (2004) 249–269

The role of MEC in SuperScaling: 2p-2h $\psi<0$

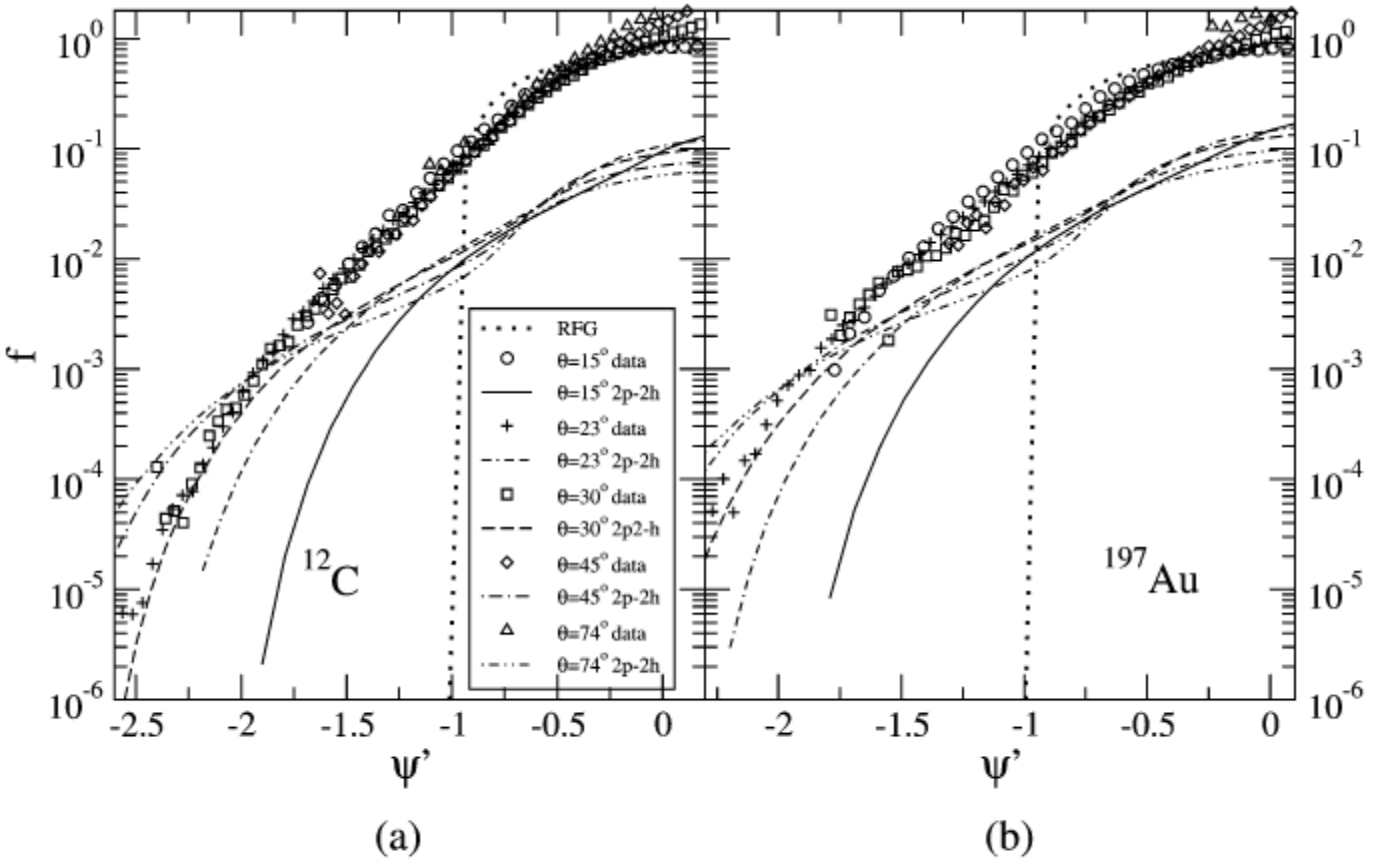

Fig. 3. The dimensionless scaling function f plotted versus the scaling variable ψ' for JLab data [39] using carbon (panel (a)) and gold (panel (b)) targets with electrons of 4045 MeV and the scattering angles given in the legend. The legend also labels the curves showing f^{MEC} computed as discussed in the text.

A. De Pace et al. / Nuclear Physics A 741 (2004) 249–269

Test of modified SuSA model (SuSA+2p2h MEC)

An example:

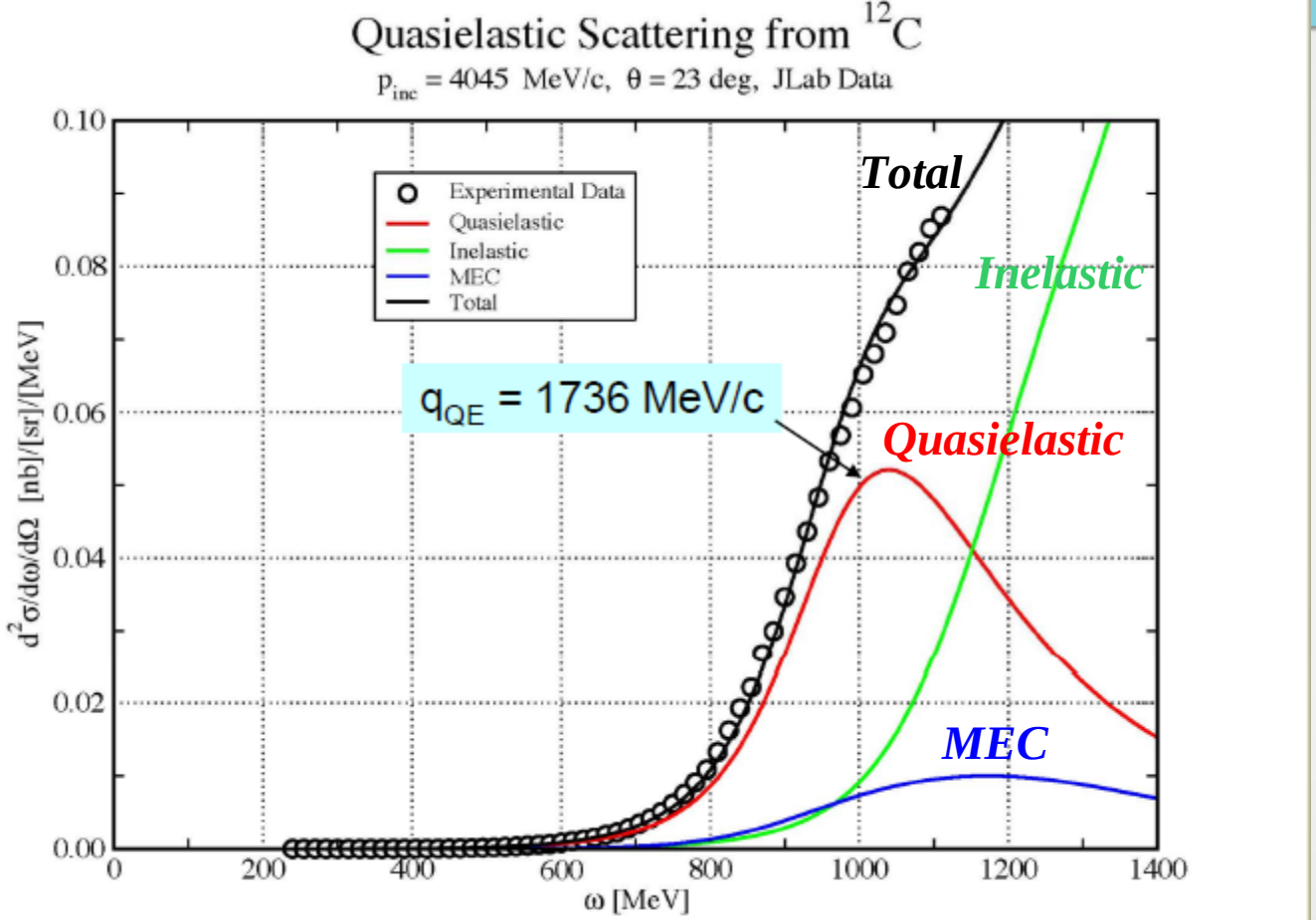

T.W. Donnelly

Relativistic effects in MEC can be mimicked

Semi-relativistic two-body currents:
non realtivistic calculations can be “relativized”
by introducing:
1) relativistic kinematics
2) kinematical factors arising from
the exact relativistic expressions

$$J^{\mu}_{\pi}(SR) = \frac{1}{\sqrt{1+\tau}} J^{\mu}_{\pi}(\mathrm{TNR})$$

$$J^{0}_{s}(SR) = \frac{1}{\sqrt{1+\tau}} J^{0}_{s}(\mathrm{TNR})$$

$$\boldsymbol{J}_{s}(SR) = \frac{1}{\sqrt{1+\tau}} \boldsymbol{J}^{(1)}_{s}(\mathrm{TNR}) + \sqrt{1+\tau}\, \boldsymbol{J}^{(2)}_{s}(\mathrm{TNR})$$

$$\boldsymbol{J}_{\Delta}(SR) = \frac{1}{\sqrt{1+\tau}} \boldsymbol{J}_{\Delta}(\mathrm{TNR})$$

J.E. Amaro et al. / Physics Reports 368 (2002) 317–407

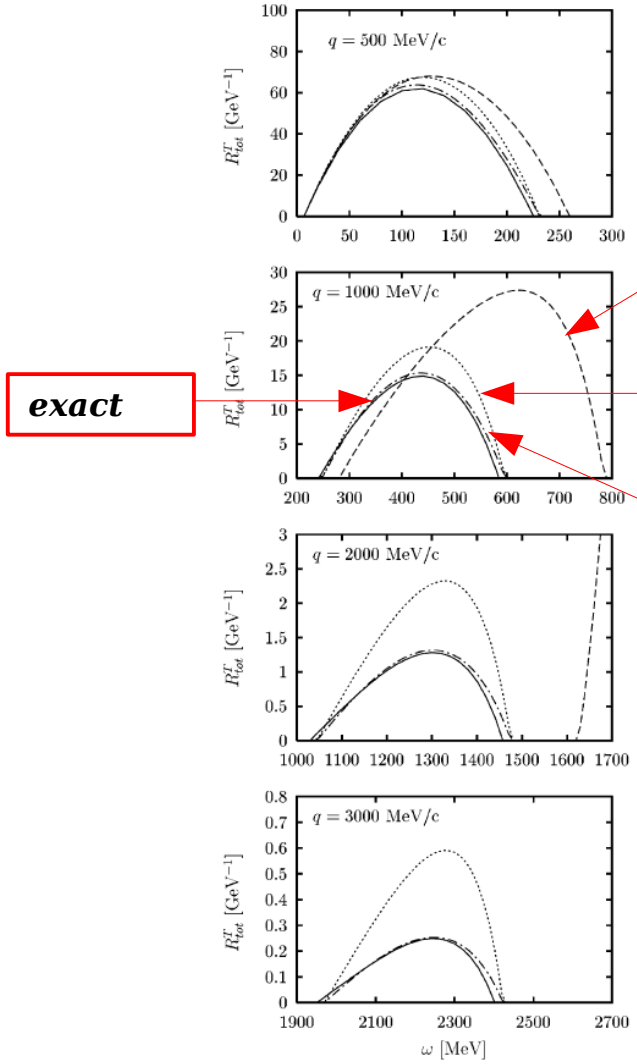

Fig. 33. Total transverse response function of ^{40}Ca including MEC for several values of the momentum transfer, and for $k_F = 237$ MeV/c. Solid: exact relativistic results. The rest of the curves have been computed using the non-relativistic Fermi gas model, with or without relativistic corrections. Dashed: traditional non-relativistic results. Dotted: including relativistic kinematics in the non-relativistic calculations. Dot–dashed: including in addition the new expansion of the OB+MEC currents. The relativistic calculations include a dynamical propagator and πN form factor, while the non-relativistic calculations do not include these corrections.

Relativistic vs non-relativistic 2p-2h MEC

direct n.r.

direct rel.

exchange n.r.

exchange rel.

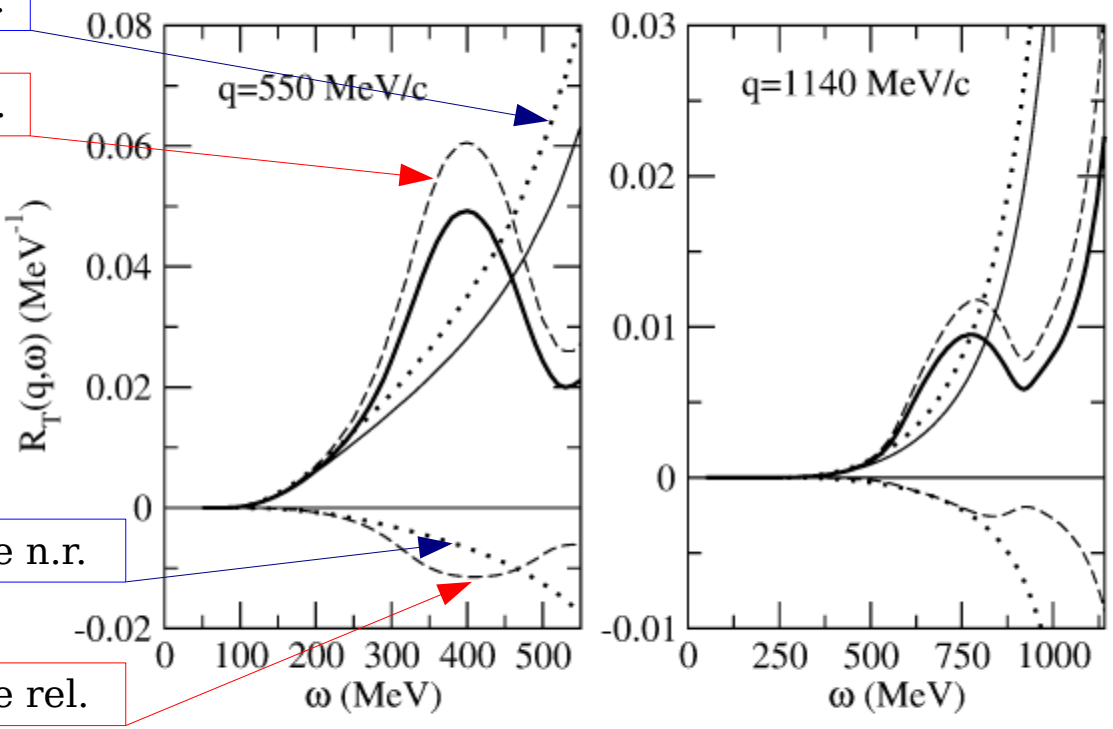

Fig. 12. The transverse response function $R_T(q,\omega)$ at $q = 550$ MeV/c and $q = 1140$ MeV/c including the exchange contributions: non-relativistic direct (positive dotted), non-relativistic exchange (negative dotted), non-relativistic total (light solid), relativistic direct (positive dashed), relativistic exchange (negative dashed) and relativistic total (heavy solid). In all instances $\bar{\epsilon}_2 = 70$ MeV and $k_F = 1.3$ fm^{-1}.

Off-shell nucleons

The usual form of the one-body nucleon EM current is

$$j^{\mu}_{(2)} = \overline{u}(\mathbf{p}) \left(F_1 \gamma^{\mu} + \frac{i}{2m} F_2 \sigma^{\mu\nu} Q_{\nu} \right) u(\mathbf{h})$$

"CC2" prescription

Gordon decomposition (valid for free spinors): the Dirac current is sum of a convection and a spin term

$$\overline{u}(\mathbf{p}) \gamma^{\mu} u(\mathbf{h}) = \overline{u}(\mathbf{p}) \left[\frac{(p+h)^{\mu}}{2m_N} + i \frac{\sigma^{\mu\nu} (p-h)_{\nu}}{2m_N} \right] u(\mathbf{h})$$

valid for free (on-shell) spinors

Equivalent currents (in the case of free spinors):

1) eliminating Q^{μ}:

$$j^{\mu}_{(1)} = \overline{u}(\mathbf{p}) \left(G_M \gamma^{\mu} - \frac{p^{\mu} + h^{\mu}}{2m_N} F_2 \right) u(\mathbf{h})$$

"CC1" prescription
($G_M = F_1 + F_2$)

2) eliminating γ^{μ}:

$$j^{\mu}_{(3)} = \overline{u}(\mathbf{p}) \left(F_1 \frac{p^{\mu} + h^{\mu}}{2m_N} + i \frac{\sigma^{\mu\nu} Q_{\nu}}{2m_N} G_M \right) u(\mathbf{h})$$

"CC3" prescription

Off-shell extrapolation and Gordon ambiguities: bound nucleons are not on-shell. This can be taken into account using the De Forest prescription (T. de Forest, NPA392, 1983) for half-off-shell nucleons:

$$E_h \to \overline{E_h} = \sqrt{\mathbf{h}^2 + m_N^2}, \quad Q^{\mu} = (\omega, \mathbf{q}) \to \overline{Q^{\mu}} = (\overline{\omega}, \mathbf{q})$$

replace the energy and momentum of the bound nucleon, but not the Q^2 at which the ff's are evaluated
⇒ the corresponding currents are no more equivalent

Gauge ambiguities

None of the above currents is conserved when nucleons are half-off-shell.
Different prescriptions are used to restore current conservation:

1. $j^3 \to \frac{\omega}{q} j^0$ Coulomb gauge

2. $j^0 \to \frac{q}{\omega} j^3$ Weyl gauge

3. $j^\mu \to \jmath^\mu - \frac{j \cdot Q}{Q^2} Q^\mu$ Landau gauge

Enforcing CC on the above currents leads to the so called “CC1”, “CC2” and “CC3” currents

For QE inclusive scattering the 3 prescriptions give similar results, but differences can arise in different observables (e.g., polarization observables)

Relativistic versus non-relativistic

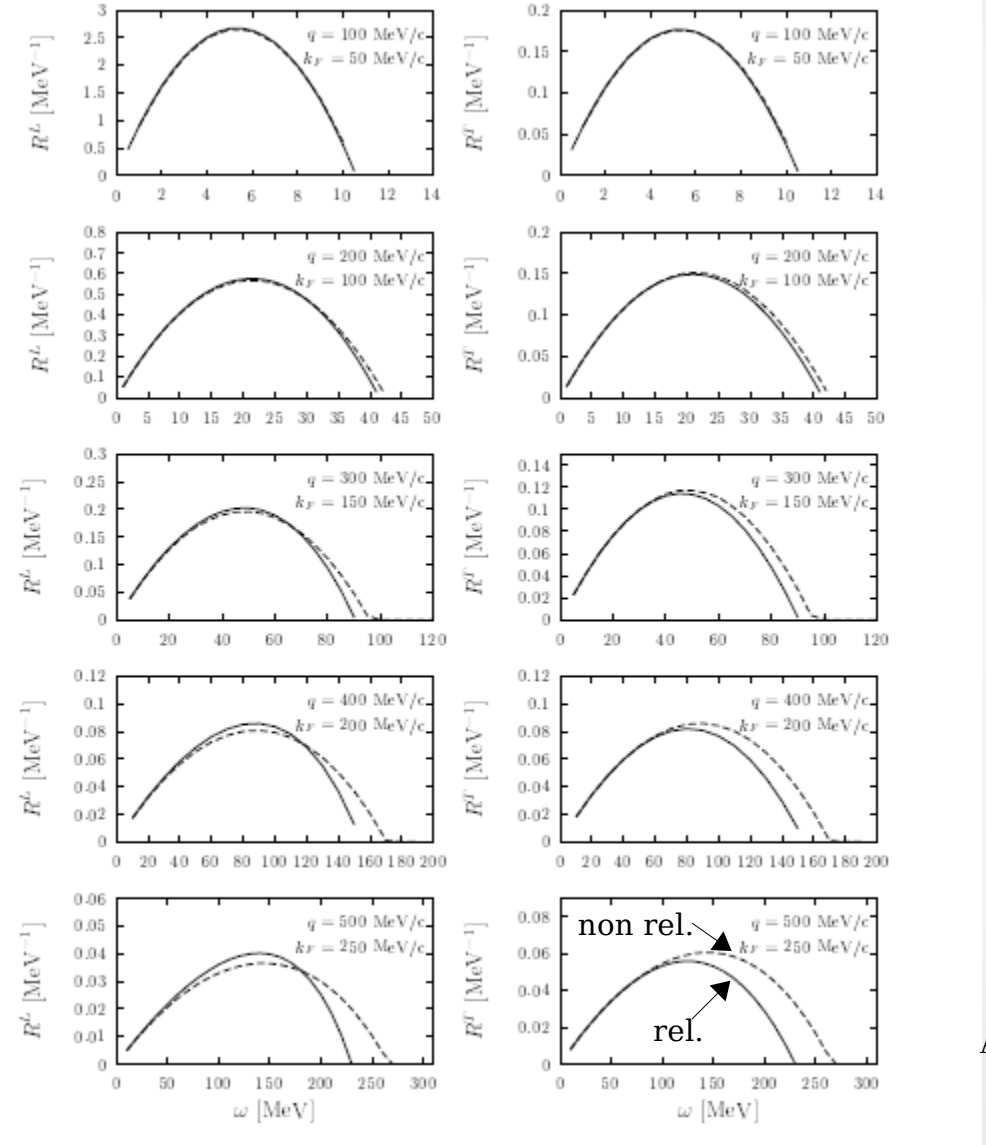

Amaro et al., Phys.Rept. 368 (2002)

Relativistic effects are important even at q~400 MeV/c

Can we mimic relativistic effects?

- Relativistic kinematics implies the replacement

$$\omega = \frac{(\mathrm{p}+\mathrm{q})^2}{2m_N} - \frac{\mathrm{p}^2}{2m_N} \Longrightarrow \omega = \sqrt{(\mathrm{p}+\mathrm{q})^2 + m_N^2} - \sqrt{\mathrm{p}^2 + m_N^2}$$

equivalent to

$$\omega \Longrightarrow \frac{\omega}{m_N}\left(\sqrt{\mathrm{p}^2 + m_N^2} + \frac{\omega}{2}\right) \simeq \omega + \frac{\omega^2}{2m_N}$$

- Relativistic operators can be accounted for by performing an expansion in the bound nucleon momentum

$$\eta = \frac{p}{m_N} \quad \text{expansion parameter} \qquad p \leq k_F \Longrightarrow \eta \leq \frac{1}{4}$$

exact in q and ω (Semi-Relativistic expansion) and therefore valid at hogh momentum transfer.

- Example: single nucleon current:

$$J^\mu(p',p) = \overline{u}(\mathrm{p}')\left(F_1\gamma^\mu + \frac{i}{2m}F_2\sigma^{\mu\nu}Q_\nu\right)u(\mathrm{p})$$

relativistic

$$J^0_{\text{non rel.}} = G_E\,, \quad \boldsymbol{J}^\perp_{\text{non rel.}} = iG_M\boldsymbol{\sigma}\times\boldsymbol{\kappa}$$

non relativistic

semi-relativistic

$$\begin{aligned} J^0(p',p) &\simeq \frac{\kappa}{\sqrt{\tau}}G_E + \frac{i}{\sqrt{1+\tau}}\left(G_M - \frac{G_E}{2}\right)(\boldsymbol{\kappa}\times\boldsymbol{\eta})\cdot\boldsymbol{\sigma} + \mathcal{O}(\eta^2) \\ \boldsymbol{J}^\perp(p',p) &\simeq \frac{\sqrt{\tau}}{\kappa}\left[iG_M\boldsymbol{\sigma}\times\boldsymbol{\kappa} + \left(G_E + \frac{\tau G_E}{2}\right)\boldsymbol{\eta}^\perp\right. \\ &\quad \left. -\frac{iG_M}{1+\tau}\left(\boldsymbol{\sigma}\times\boldsymbol{\kappa}\boldsymbol{\kappa}\cdot\boldsymbol{\eta} + \frac{1}{2}\boldsymbol{\sigma}\cdot\boldsymbol{\kappa}\boldsymbol{\kappa}\times\boldsymbol{\eta}\right)\right] + \mathcal{O}(\eta^2) \end{aligned}$$

The semi-relativistic approximation

$$\tau = \kappa^2 - \lambda^2 \Longrightarrow \frac{\kappa^2}{\tau} > 1$$

→ enhancement of R_L
reduction of R_T

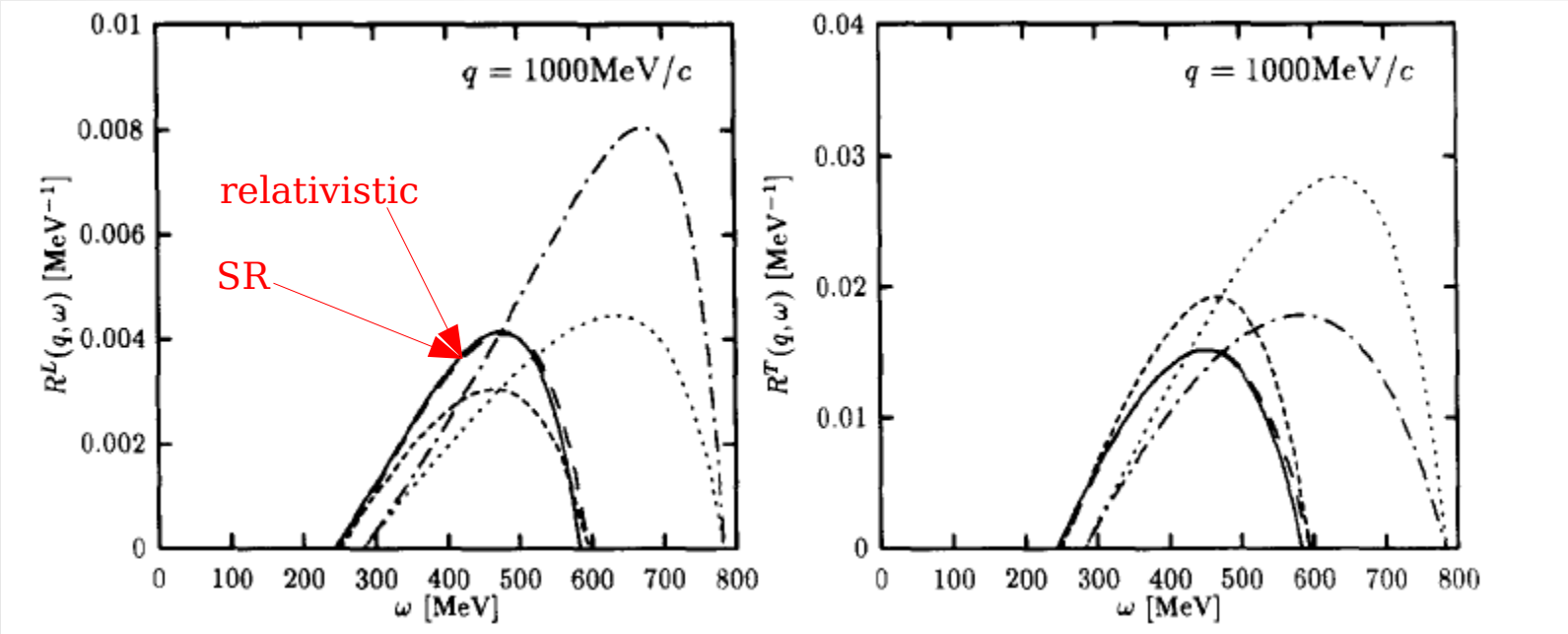

J.E. Amaro, J.A. Caballero, T.W. Donnelly, A.M. Lallena, E. Moya de Guerra, J.M. Udías, NPA602 (1996) 263

The Coulomb Sum Rule

The CSR states that the integral of the QE longitudinal response of a nucleus should be equal, at high q, to the total number of protons:

$$S_L(q)=\frac{1}{Z}\int_{0+}^{\infty}\frac{R_L(q,\omega)}{G_L^2(q,\omega)}\,d\omega$$

$$G_L^2(q,\omega)=\frac{1+\tau}{1+2\tau}\left[G_{Ep}^2(\tau)+\frac{N}{Z}G_{En}^2(\tau)\right]$$

$$\rightarrow \quad \lim_{q\to\infty} S_L(q)=1$$

Model-independent theorem: the CSR measures a property of the nuclear ground state, independent of the final state. It is a consequence of unitarity (summation over a complete set of intermediate states).

Controversy between Saclay and Bates data:
- Saclay data showed a quenching of R_L of ~40% on ^{12}C, ^{40}Ca, ^{48}Ca, ^{56}Fe, inconsistent with $S_L(q)=1$
- Bates data showed no quenching
- Re-analysis of world data accounting for Coulomb corrections and relativistic effects (Jourdan,NPA603,1996): no quenching
- New experiment al Jlab ($0.55<q<1$ GeV/c), no published data yet.

H. Yao, PANIC 2011

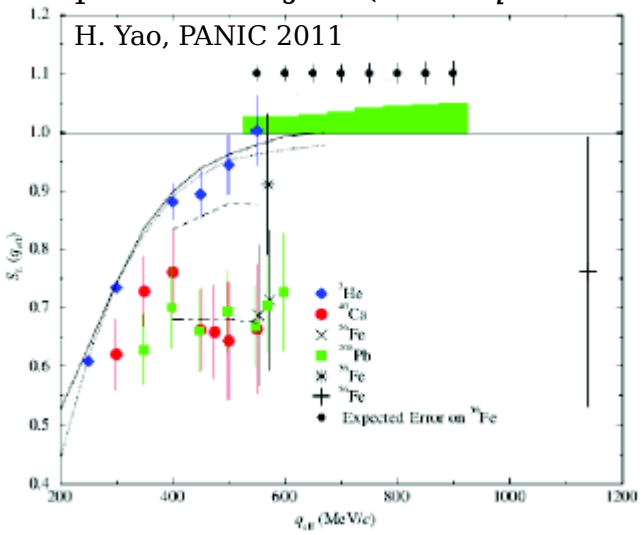

H. Yao, PANIC 2011

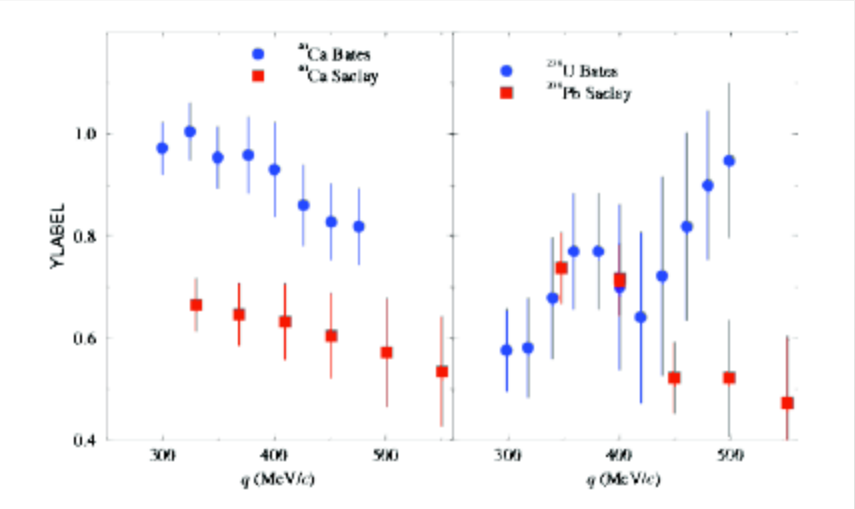

Some references on the general framework

- "**Relativistic Quantum Mechanics**",
  J.D. Bjorken and S.D, Drell,
  McGraw-Hill, NY (1964)

- "**Quantum Electrodynamics**",
  W. Greiner and J. Reinhardt,
  Springer-Verlag (1994)

- "**Electron Scattering from Nuclear and Nucleon Structure**",
  J.D. Walecka,
  Cambridge University Press (2001)

- "**Electromagnetic Response of Atomic Nuclei**",
  S. Boffi, C. Giusti, F. Pacati, M. Radici,
  Clarendon Press, Oxford (1996); Phys. Rep. 226, (1993)

- "**The Atomic Nucleus observed with Electromagnetic Probes**",
  T.W. Donnelly,
  An Advanced Course in Modern Nuclear Physics – Lecture Notes in Physics, Springer-Verlag (2001)

Some references on superscaling and relativistic MEC

- *Scaling and super-scaling*
  - *G.B. West, Phys.Rept. 18 (1975)*
  - *W.M. Alberico, A. Molinari, T.W. Donnelly, E.L. Kronenberg, J.W. Van Orden, Phys.Rev. C38 (1988)*
  - *D.B. Day, J.S. McCarthy, T.W. Donnelly, I. Sick, Ann.Rev.Nucl.Part.Sci. 40 (1990)*
  - *T.W. Donnelly, I. Sick, Phys.Rev.Lett. 82 (1999), Phys.Rev. C60 (1999)*
  - *C. Maieron, T.W. Donnelly, Ingo Sick (Basel U.), Phys.Rev. C65 (2002)*
  - *C. Maieron, J.E. Amaro, MBB, T.W. Donnelly, J.A.Caballero, C.F.Williamson, Phys.Rev. C80 (2009)*
- Relativistic MEC
  - J.W. Van Orden, T.W. Donnelly, Ann. Phys. 131 (1980)
  - W.M. Alberico, T.W. Donnelly, A. Molinari, Nucl.Phys. A512 (1990)
  - M.J. Dekker, P.J. Brussaard, J.A. Tjon, Phys.Lett. B289 (1992); Phys.Rev. C49 (1994)
  - J.E. Amaro, MBB, J.A. Caballero, T.W. Donnelly, A. Molinari, Nucl.Phys. A697(2002); Phys.Rep. 368(2002); Nucl.Phys. A723(2003)
  - A. De Pace, M. Nardi, W.M. Alberico, T.W. Donnelly, A. Molinari, Nucl.Phys. A726(2003); Nucl.Phys. A741(2004)

Scuola di Fisica Nucleare Raimondo Anni

3. Quasielastic neutrino scattering

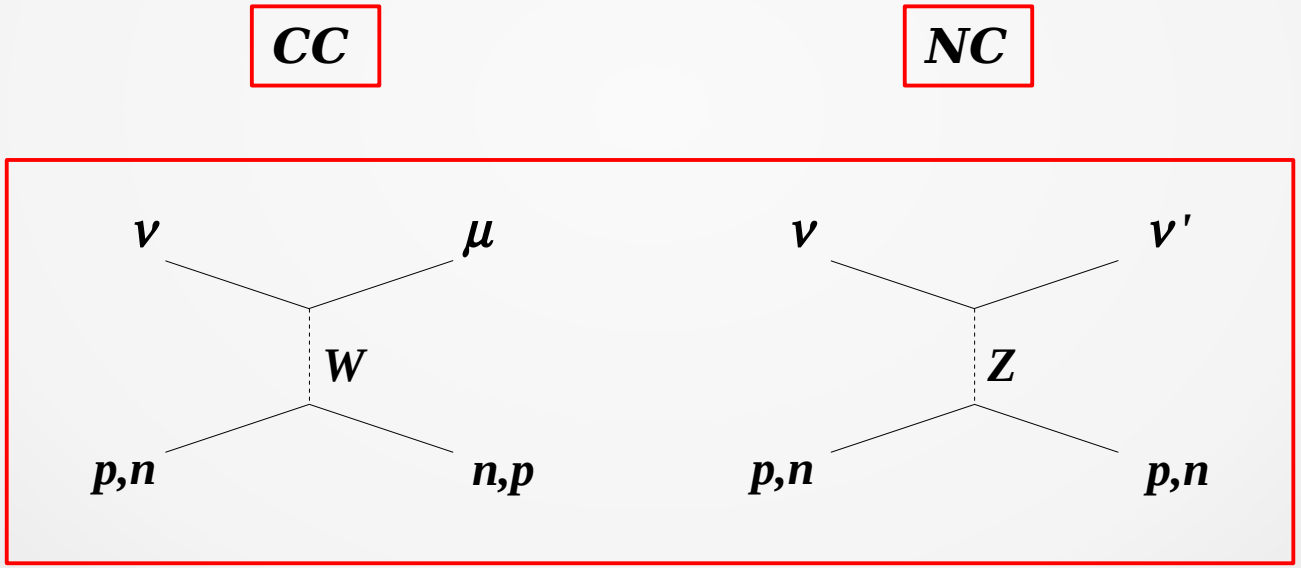

Neutrino Experiments

- Enormous experimental effort to study neutrino properties:
  great amount of neutrino detectors, experiments and facilities, both operating and under construction.

- Main goal: study neutrino properties (precision measurements of oscillation parameters, θ_{13} and CP violation, mass hierarchy, sterile neutrinos...).

- 2 strategies:

  1) disappearance expt's: a known number of ν's of a certain type is produced and the number of the same type ν's is detected at a distance L
  2) appearance expt's: ν's of a certain type are produced and ν's of a different type are detected

- Many experiments use complex nuclei as targets: detailed studies of the nuclear dynamics are needed in order to interpret the data.

- New information on nuclear and nucleonic structure, complementary to electron scattering, can be extracted from neutrino experiments.

- FermiLab, Illinois: MiniBooNE, SciBooNE, MicroBooNE, MINERνA, NoνA, MINOS, ArgoNeuT;
  $\nu_\mu, \nu_e, \nu_\mu, \nu_e$;
  Targets: C, O, Fe, Pb, Ar, He; ν+nucleus $\rightarrow$ l+X, Neutrino energy ~ 1 GeV (~0.5 – 10 GeV)

- J-Parc, Japan: T2K, K2K; Targets: C_8H_8, ^{16}O; E_ν ~ 1 GeV

- Previous expt's: LSND (Los Alamos, 1993-98, E_ν ~ 200 MeV); NOMAD (CERN, C, 90's, E_ν ~ 3 – 100 GeV)

Quasielastic Neutrino Scattering

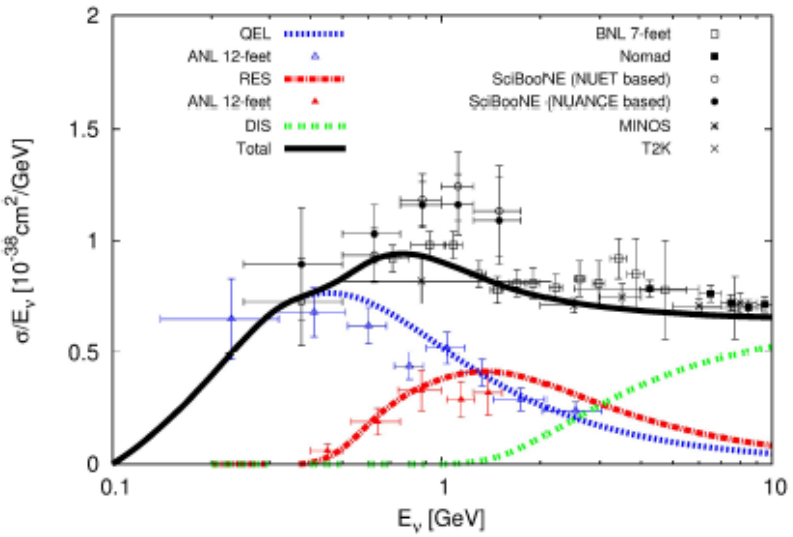

Figure 1: Breakdown of the inclusive CC muon neutrino cross section on free isoscalar target to QE, RES and DIS contributions, as viewed by NuWro MC event generator.

J.Morfin, J.Nieves, J.Sobczyk, Adv.High Energy Phys. 2012 (2012)

QE scattering dominates at neutrino energies below ~ 1 GeV

Neutrino and Antineutrino Data

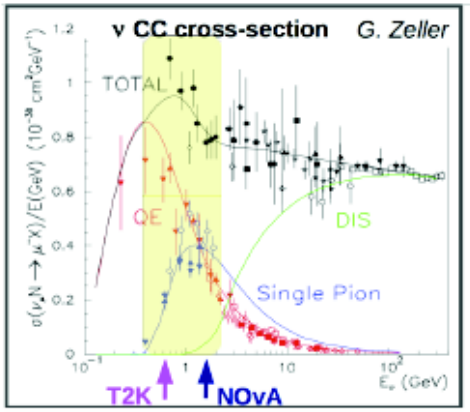

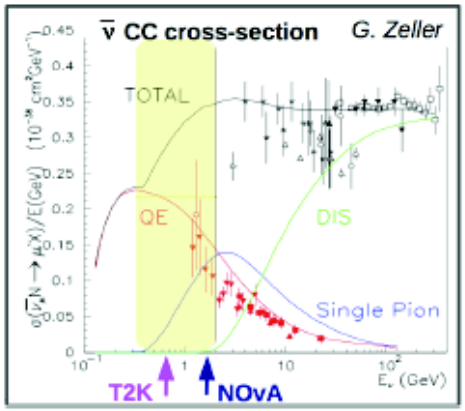

MiniBooNE

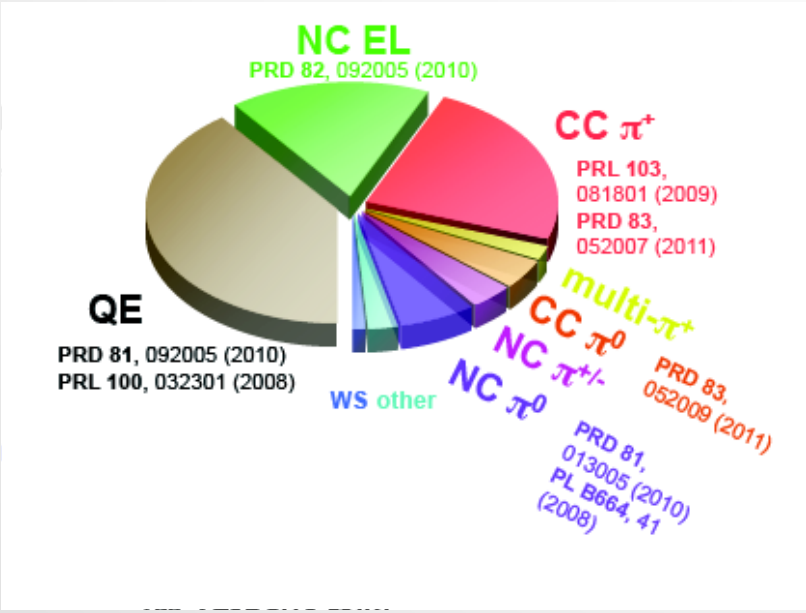

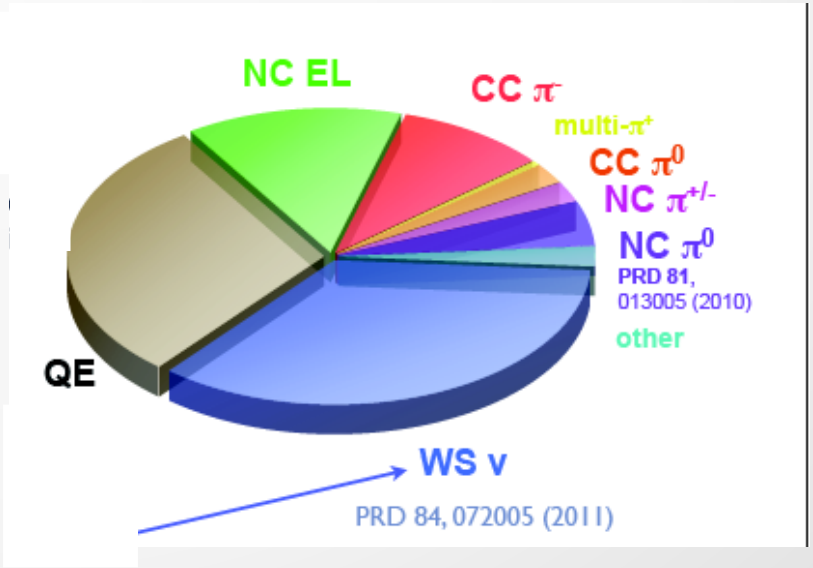

Connection with electron scattering (SuSA)

- Many high quality data are available for quasi-elastic electron scattering
- Although not sufficient, it is necessary that nuclear models to be used in neutrino scattering analyses reproduce these data
- The SuSA approach makes use of (e,e') data to predict CC and NC ν-scattering cross sections in the QE region exploiting **SuperScaling**:

  1) extract the super-scaling function from QE (e,e') data → $f(\psi) \sim R^{em}/G^{em}_{s.n.}$

  2) plug it into neutrino cross sections → $R^{weak} \sim G^{weak}_{s.n.} * f(\psi)$

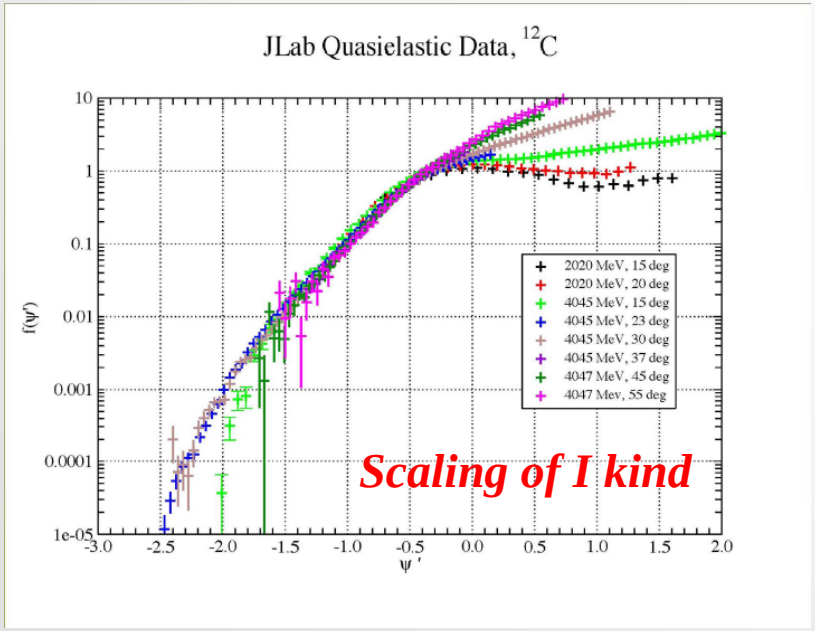

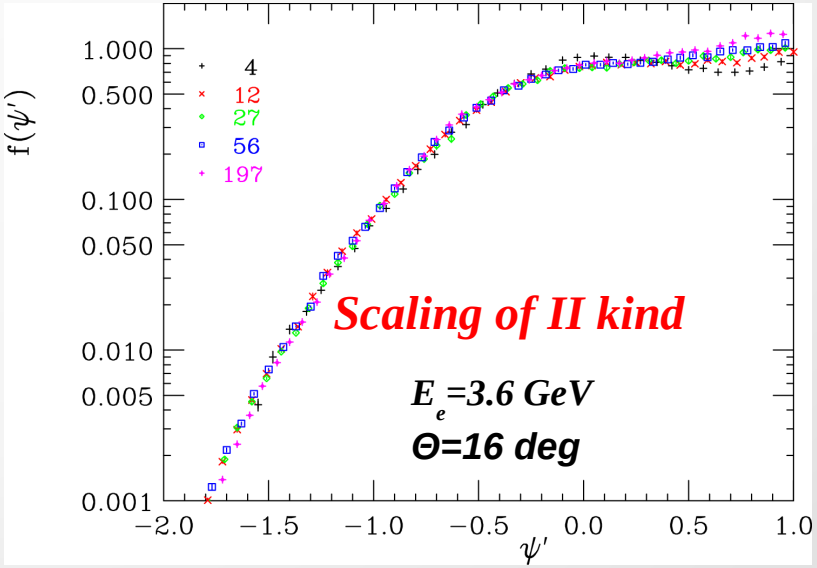

[Day,McCarthy,Donnelly,Sick,Ann.Rev.Nucl.Part.Sci.40(1990); Donnelly & Sick, PRC60(1999),PRL82(1999)]

Charged Current Neutrino Scattering

Cross section:

$$\left[\frac{d^2\sigma}{d\Omega dk'}\right]_\chi \equiv \sigma_0 \mathcal{F}_\chi^2,$$

$$\sigma_0 \equiv \frac{(G\cos\theta_c)^2}{2\pi^2}[k'\cos\tilde{\theta}/2]^2,$$

finite lepton mass
(ERL not valid!)

$$\tan^2\tilde{\theta}/2 \equiv \frac{|Q^2|}{v_0},$$

$$v_0 \equiv (\epsilon+\epsilon')^2 - q^2 = 4\epsilon\epsilon' - |Q^2|.$$

$$\mathcal{F}_\chi^2 = [\hat{V}_{CC}R_{CC} + 2\hat{V}_{CL}R_{CL} + \hat{V}_{LL}R_{LL} + \hat{V}_T R_T] + \chi[2\hat{V}_{T'}R_{T'}],$$

Rosenbluth-like decomposition: 5 response functions

$$\begin{aligned} R_{CC} &= R_{CC}^{VV} + R_{CC}^{AA}, \\ R_{CL} &= R_{CL}^{VV} + R_{CL}^{AA}, \\ R_{LL} &= R_{LL}^{VV} + R_{LL}^{AA}, \\ R_T &= R_T^{VV} + R_T^{AA}, \\ R_{T'} &= R_{T'}^{VA}. \end{aligned}$$

CC charge-charge
CL charge-longitudinal
LL longitudinal-longitudinal
T trasverse
T' transverse axial-vector

Each response has
VV (vector-vector), AA (axial-axial), VA (vector-axial)
components arising from the V and A
weak nuclear currents:

$$j_V^\mu = \bar{u}(P')\left[F_1\gamma^\mu + \frac{i}{2m_N}F_2\sigma^{\mu\nu}Q_\nu\right]u(P),$$

$$j_A^\mu = \bar{u}(P')\left[G_A\gamma^\mu + \frac{1}{2m_N}G_P Q^\mu\right]\gamma^5 u(P),$$

Leptonic vertex

Leptonic kinematical factors

$$\widehat{V}_{CC} = 1 - \tan^2\widetilde{\theta}/2 \cdot \delta^2,$$
$$\widehat{V}_{CL} = \nu + \frac{1}{\rho'}\tan^2\widetilde{\theta}/2 \cdot \delta^2,$$
$$\widehat{V}_{LL} = \nu^2 + \tan^2\widetilde{\theta}/2\left(1 + \frac{2\nu}{\rho'} + \rho \cdot \delta^2\right) \cdot \delta^2,$$
$$\widehat{V}_T = \left[\frac{1}{2}\rho + \tan^2\widetilde{\theta}/2\right] - \frac{1}{\rho'}\tan^2\widetilde{\theta}/2 \times \left(\nu + \frac{1}{2}\rho\rho' \cdot \delta^2\right) \cdot \delta^2,$$
$$\widehat{V}_{T'} = \left[\frac{1}{\rho'}\tan^2\widetilde{\theta}/2\right](1 - \nu\rho' \cdot \delta^2).$$
$$\widehat{V}_L \equiv \widehat{V}_{CC} - 2\nu\widehat{V}_{CL} + \nu^2\widehat{V}_{LL}.$$

$$\delta \equiv \frac{m'}{\sqrt{|Q^2|}}.$$

$$\nu \equiv \frac{\omega}{q} = \frac{\lambda}{\kappa},$$
$$\rho \equiv \frac{|Q^2|}{q^2} = \frac{\tau}{\kappa^2} = 1 - \nu^2,$$
$$\rho' \equiv \frac{q}{\epsilon + \epsilon'},$$

In the ERL (e,e')

$$\widehat{V}_{CC} \to v_{CC} = 1,$$
$$\widehat{V}_{CL} \to v_{CL} = \nu,$$
$$\widehat{V}_{LL} \to v_{LL} = \nu^2,$$
$$\widehat{V}_L \to v_L = \rho^2,$$
$$\widehat{V}_T \to v_T = \tfrac{1}{2}\rho + \tan^2\theta/2,$$
$$\widehat{V}_{T'} \to v_{T'} = \tan\theta/2\sqrt{\rho + \tan^2\theta/2},$$

Coulomb corrections (EMA)

$$\mathbf{k}'_\infty = D(k')\mathbf{k}',$$
$$\epsilon'_\infty = \sqrt{m'^2 + k'^2},$$
$$D(k') = 1 - \chi\frac{3Z\alpha}{2Rk'},$$

Hadronic vertex

The nuclear vector current is conserved:

$$R_{CL}^{VV} = -\nu R_{CC}^{VV},$$
$$R_{LL}^{VV} = \nu^2 R_{CC}^{VV}.$$

$$\widehat{V}_{CC} R_{CC}^{VV} + 2\widehat{V}_{CL} R_{CL}^{VV} + \widehat{V}_{LL} R_{LL}^{VV} = \widehat{V}_L R_L^{VV} \equiv X_L^{VV}$$

The nuclear axial current is not conserved:

$$\widehat{V}_{CC} R_{CC}^{AA} + 2\widehat{V}_{CL} R_{CL}^{AA} + \widehat{V}_{LL} R_{LL}^{AA} \equiv X_{C/L}^{AA}$$

Defining:

$$\widehat{V}_T \left[R_T^{VV} + R_T^{AA}\right] \equiv X_T,$$
$$2\widehat{V}_{T'} R_{T'}^{VA} \equiv X_{T'}.$$

we finally get

$$\mathcal{F}_\chi^2 = X_L^{VV} + X_{C/L}^{AA} + X_T + \chi X_{T'}.$$

general expression, valid in any kinematic region

The single-nucleon responses in the QE region:

$$j_V^\mu = \bar{u}(P')\left[F_1\gamma^\mu + \frac{i}{2m_N}F_2\sigma^{\mu\nu}Q_\nu\right]u(P),$$
$$j_A^\mu = \bar{u}(P')\left[G_A\gamma^\mu + \frac{1}{2m_N}G_P Q^\mu\right]\gamma^5 u(P),$$

$$G_A'^{(1)}(\tau) = G_A^{(1)}(\tau) - \tau G_P^{(1)}(\tau),$$

$$R_L^{VV} = \frac{1}{\rho}\left[G_E^{(1)}\right]^2$$
$$R_T^{VV} = 2\tau\left[G_M^{(1)}\right]^2,$$

$$R_{T'}^{VA} = 2\sqrt{\tau(1+\tau)}\,G_M^{(1)}G_A^{(1)}.$$

$$R_{CC}^{AA} = \frac{\nu^2}{\rho}\left[G_A'^{(1)}\right]^2,$$
$$R_{CL}^{AA} = -\frac{\nu}{\rho}\left[G_A'^{(1)}\right]^2,$$
$$R_{LL}^{AA} = \frac{1}{\rho}\left[G_A'^{(1)}\right]^2,$$
$$R_T^{AA} = 2(1+\tau)\left[G_A^{(1)}\right]^2,$$

Response Functions in *(e,e')* and CC *(ν,l)*

(e,e')

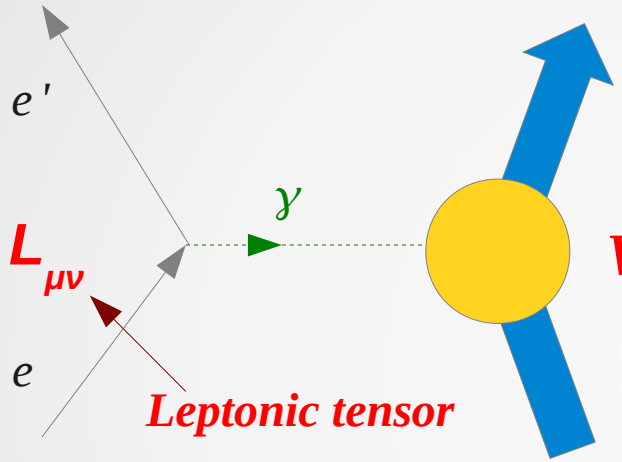

$$\frac{d^2\sigma}{d\epsilon' d\Omega'} = \sigma_{Mott}\left(v_L R_L + v_T R_T\right)$$

2 electromagnetic response functions

CC

(ν,l)

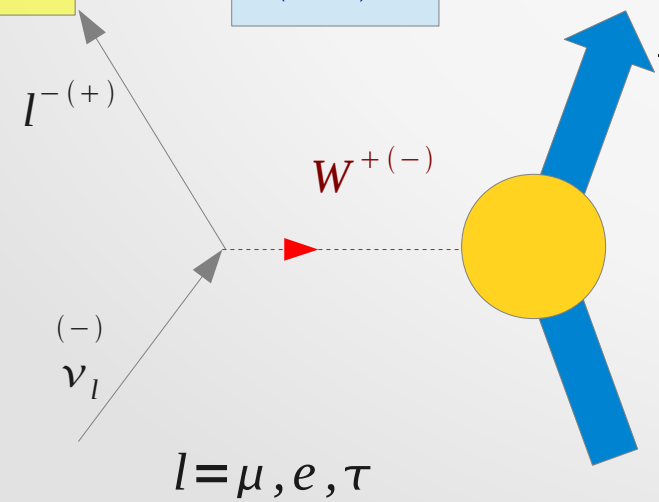

$$\frac{d^2\sigma}{d\epsilon' d\Omega'} = \sigma_0\left(\boxed{V_{CC}R_{CC} + 2V_{CL}R_{CL} + V_{LL}R_{LL}} + V_T R_T \pm 2V_{T'}R_{T'}\right)$$

$$\downarrow$$

$$V_L R_L$$

5 (3) weak response functions

Purely isovector

Typically transverse (CC,CL,LL small)

Have VV, AA and VA components generated by

$J_\mu = J_\mu^V + J_\mu^A$

+ ν

– ν

CCQE L-T-T' separation

MiniBooNE kinematics

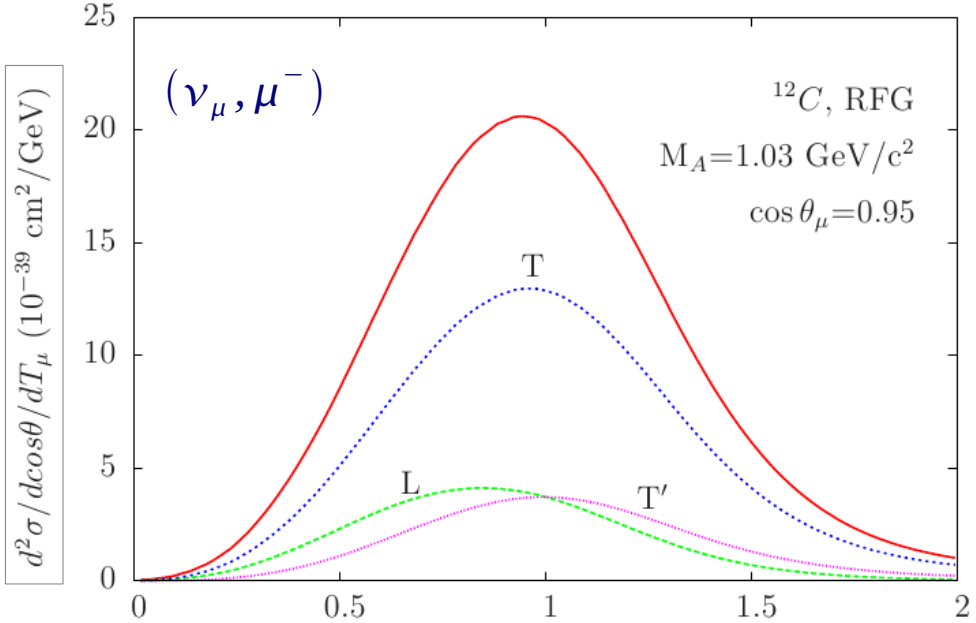

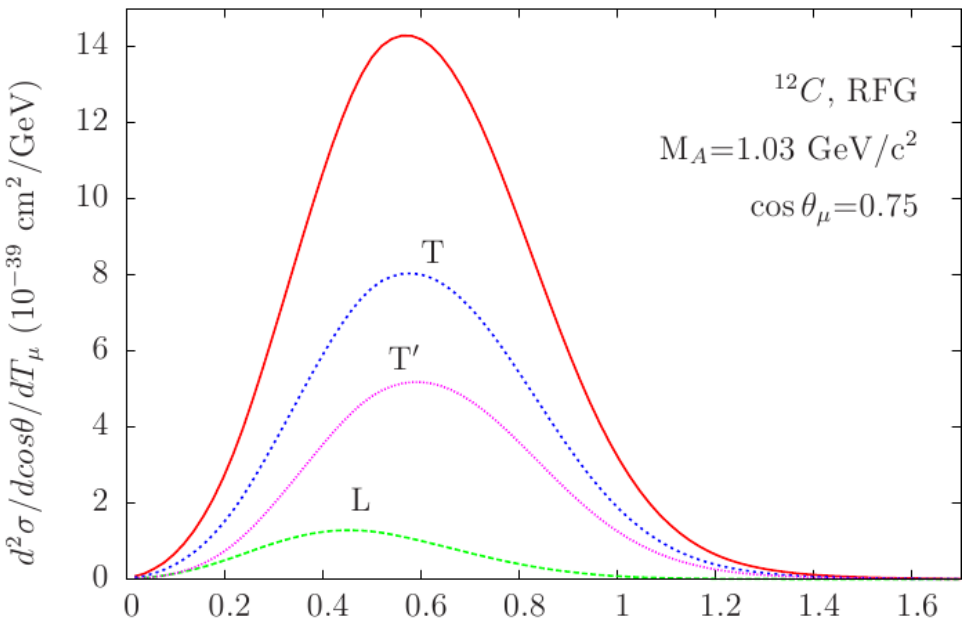

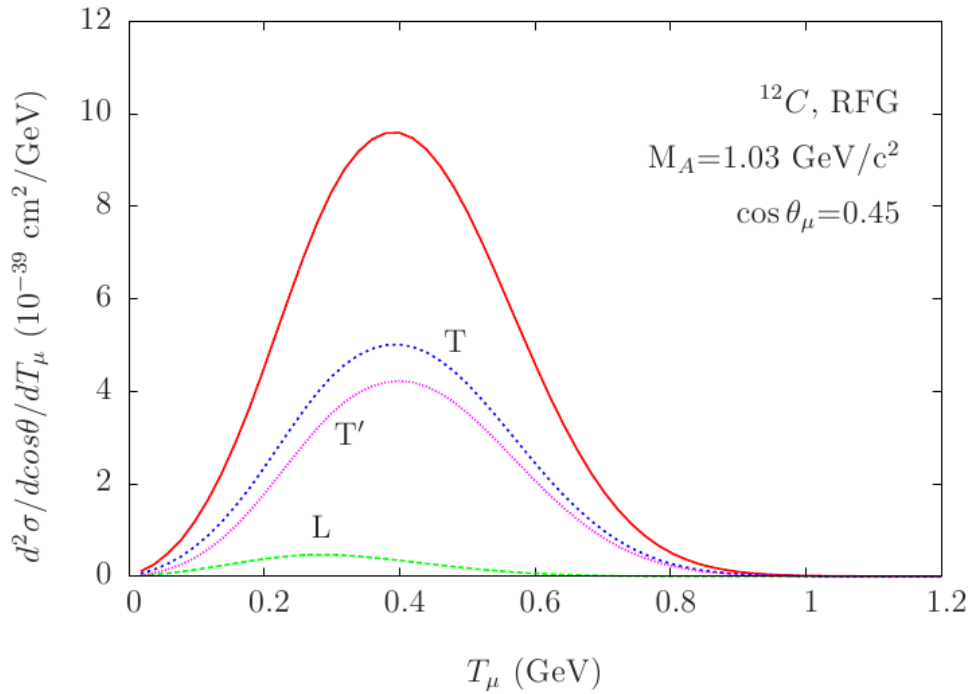

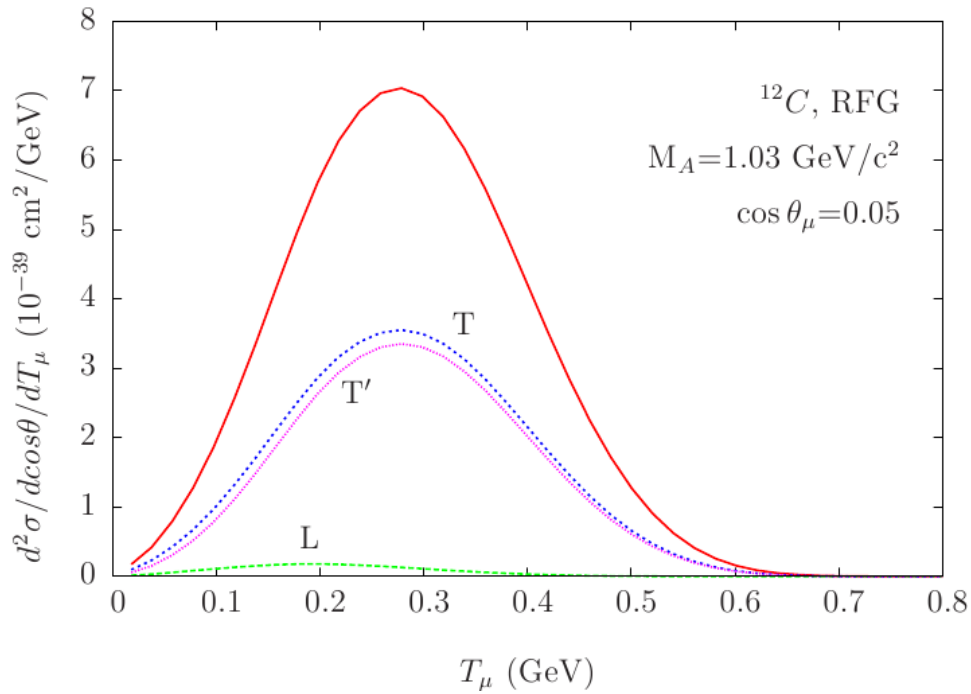

CCQE VV-AA-VA separation

MiniBooNE kinematics

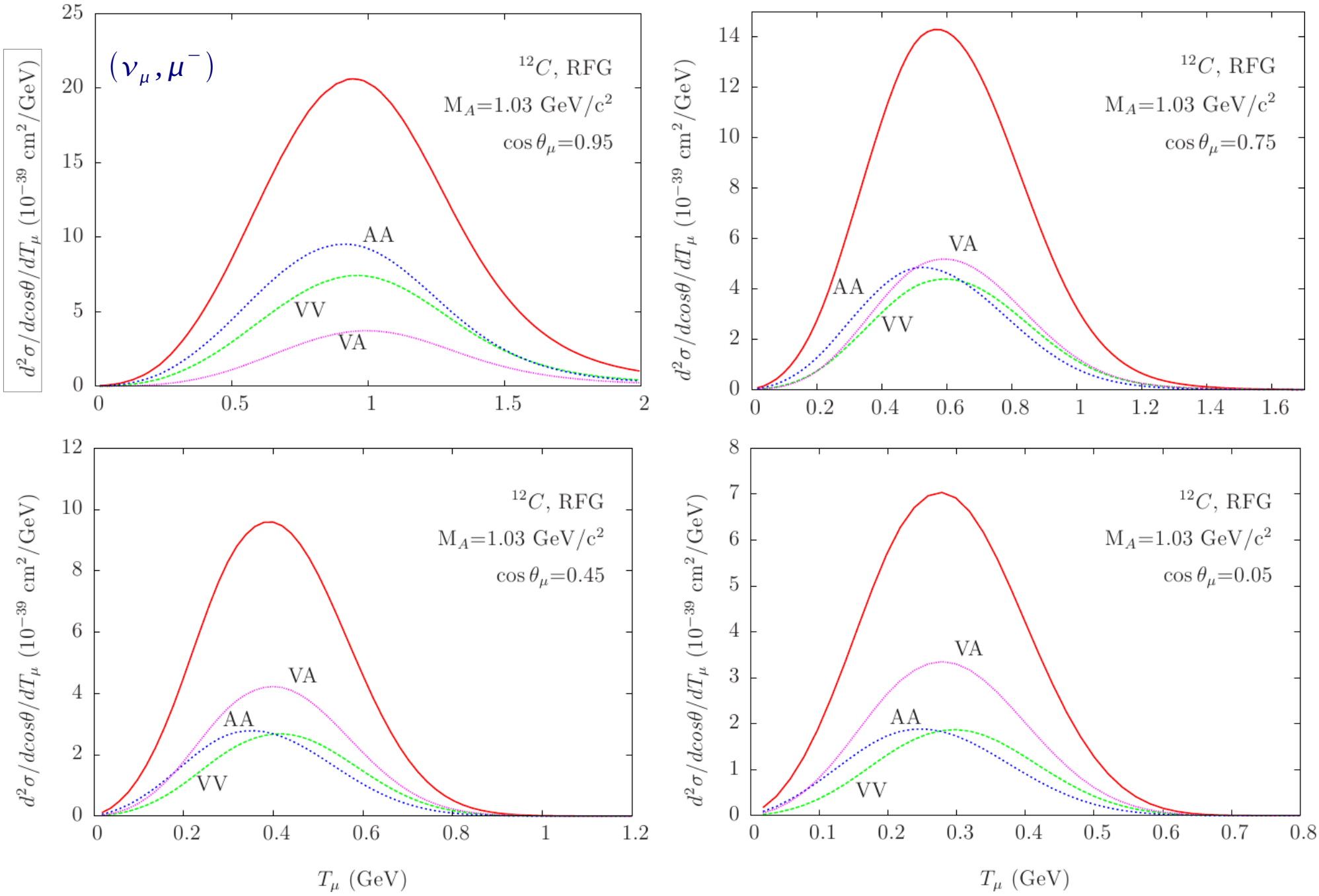

L-T-T' separation in the total CCQE cross section

Total cross section (integrated over all allowed muon kinemtics)

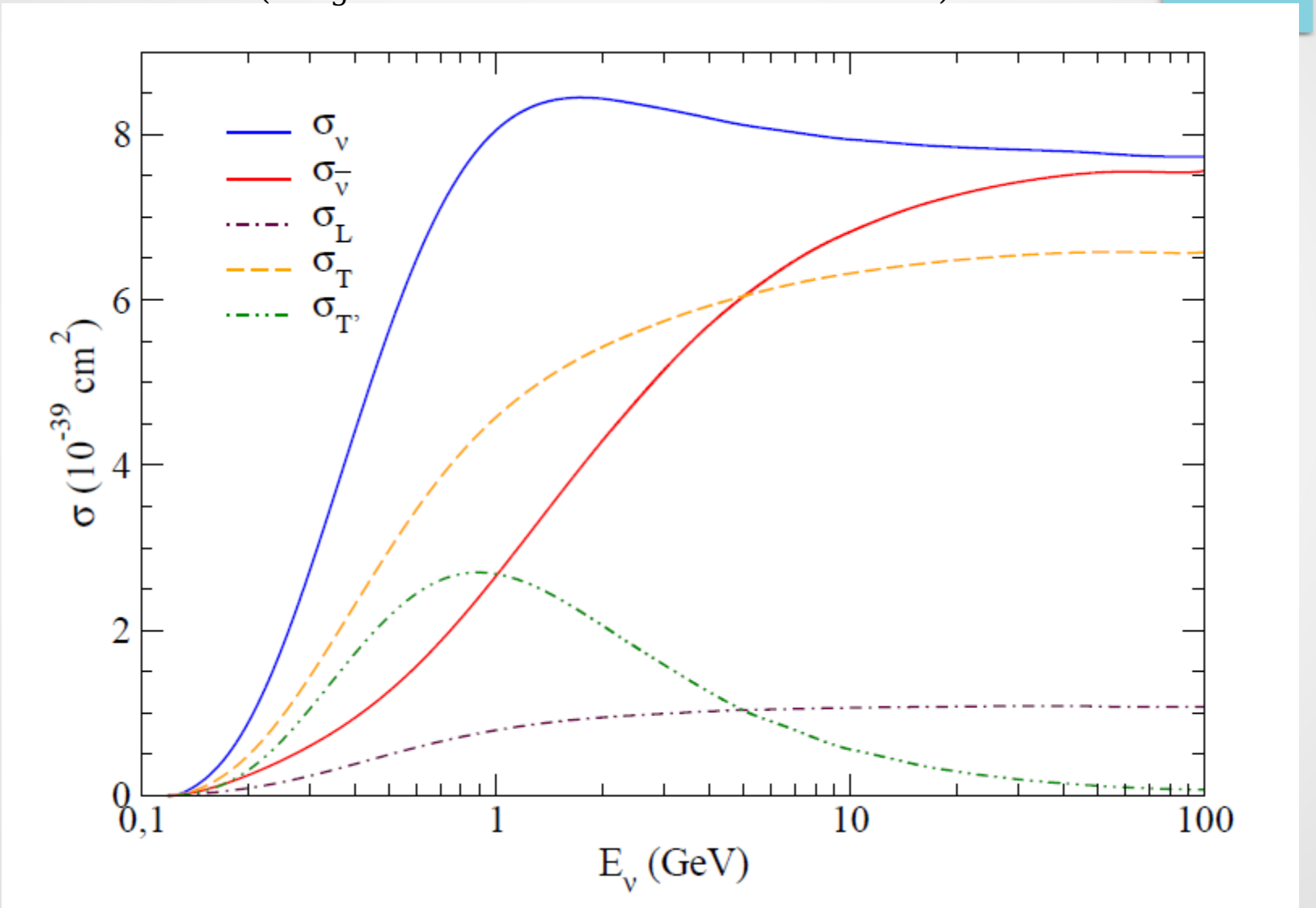

CC neutrino scattering in the Δ region

Elementary reactions:

$$\nu_\mu p \to \mu^- \Delta^{++},$$
$$\nu_\mu n \to \mu^- \Delta^{+},$$
$$\bar{\nu}_\mu p \to \mu^+ \Delta^{0},$$
$$\bar{\nu}_\mu n \to \mu^+ \Delta^{-}.$$

Current:

$$J^\mu(q) = \mathcal{T}\bar{u}^{(\Delta)}_\alpha(p', s')\Gamma^{\alpha\mu}u(p, s),$$

$$\Gamma^{\alpha\mu} = \left[\frac{C_3^V}{m_N}(g^{\alpha\mu}\not{q} - q^\alpha\gamma^\mu) + \frac{C_4^V}{m_N^2}(g^{\alpha\mu}q\cdot p' - q^\alpha p'^\mu) + \frac{C_5^V}{m_N^2}(g^{\alpha\mu}q\cdot p - q^\alpha p^\mu)\right]\gamma_5 + \left[\frac{C_3^A}{m_N}(g^{\alpha\mu}\not{q} - q^\alpha\gamma^\mu + \frac{C_4^A}{m_N^2}(g^{\alpha\mu}q\cdot p' - q^\alpha p'^\mu) + C_5^A g^{\alpha\mu} + \frac{C_6^A}{m_N^2}q^\alpha q^\mu\right].$$

CVC

$C_6^V = 0$

PCAC

$C_6^A = C_5^A(\mu_\pi^2 + 4\tau)^{-1}$

5 form factors

Hadronic tensor:

$$w^{\mu\nu} = \mathcal{T}^2\mu_\Delta \mathrm{Tr}\{P_{\beta\alpha}(p')(\gamma_0\Gamma^{\dagger\alpha\mu}\gamma_0)\Lambda(p)\Gamma^{\beta\nu}\},$$

Rarita-Schwinger projector

$$w^{\mu\nu} = w^{\mu\nu}_{VV} + w^{\mu\nu}_{AA} + w^{\mu\nu}_{VA}$$

$$w^{\mu\nu}_{VV} = -w_{1V}\left(g^{\mu\nu} + \frac{\kappa^\mu\kappa^\nu}{\tau}\right) + w_{2V}(\eta^\mu + \rho_\Delta\kappa^\mu)(\eta^\nu + \rho_\Delta\kappa^\nu),$$

$$w^{\mu\nu}_{AA} = -w_{1A}\left(g^{\mu\nu} + \frac{\kappa^\mu\kappa^\nu}{\tau}\right) + w_{2A}(\eta^\mu + \rho_\Delta\kappa^\mu)(\eta^\nu + \rho_\Delta\kappa^\nu) - u_{1A}\frac{\kappa^\mu\kappa^\nu}{\tau} + u_{2A}(\kappa^\mu\eta^\nu + \eta^\mu\kappa^\nu),$$

$$w^{\mu\nu}_{VA} = 2i\,w_3\epsilon^{\alpha\beta\mu\nu}\eta_\alpha\kappa_\beta$$

PHYSICAL REVIEW C **71**, 015501 (2005)

SuperScaling Approximation to CC QE+Δ

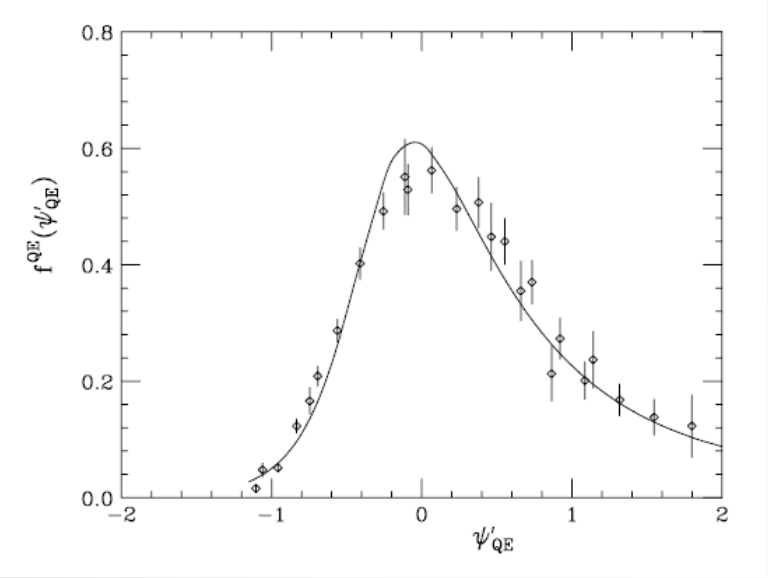

⇨

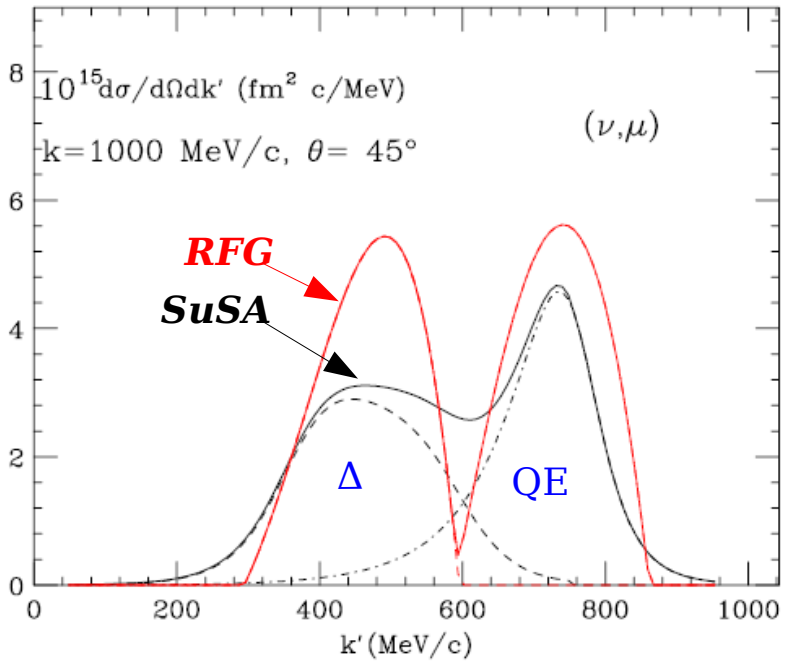

FIG. 9. (Color online) Neutrino reaction cross sections as in Fig. 6 for $\theta = 45$ degrees, showing a comparison of the full results obtained using the empirical scaling functions f^{QE} and f^{Δ} as discussed in the text with results obtained using the RFG scaling function f_{RFG} (heavier lines). The former lie somewhat lower and extend over a wider range in k' than the latter.

J.E.Amaro, MBB, J.A.Caballero, T.W.Donnelly, A.Molinari, I.Sick,Phys. Rev. C 71 (2005)

Limitations of the SuSA approach

The SuSA approach is based on some assumptions:

1. Super-scaling violations (beyond impulse approximation) are neglected:

-collective effects (like giant resonances), important at low momentum and energy transfer: here SuSA is bound to fail and RPA calculations are appropriate.

-Meson Exchange Currents (MEC), involving two-body operators.

2. Scaling of 0^{th} kind: $f_L = f_T$ Longitudinal-Transverse
holds exactly in RFG but not in more sophisticated models (e.g. RMF)

3. Scaling of the 3^{rd} kind : $f(T=0) = f(T=1)$ Isoscalar-Isovector

-CC neutrino reactions are isovector only

-f_L extracted from electron scattering contains both isospin components:

$$f_L \approx \tfrac{1}{2} f_L(T=0) + \tfrac{1}{2} f_L(T=1)$$

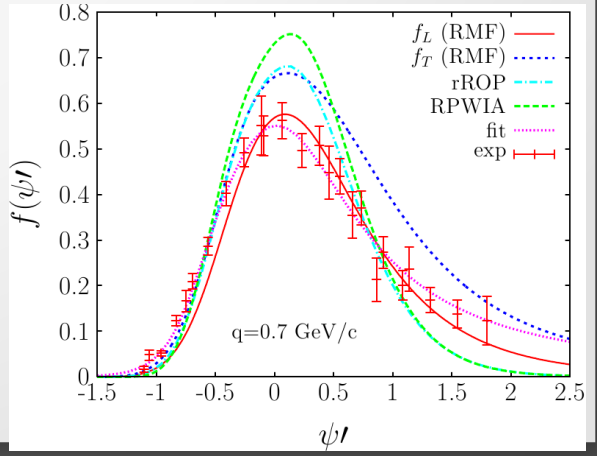

MEC in “CCQE” neutrino scattering

Why should MEC be relevant in quasielastic neutrino scattering?

In (e,e') experiments E_e is well-known and “QE” means that the electron is scattered by an individual nucleon moving inside the nucleus

In (ν_μ,μ) the neutrino the situation is different: the neutrino beam is not monochromatic, but it spans a wide range of energies:

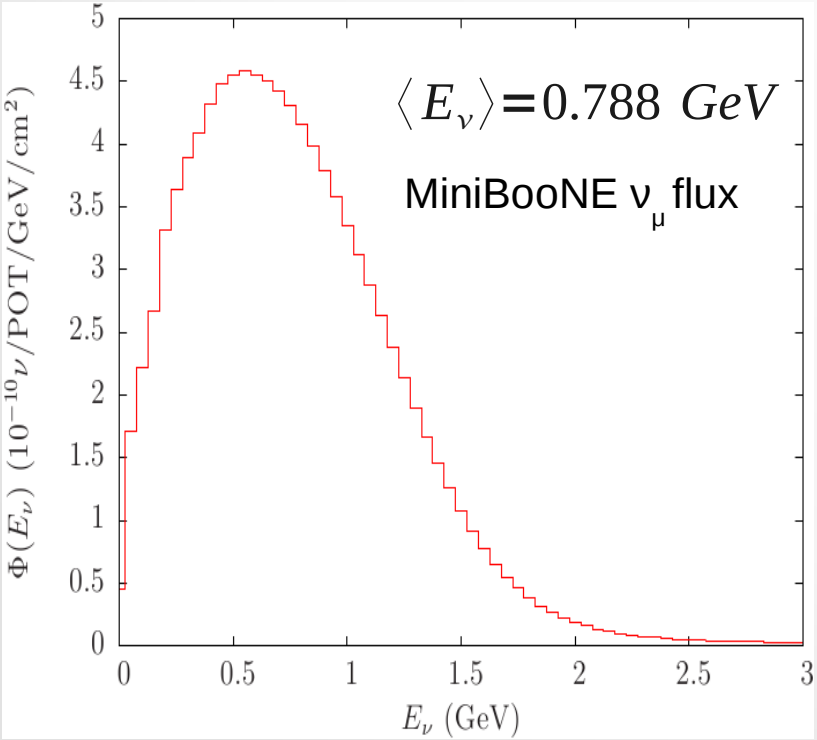

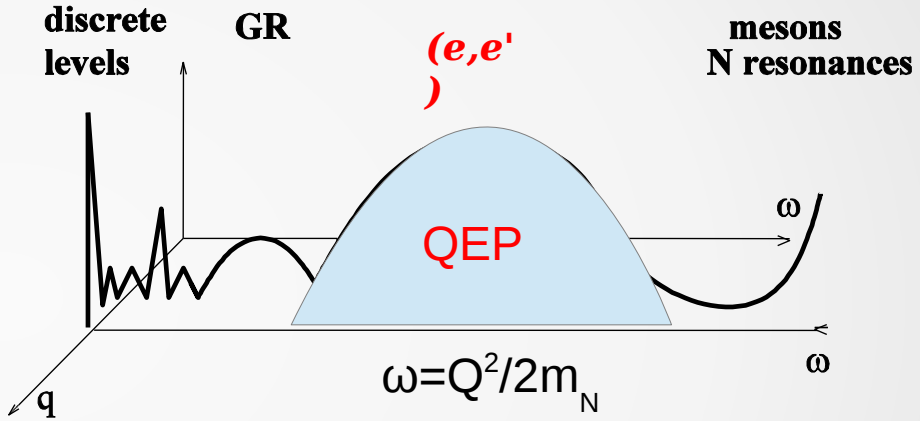

Flux-averaged cross section:

$$< \frac{d^2\sigma}{d\cos\theta\, dT_\mu} > = \frac{1}{\phi_{tot}} \int \frac{d^2\sigma(E_\nu)}{d\cos\theta\, dT_\mu} \phi(E_\nu)\, dE_\nu$$

As a consequence, different regions in the (q,ω) plane, corresponding to different reaction mechanisms, contribute to each experimental point (θ,T_μ).

MEC in “CCQE” neutrino scattering

- “QE” for many neutrino experiments (e.g., MiniBooNE) means

  “no pions ares detected in the final state”

- Processes involving scattering off two or more nucleons can give a non-negligible contribution to the cross section

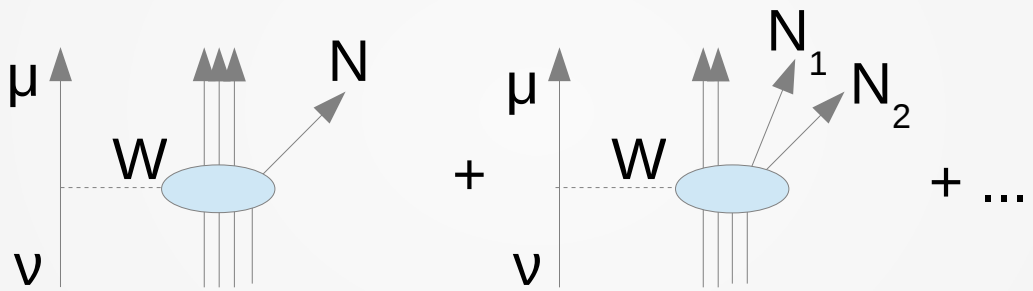

- The situation is different from electron scattering, where the quasielastic region can be clearly identified.

- These mechanisms may be (at least partially) responsible for the so-called “axial mass puzzle” of the MiniBooNE data

The nucleon axial mass

- The nucleon “axial mass” is the cutoff parameter entering the dipole parametrization of the axial-vector form factor of the nucleon

$$G_A(Q^2) = g_A/(1+Q^2/M_A^2)^2$$

g_A=1.2673±0.0035
from neutron β decay

World average from neutrino experiments:

$$M_A = (1.026 \pm 0.021)\,\mathrm{GeV}$$

Bernard, Elouadrhiri, Meissner, J. Phys. G28 (2002)

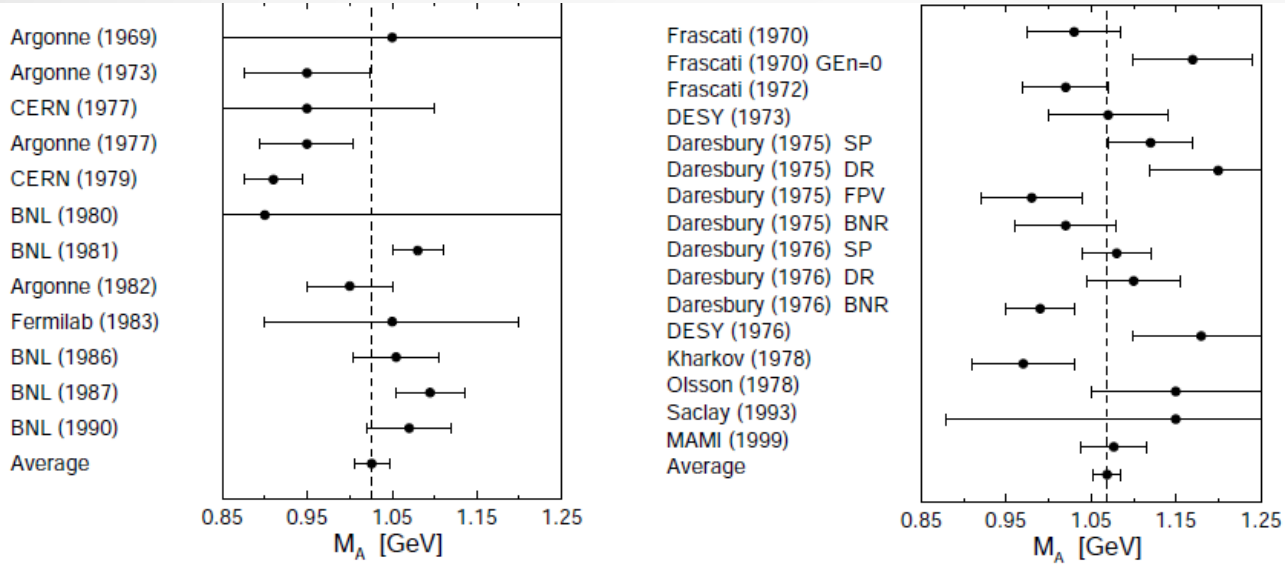

Figure 1. Axial mass M_A extractions. Left panel: From (quasi)elastic neutrino and antineutrino scattering experiments. The weighted average is $M_A = (1.026 \pm 0.021)\,\mathrm{GeV}$. Right panel: From charged pion electroproduction experiments. The weighted average is $M_A = (1.069 \pm 0.016)\,\mathrm{GeV}$. Note that value for the MAMI experiment contains both the statistical and systematical uncertainty; for other values the systematical errors were not explicitly given. The labels SP, DR, FPV and BNR refer to different methods evaluating the corrections beyond the soft pion limit as explained in the text.

The “Nucleon Axial Mass Puzzle”

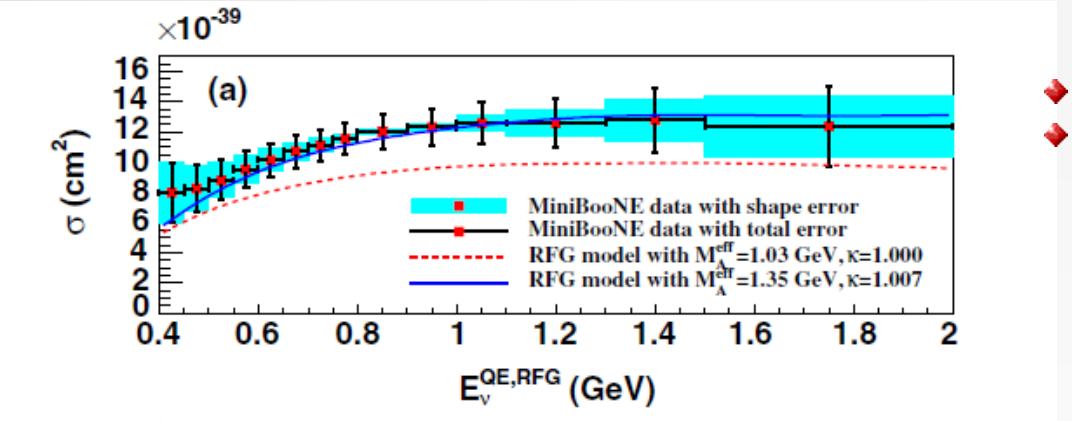

- MiniBooNE data are ~20% higher than RFG
- They can be fitted by RFG using an effective nucleon axial mass in the dipole parametrization

$$M_A^{eff}=1.35\ GeV/c^2$$

higher than the standard value ~1 GeV/c^2

The reconstruction of the neutrino energy and Q^2 is based on the assumption that the process in quasielastic:

$$E_\nu^{QE}=\frac{2(M_n')E_\mu-((M_n')^2+m_\mu^2-M_p^2)}{2\cdot[(M_n')-E_\mu+\sqrt{E_\mu^2-m_\mu^2}\cos\theta_\mu]},$$

$$Q^2_{QE}=-m_\mu^2+2E_\nu^{QE}(E_\mu-\sqrt{E_\mu^2-m_\mu^2}\cos\theta_\mu),$$

- Is this a measure of the axial mass or just an indication that the RFG is not adequate?
- Tension between MiniBooNE result and high energy NOMAD data

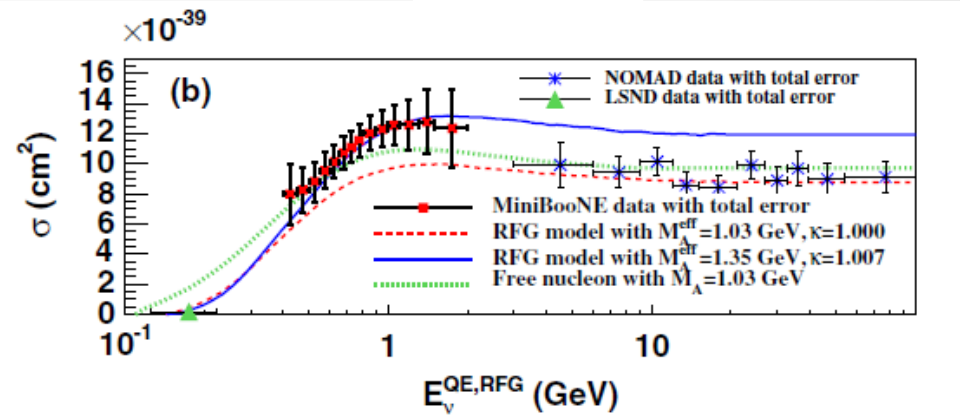

Various recent calculations of MEC mechanisms in QE neutrino scattering:

1. M.Martini et al., PRC81(2010);
2. J.E.Amaro et al.,PLB696(2011);
3. Nieves et al.,PLB707(2012);
4. G.Shen et al., PRC86(2012)

- In the approach of ref.2 a fully relativistic, RFG-based, pionic model for 2p2h MEC, performed for inclusive electron scattering ***[De Pace et al. NPA741, 249 (2004)]*** is applied to neutrino scattering. This induces a modification of the polar-vector transverse response function according to CVC.

$$R_T = R_T^{VV} + R_T^{AA}$$

- The MEC contribution to the axial-vector response is neglected because the 2p2h sector is not directly reachable in lowest relativistic order for the axial-vector matrix elements:

$$J_0^{V(MEC)} \sim O(\kappa^2) \qquad J_0^{A(MEC)} \sim O(\kappa) \qquad \kappa = q/2m_N$$
$$\vec{J}^{V(MEC)} \sim O(\kappa) \qquad \vec{J}^{A(MEC)} \sim O(\kappa^2)$$

[Donnelly&Van Orden,Annals Phys. 131 (1981); Alberico et al., Nucl.Phys. A512 (1990) 541]

- A fully consistent gauge invariant calculation would require also the inclusion of the associated correlation diagrams, not explicitly included in present calculation. However:
  1) these are hard to compute because in RFG because of divergences that need to be renormalized ***[Amaro et al., Phys.Rev.C82:044601 (2010)]***
  2) when MEC effects are added on top of the SuSA result, correlation effects are possibly already included in the phenomenological susperscaling function, since they also contribute to longitudinal channel

Results for CCQE neutrino and antineutrino scattering and comparison with data

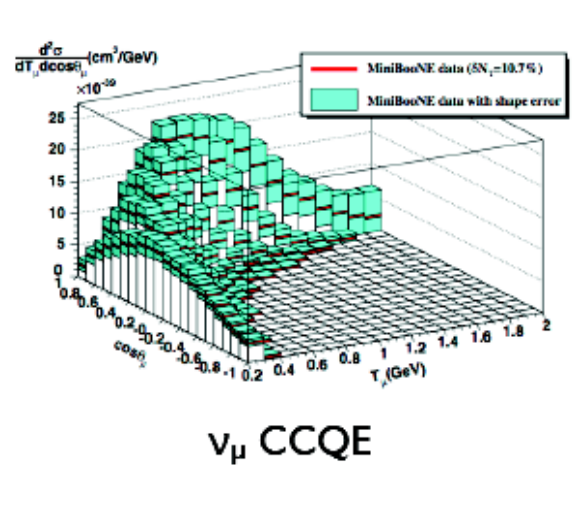

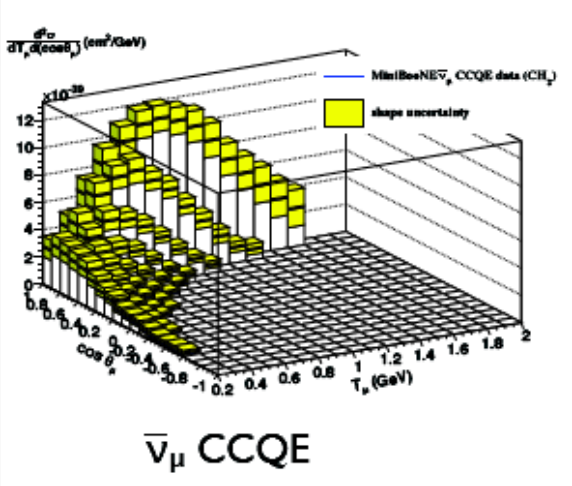

Aguilar-Arevalo et al., MiniBooNE, PHYSICAL REVIEW D 81, 092005 (2010)

Aguilar-Arevalo et al., MiniBooNE, PHYSICAL REVIEW D 81, 092005 (2010)

Double differential c.s. measured vs the muon kinetic energy ans scattering angle

MiniBooNE double differential CCQE cross sections at forward angles

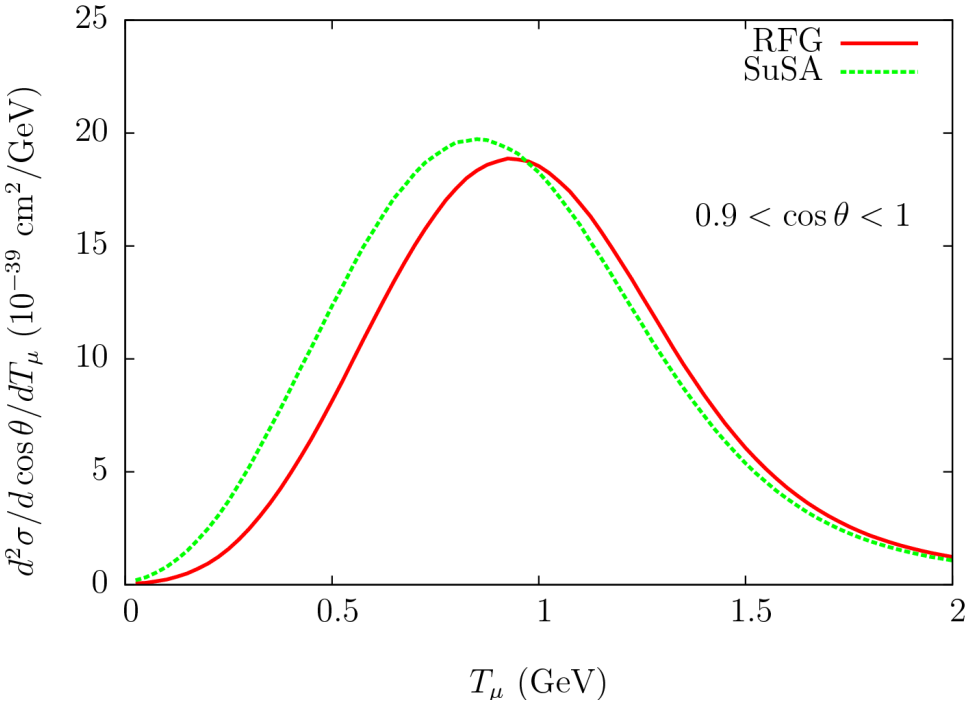

MiniBooNE double differential CCQE cross sections at forward angles

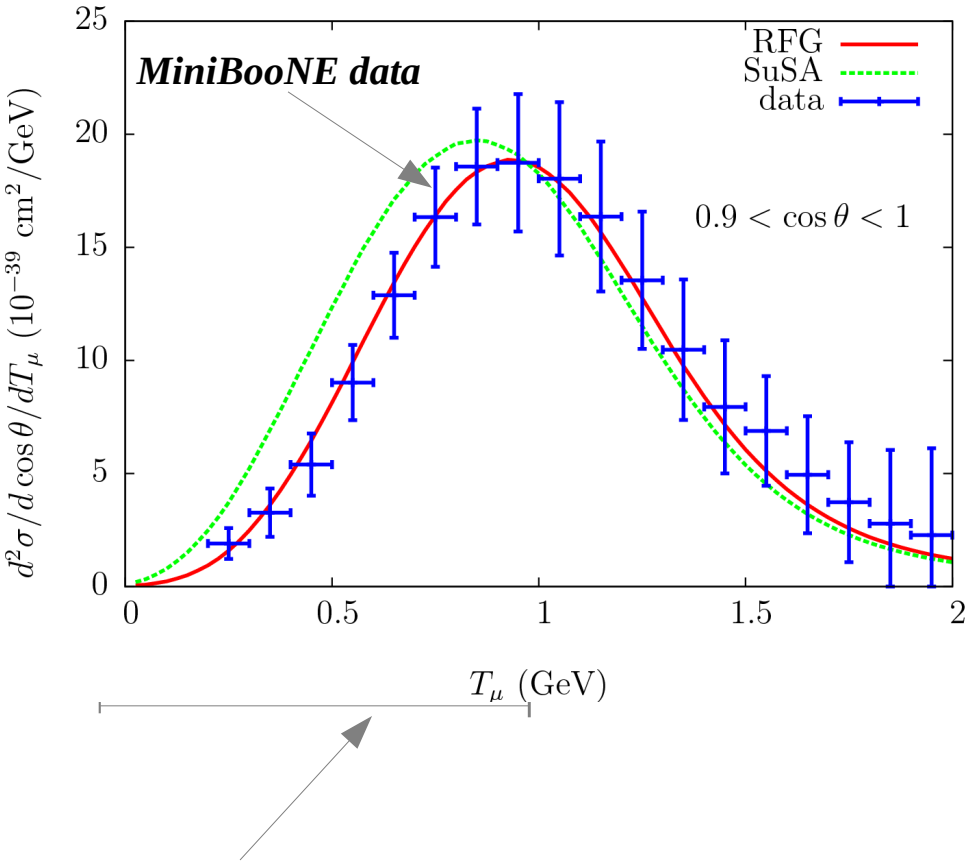

Pauli blocking is active in this region (low momentum transfers, q≲0.4 GeV/c): this explains the big difference between the RFG (where PB is included by definition) and the SuSA (which has no PB) results.

At very low angles both RFG and SuSA are compatible with the data, except for the Pauli-blocked region, where super-scaling ideas are not applicable.

MiniBooNE double differential CCQE cross sections at forward angles

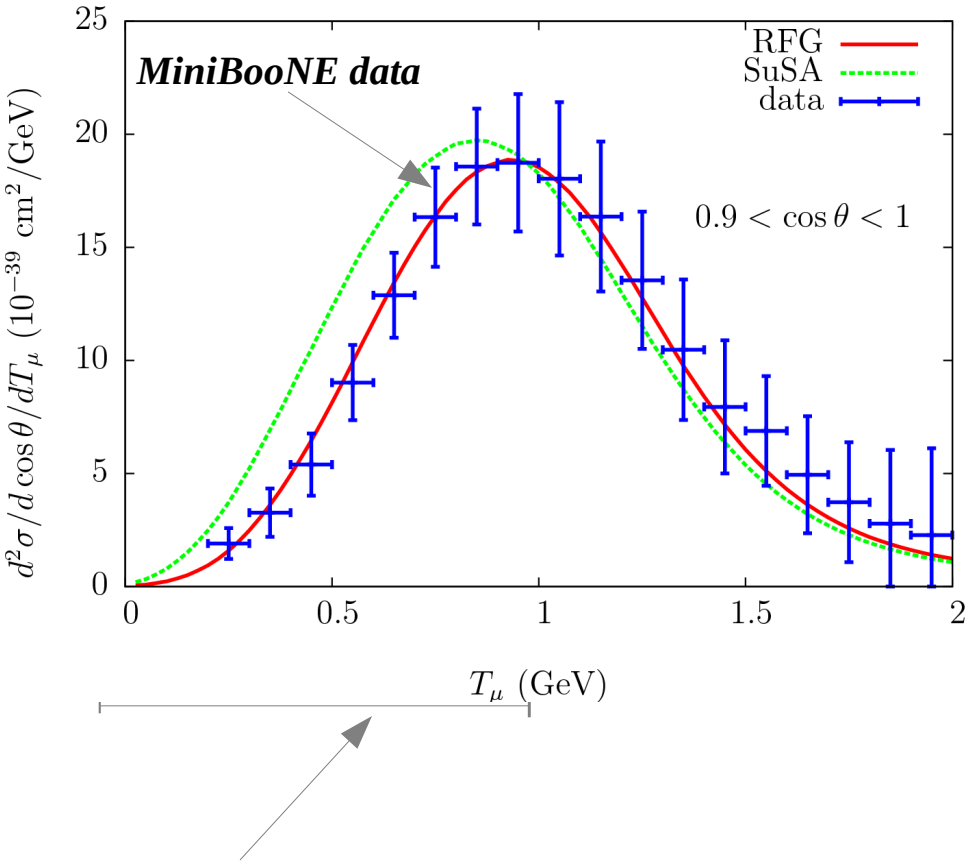

Pauli blocking is active in this region (low momentum transfers, q≲0.4 GeV/c): this explains the big difference between the RFG (where PB is included by definition) and the SuSA (which has no PB) results.

At very low angles both RFG and SuSA are compatible with the data, except for the Pauli-blocked region, where super-scaling ideas are not applicable.

However: about ½ of the cross section for such kinematics arises from the first 50 MeV of excitation, where none of the two approaches should be trusted.

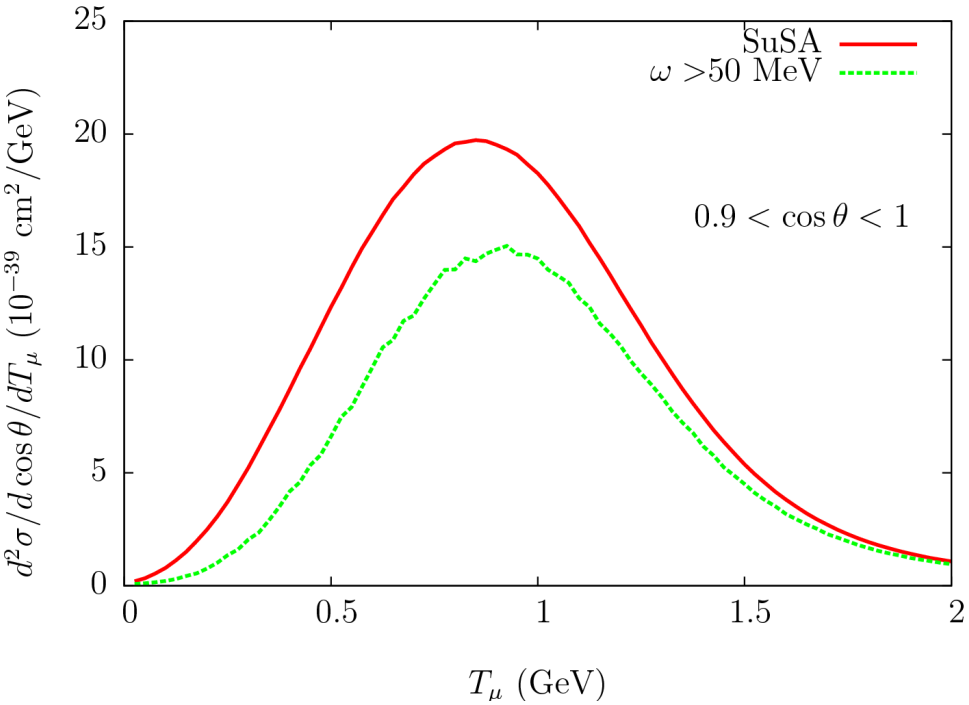

Here a proper treatment of collective excitations, like RPA with realistic nuclear wave functions, is required.

Comparison with MiniBooNE differential CC cross sections

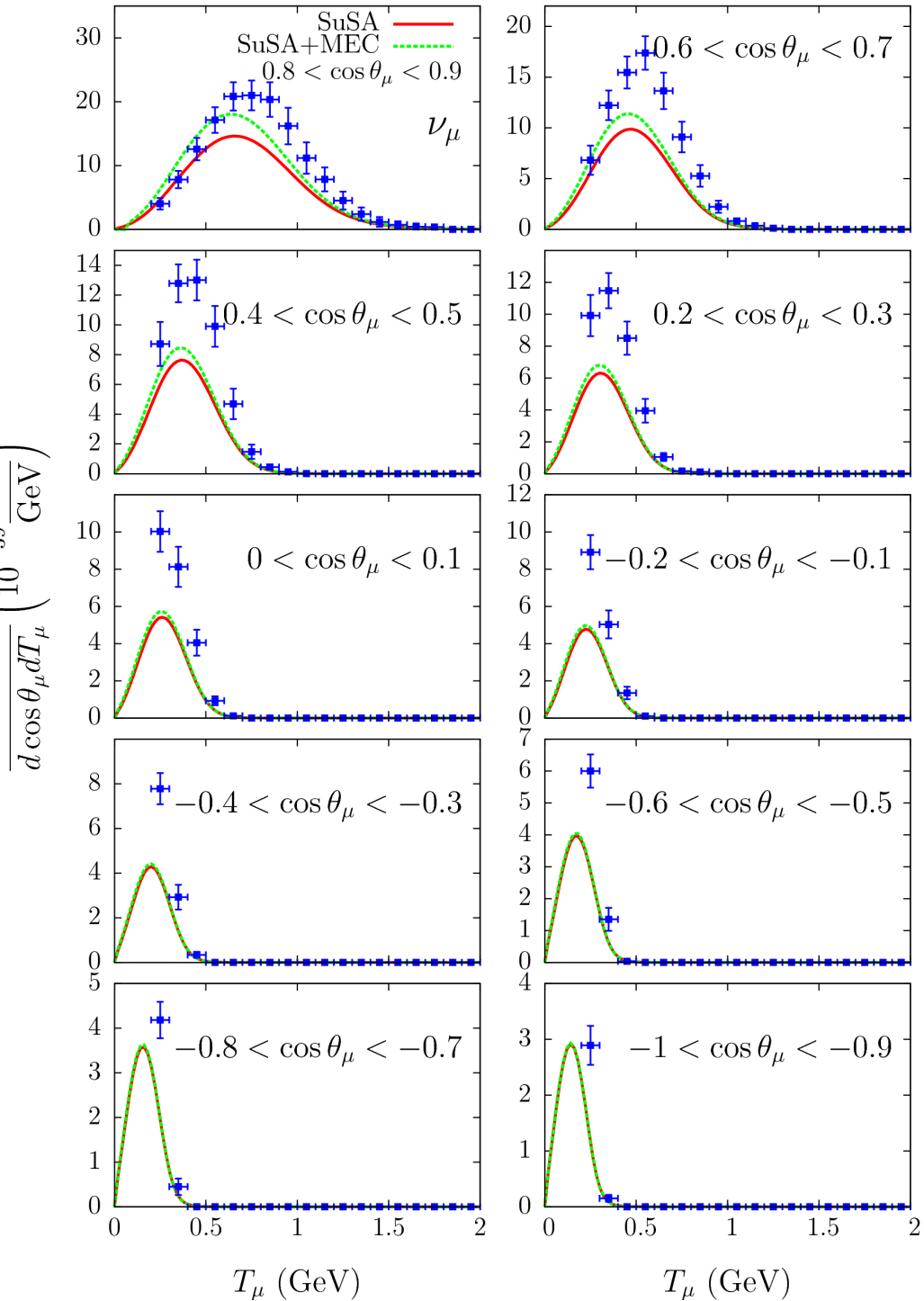

- SuSA predictions fall below the data for most kinematics

- 2p2h MEC improve the agreement but are not enough to explain the data

- The effect of 2p2h diagrams decreases with increasing scattering angle

Amaro et al., PLB696 (2011)

Comparison with MiniBooNE differential CC cross sections

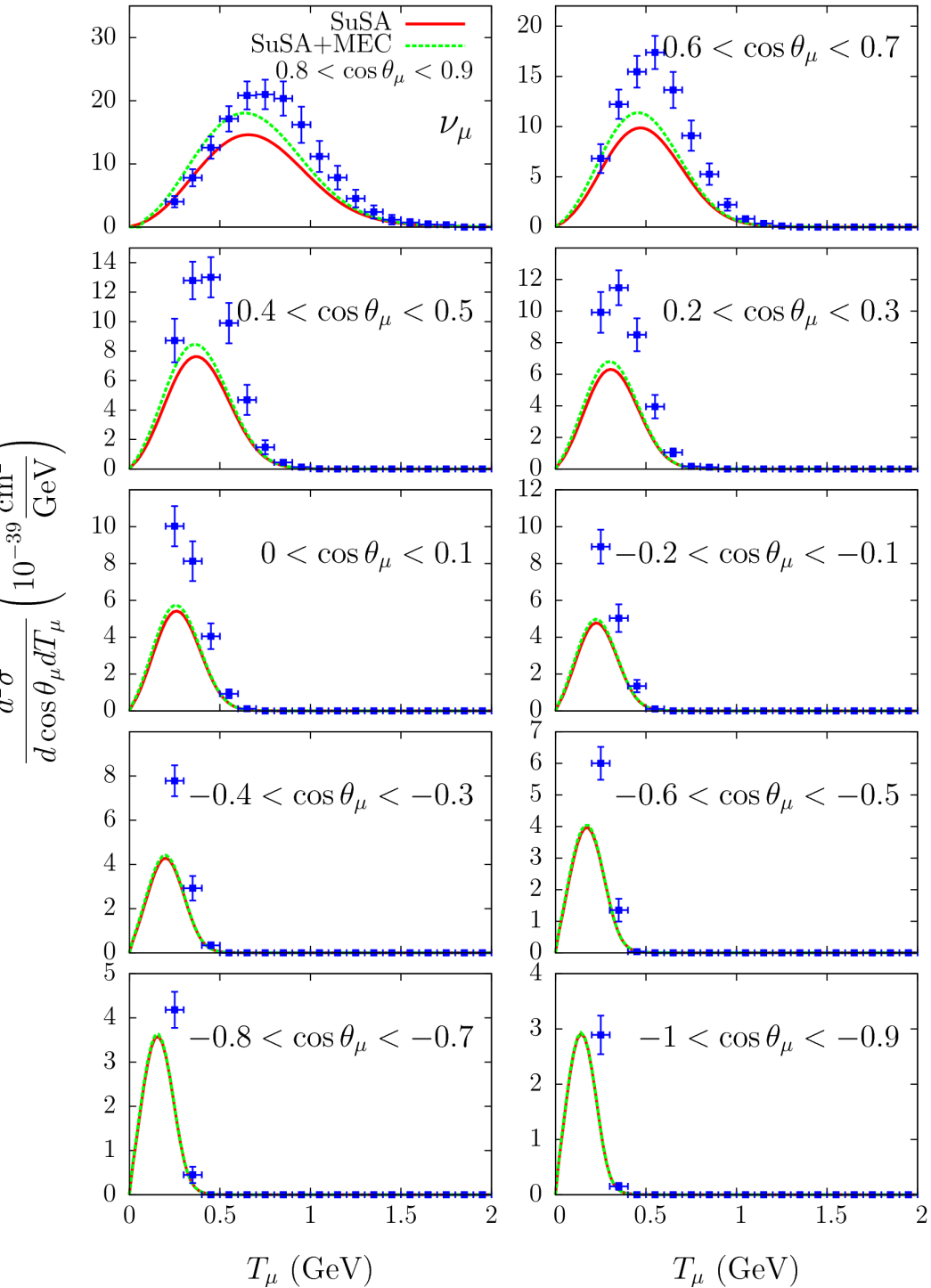

- SuSA predictions fall below the data for most kinematics

- 2p2h MEC improve the agreement but are not enough to explain the data

- The effect of 2p2h diagrams decreases with increasing scattering angle

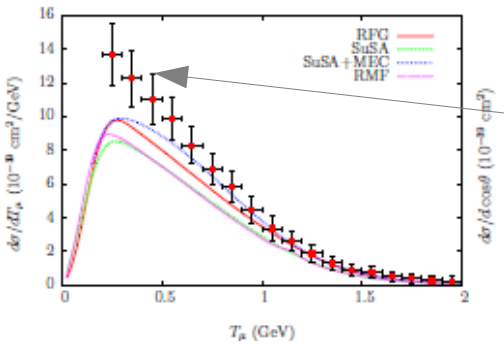

Strength is missing at lower muon energies

and larger scattering angles

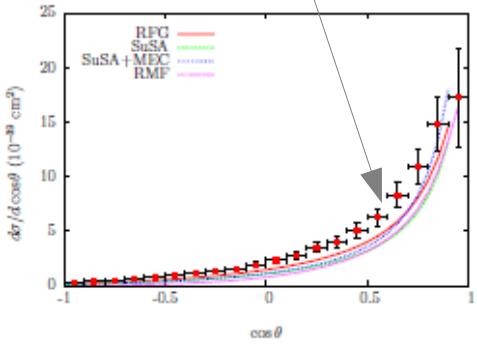

Amaro et al., PLB696 (2011)

Total CC cross section

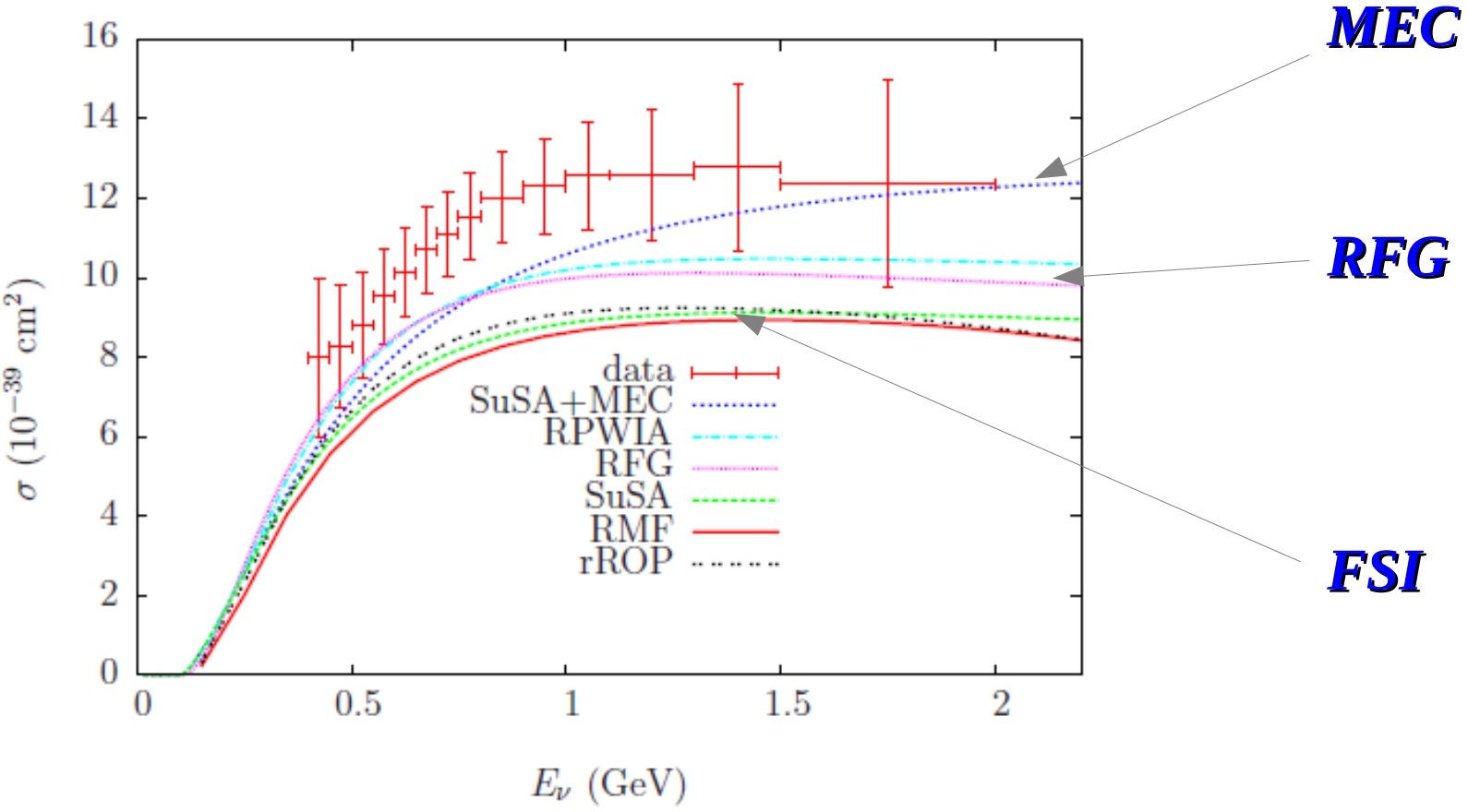

Amaro et al., PLB696 (2011)

CCQE antineutrino cross section

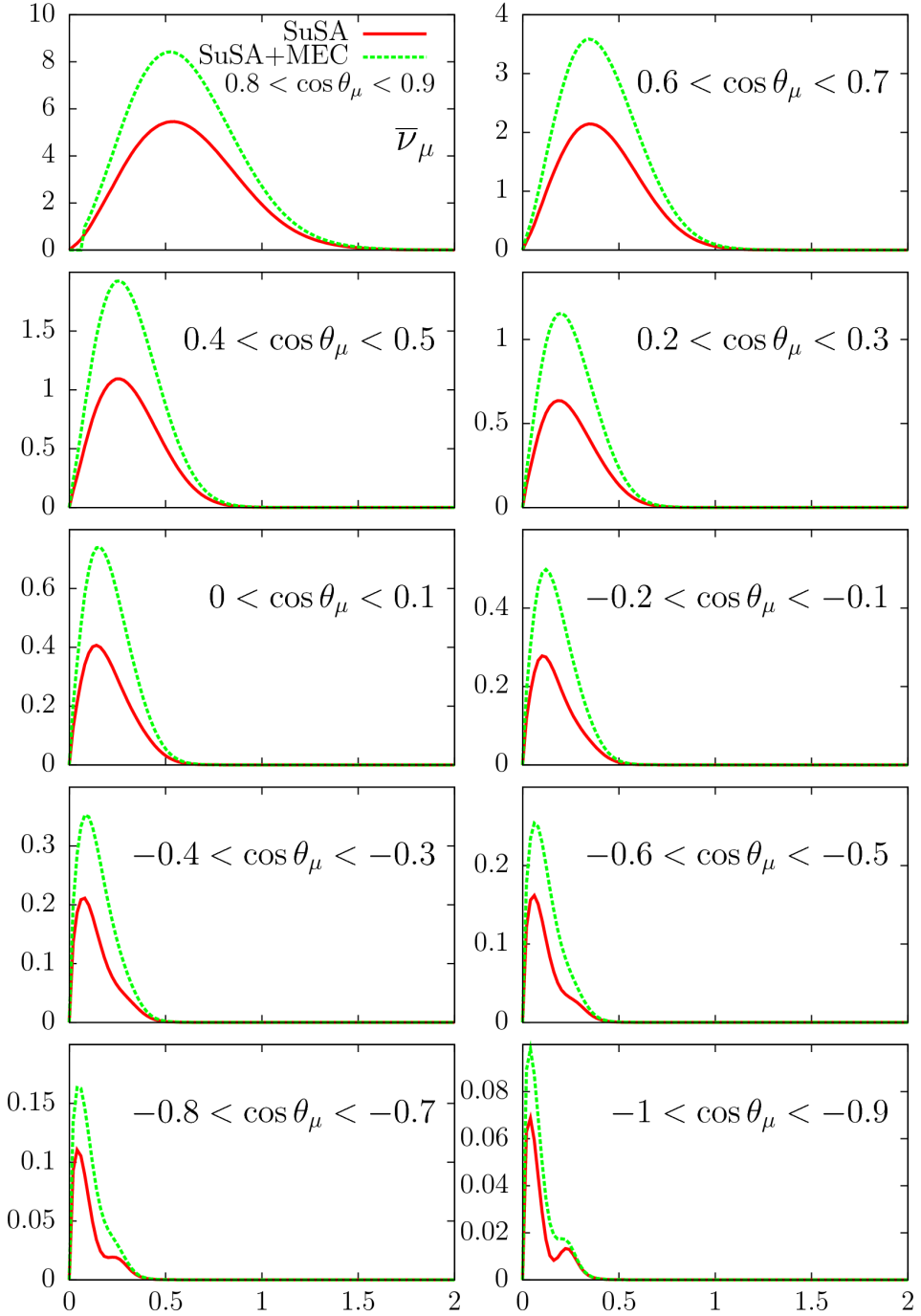

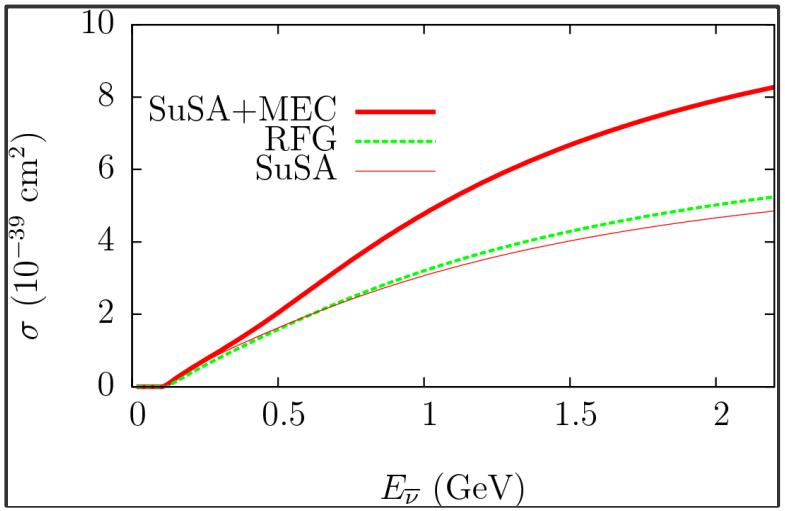

- The effects of MEC in the present model are found to be very important and significantly larger than for neutrino scattering

- MEC enhance the transverse response: Hence the transverse-axial cancellation mechanism occurring for antineutrinos is suppressed

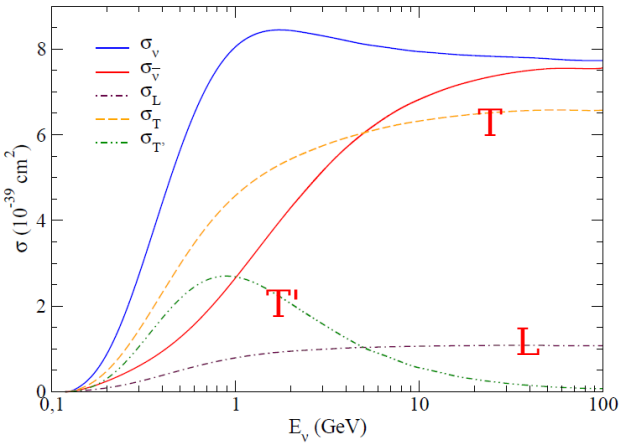

Amaro et al., PRL 108 (2012)

Comparison with antineutrino data

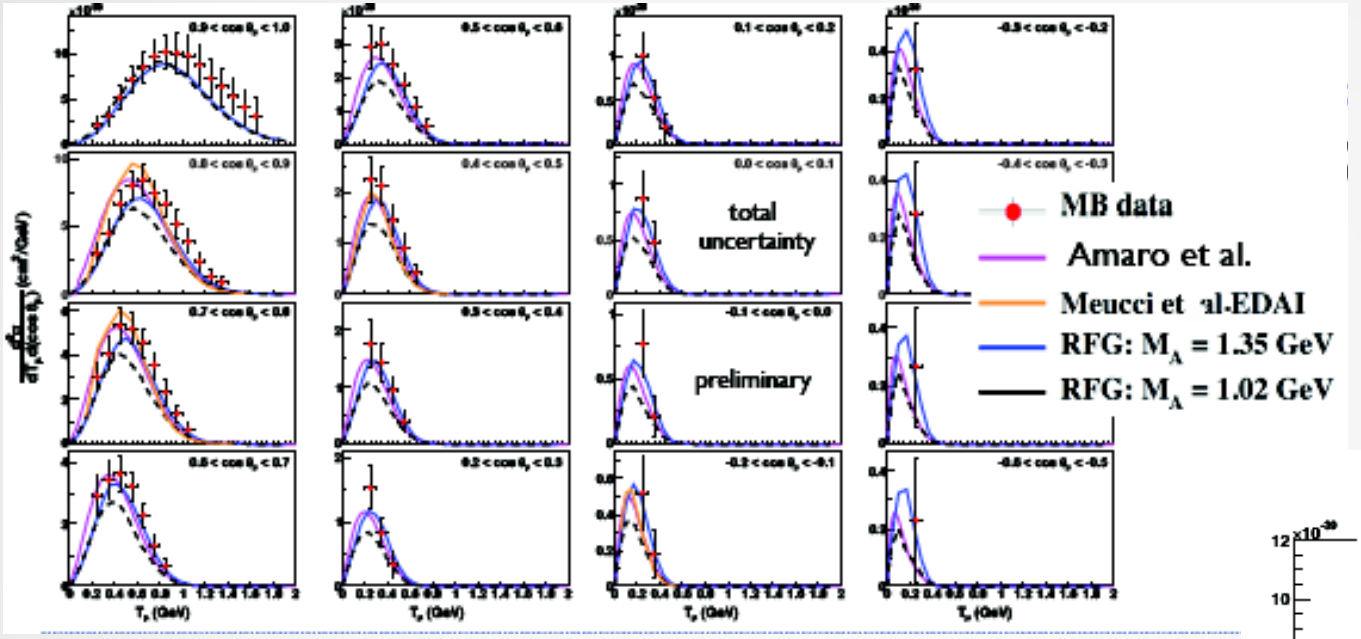

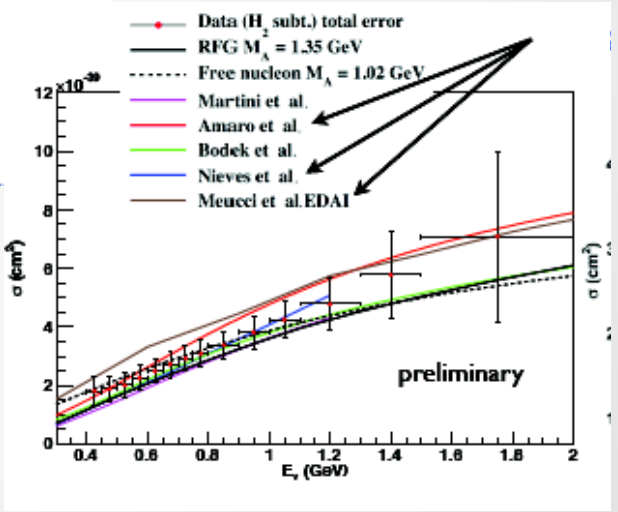

MiniBooNE coll., arXiv:1301.7067

Neutral Current Neutrino Scattering

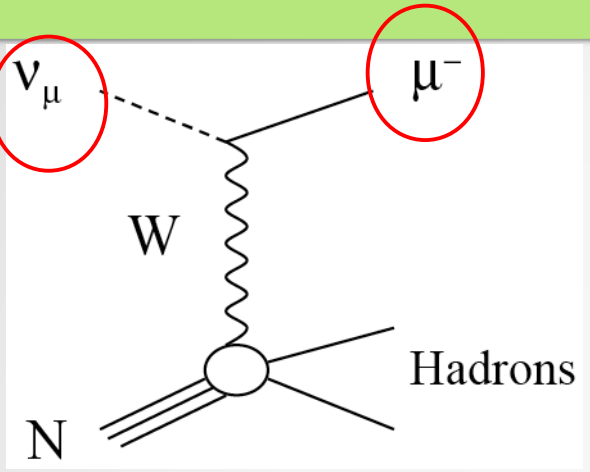

Charged Current (CC)

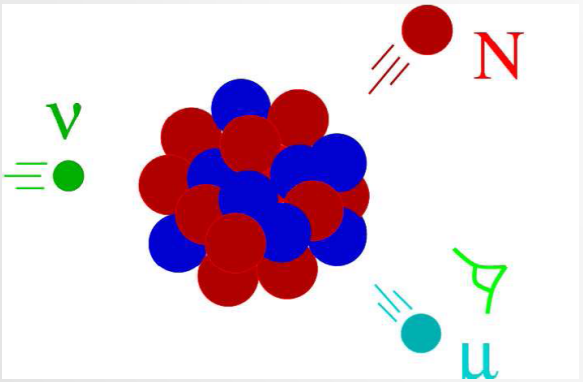

Q^2 fixed, as in (e,e')
t-channel kniematics

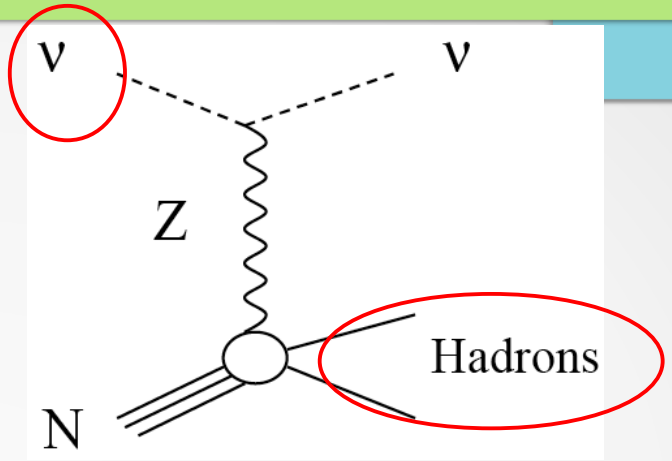

Neutral Current (NC)

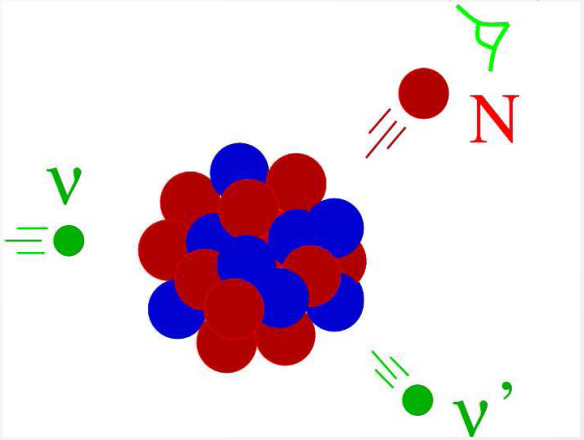

Q^2 in son fixed:
u-channel kniematics

The two processes correspond to different kinematical situations:
do they reveal different sensitivity to the dynamics underlying scaling?

Kinematics and scaling in NC processes

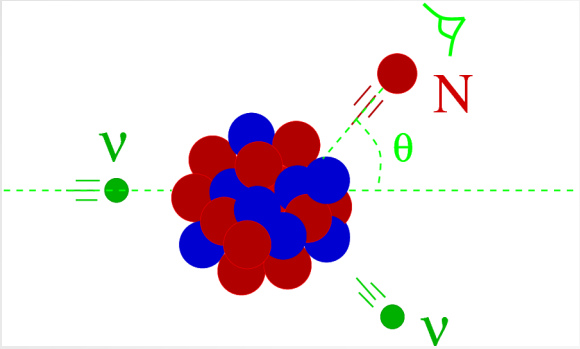

Let us assume to know

- the neutrino beam energy E_ν
- the outgoing nucleon energy E_N and scattering angle θ_{kN}

- u-channel kinematics: the scattered lepton is not observed, hence Q_μ is unknown.
- A new transferred momentum $Q'_\mu = K_\mu - P_{N\mu}$ can be defined
- New scaling variables $y^{(u)}(q', \omega')$ and $\psi^{(u)}(q', \omega')$ can be introduced
- Validity of the scaling approach for NC reactions?
  - Mild dependence of νN cross section upon (p, ε)
  - Reduced cross section depends weakly on q'

t- and u-scattering

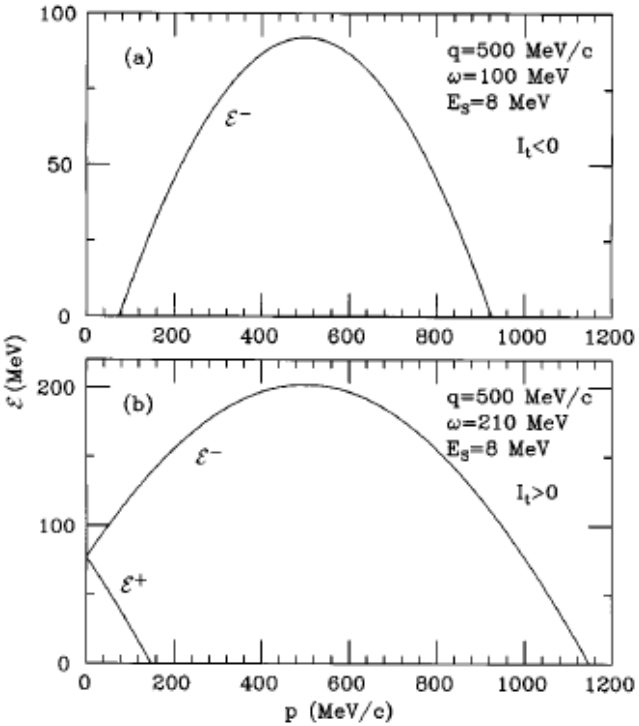

FIG. 2. The domain $\mathcal{D}$ over which one integrates for the t-inclusive cross section at typical values of momentum and energy transfer. Note the more complex structure of the boundary when the intercept I_t given by Eq. (5) is positive.

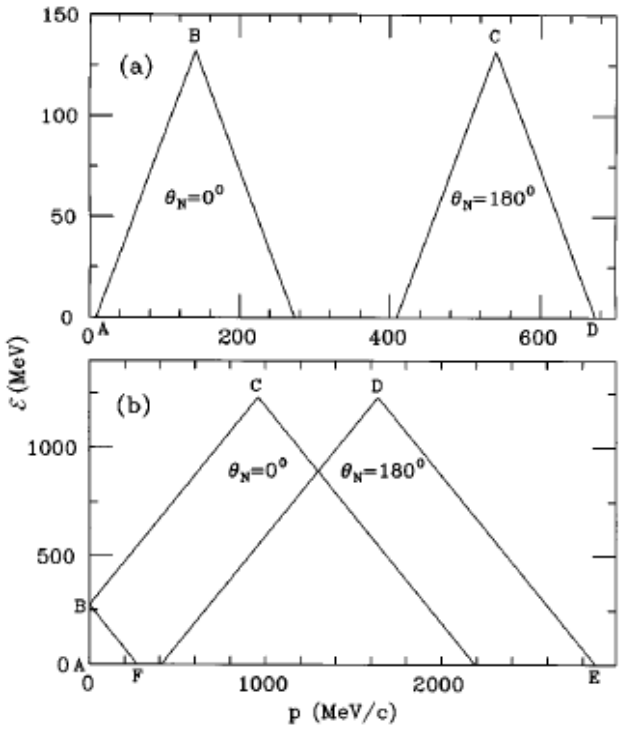

FIG. 3. The same as Fig. 2 for the u-inclusive cross section: (a) LSND kinematics (ϵ=200 MeV, T_N=60 MeV); (b) BNL kinematics (ϵ=1.3 GeV, T_N=60 MeV). The boundaries shown all involve $\mathcal{E}^-$ except for line BF which involves $\mathcal{E}^+$. Note that when the neutrino and outgoing nucleon momenta are antiparallel quite remote regions of the $(\mathcal{E}, p)$ plane are explored.

Different regions of the missing energy-missing momentum plane are explored by the two processes

MB, A.De Pace, T.W.Donnelly, A-Molinari, M.Musolf, Phys.Rev. C54 (1996)

Scaling and factorization for NC in RFG

To apply scaling ideas to the NC process one must assume that factorization of the c.s. into (nucleonic cross section)*(scaling function) holds.

$$\frac{d\sigma}{dp_N d\Omega_N} = \frac{1}{32\pi\epsilon}\frac{1}{q'}\left(\frac{p_N^2}{E_N}\right) g^4 \int_{\mathcal{D}_u} pdp \int \frac{d\varepsilon}{E} S(p,\varepsilon) \int_0^{2\pi} \frac{d\phi'}{2\pi} \ell_{\mu\nu} w^{\mu\nu} D_V^2(Q^2)$$

$$Factorization: \quad \frac{d\sigma}{d\Omega_N dp_N} \approx \overline{\sigma}_{sn}^{(u)} F(\psi^{(u)}, q') \approx \overline{\sigma}_{sn}^{(u)} F(\psi^{(u)})$$

How good is it?

Factorized RFG

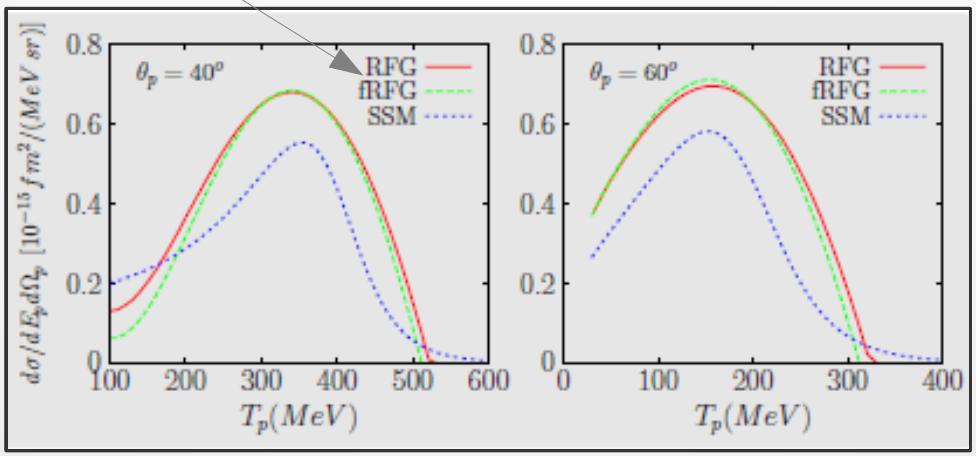

Amaro et al., Phys.Rev. C73 (2006) 035503

NC neutrino cross section and strangeness

NC neutrino reactions are sensitive to the strange form factors of the nucleon.
In particular, the ratio of cross sections corresronding to proton and neutron knockout can be used to measure the strange axial form factor g_A^s.

$$
\begin{aligned}
w_{1a}(\tau) &= \tau\widetilde{G}_{Ma}^2(\tau) + (1+\tau)\widetilde{G}_{Aa}^2(\tau) \\
w_{2a}(\tau) &= \frac{\widetilde{G}_{Ea}^2(\tau) + \tau\widetilde{G}_{Ma}^2(\tau)}{1+\tau} + \widetilde{G}_{Aa}^2(\tau) \\
w_{3a}(\tau) &= \widetilde{G}_{Ma}(\tau)\widetilde{G}_{Aa}(\tau)\ ,
\end{aligned}
\qquad (a = p, n):
$$

$$
\begin{aligned}
\widetilde{G}_{Ep}(\tau) &= (2 - 4\sin^2\theta_W)G_E^{T=1}(\tau) - 4\sin^2\theta_W G_E^{T=0}(\tau) - G_E^{(s)}(\tau) \\
\widetilde{G}_{En}(\tau) &= -(2 - 4\sin^2\theta_W)G_E^{T=1}(\tau) - 4\sin^2\theta_W G_E^{T=0}(\tau) - G_E^{(s)}(\tau) \\
\widetilde{G}_{Mp}(\tau) &= (2 - 4\sin^2\theta_W)G_M^{T=1}(\tau) - 4\sin^2\theta_W G_M^{T=0}(\tau) - G_M^{(s)}(\tau) \\
\widetilde{G}_{Mn}(\tau) &= -(2 - 4\sin^2\theta_W)G_M^{T=1}(\tau) - 4\sin^2\theta_W G_M^{T=0}(\tau) - G_M^{(s)}(\tau) \\
\widetilde{G}_{Ap}(\tau) &= -2G_A^{(3)}(\tau) + G_A^{(s)}(\tau) \\
\widetilde{G}_{An}(\tau) &= 2G_A^{(3)}(\tau) + G_A^{(s)}(\tau)\ .
\end{aligned}
$$

$$
\begin{aligned}
G_E^{(s)}(\tau) &= \rho_s\tau G_V^D(\tau) \\
G_M^{(s)}(\tau) &= \mu_s G_V^D(\tau) \\
G_S^{(s)}(\tau) &= g_A^s G_A^D(\tau)\ ,
\end{aligned}
$$

p/n ratio

MB et al., PRC54 (1996)

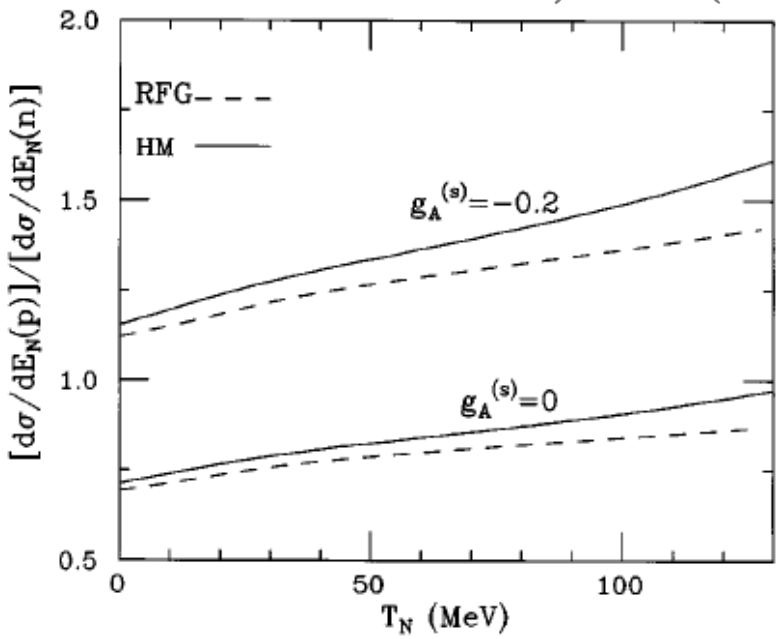

FIG. 9. Ratio between the angle-integrated cross sections for proton and neutron ejection at LSND kinematics. Both the RFG (dashed line) and HM (solid line) results are displayed.

Alberico et al., PLB438 (1998)

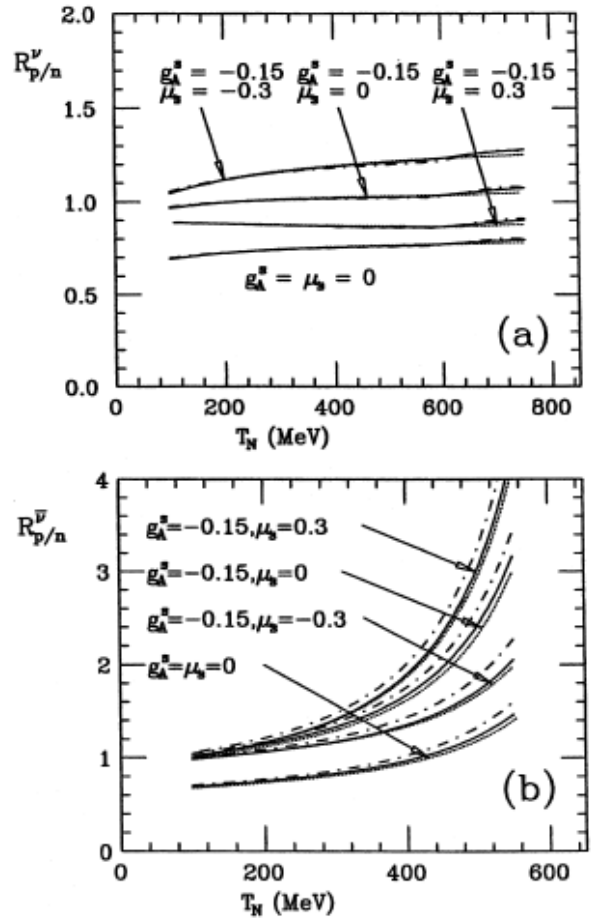

Fig. 1. The ratio $\mathcal{R}^{\nu}_{p/n}$ (a) and $\mathcal{R}^{\bar{\nu}}_{p/n}$ (b) for NC neutrino processes, versus the kinetic energy of the final nucleon $T_N = T_p = T_n$, at incident energy $E_{\nu(\bar{\nu})} = 1$ GeV. The dotted lines correspond to the RFG model, the solid lines to the RSM calculation, the dot–dashed lines include the effect of FSI accounted for by the ROP model. Four different choices of the strangeness parameters are shown, as indicated in the figure.

NC results: comparison with MiniBooNE data

The dependence upon the nuclear model is essentially canceled in the p/n ratio:

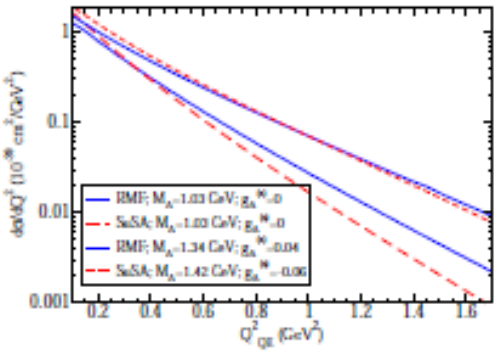

Figure 4: NCQE antineutrino cross section computed using RMF and SuSA models for different values of $g_A^{(s)}$ and M_A. We employed the antineutrino flux prediction for MiniBooNE given in Ref. [27].

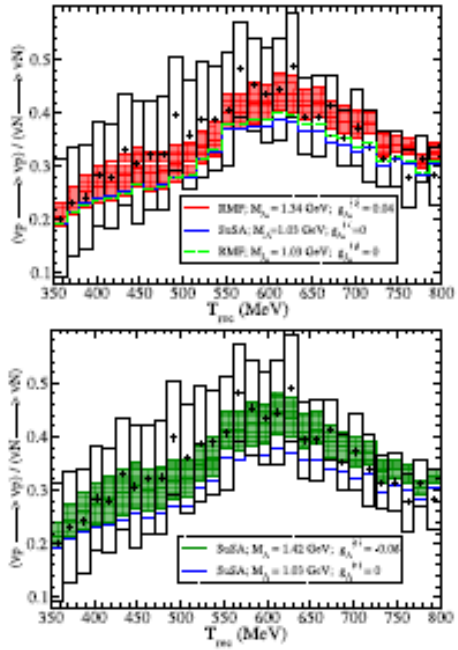

Figure 3: Ratio $(\nu p \to \nu p)/(\nu N \to \nu N)$ computed within RMF and SuSA models. Shadowed areas represent the 1-σ region allowed for $g_A^{(s)}$ (see text). The ratio computed with the best-$g_A^{(s)}$ is presented as well as those obtained with the standard axial mass and no strangeness. Data from Ref. [10].

R. Gonzalez-Jimenez et al., PLB718 (2013)

Summary of SuSA approach to neutrino scattering

Plus

- The SuSA approach gives (by construction) reasonable agreement with electron scattering data in a wide range of kinematics;
- It can be applied to all nuclei (II kind scaling);
- The superscaling function is phenomenological, but it is well reproduced by the relativistic mean field model.

Minus

- It is based on some assumptions:

1. The superscaling function is extracted from longitudinal data and the approach assumes $f_L=f_T=f_{T'}$ (true in some, but not all, microscopic models)
2. Superscaling violations are not accounted for and must be added (MEC).
   This is difficult to do in a consistent way.
   However, RFG exact calculations can be used as a guideline.

Results

- Application to the CCQE process: cross sections are lower than the MiniBooNE data
- Addition of 2p2h MEC diagrams improves the agreement but still misses the data at higher scattering angles and lower muon energies
- Application to the NCQE process gives results lower than the MiniBooNE data at low Q^2 (but no MEC in the present model)

Future work

- Improvements of the model (in progress):

1. Inclusion of axial MEC in the 2p2h sector
2. Inclusion of correlations associated to MEC, necessary to preserve gauge invariance

Scuola di Fisica Nucleare Raimondo Anni

4. Parity-Violating Electron Scattering

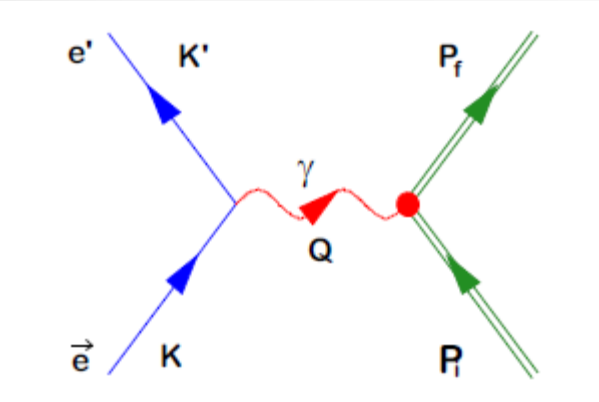

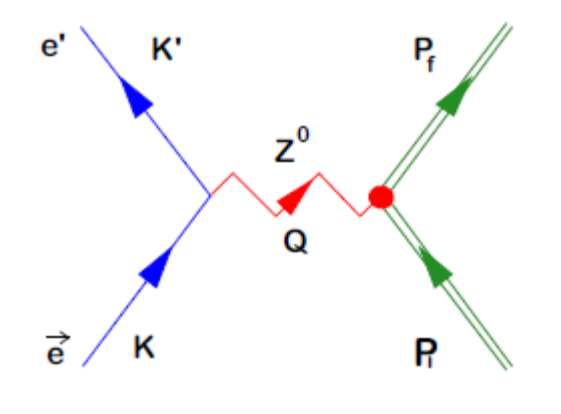

Parity violating electron scattering

Electrons interact with hadrons via e.m. (PC) and weak (PV) interaction.
Longitudinally polarized electrons measurements allows to isolate the PV contribution to the c.s.

$M_\gamma \propto (e^2/Q^2) j_\mu^{\rm EM} J_{\rm EM}^\mu$

$M_{Z^0} \propto (g^2/M_Z^2) j_\mu^{\rm WNC} J_{\rm WNC}^\mu$

$|M_\gamma + M_{Z^0}|^2 \longrightarrow$ 3 classes of terms:

$|M_\gamma|^2$ PC problem, typical strength α^2

$|M_{Z^0}|^2$ typical strength G^2, very small

$M_\gamma^* M_{Z^0}$ interference, typical strength αG

$$\left(\frac{d^2\sigma}{d\Omega d\epsilon'}\right)^{PC} = \frac{1}{2}\left(\frac{d^2\sigma^+}{d\Omega d\epsilon'} + \frac{d^2\sigma^-}{d\Omega d\epsilon'}\right) \sim |M_\gamma|^2 \sim \eta_{\mu\nu}^{\rm PC} W_{\rm PC}^{\mu\nu}$$

$$\left(\frac{d^2\sigma}{d\Omega d\epsilon'}\right)^{PV} = \frac{1}{2}\left(\frac{d^2\sigma^+}{d\Omega d\epsilon'} - \frac{d^2\sigma^-}{d\Omega d\epsilon'}\right) \sim M_\gamma^* M_{Z^0} \sim \eta_{\mu\nu}^{\rm PV} W_{\rm PV}^{\mu\nu}$$

$$\mathcal{A} = \frac{d\sigma^{+1} - d\sigma^{-1}}{d\sigma^{+1} + d\sigma^{-1}} = \mathcal{A}_0 \times \frac{W^{\rm PV}}{W^{\rm PC}}$$

Access to the WNC electron-hadron interaction

PV Asymmetry

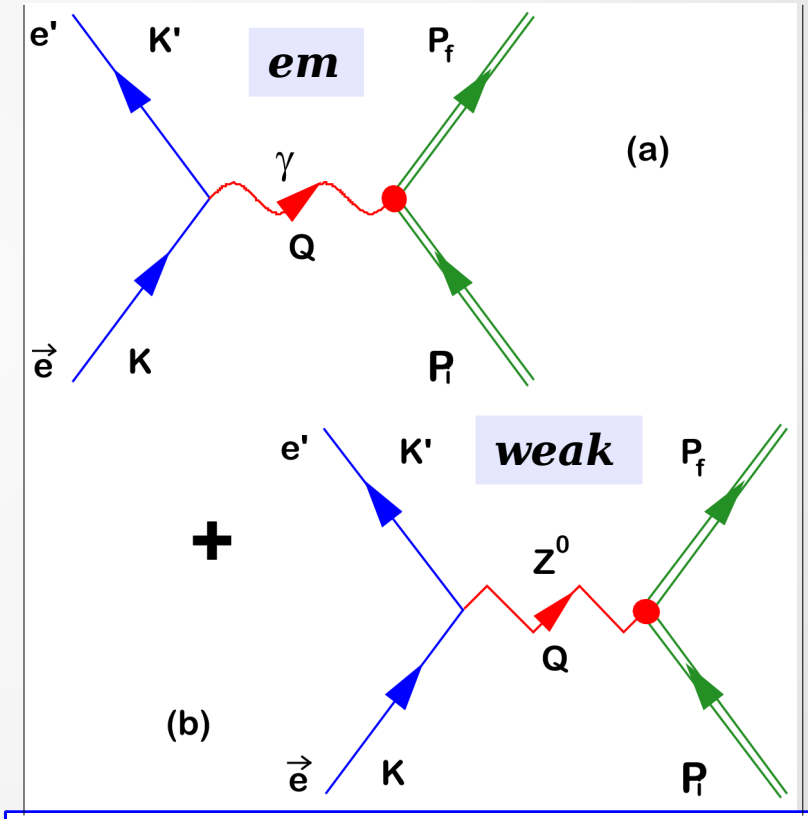

$$\mathcal{A}_0 \equiv \frac{G}{2\pi\alpha\sqrt{2}} |Q^2| \cong 3.25 \times 10^{-6} \, |Q^2({\rm fm}^{-2})|$$

Characteristic size = 1 ppm

Parity-violating electron scattering

- Why

  - Test of Standard Model
  - Electroweak form factors of the nucleon (strangeness)
  - Probe nuclear structure

- How

  -Elastic scattering off proton and nuclei
  -Inelastic scattering from discrete nuclear levels
  -Quasielastic scattering
  -Delta resonance region
  -DIS

- Why nuclei?

  -3 flavors (u,d,s) and 3 types of form factors (E, M, A) → 9 ff's to be separated: this cannot be accomplished using only elastic scattering from the proton, neutrons must also be used
  -Combining cross section and asymmetry measurements for electron scattering from the proton and from nuclei provides useful constraints on this set of form factors
  -PV can also be used to study nuclear dynamics

Doability

The fractional precision with which the PV asymmetry can be measured is

$$\left|\frac{\Delta\mathcal{A}}{\mathcal{A}}\right| = \frac{1}{\sqrt{X_0\mathcal{F}}}$$

$X_0 \sim 10^{42}\ \mathrm{cm}^{-2}$ = (integrated luminosity) X
(detector solid angle) X
(squared electron polarization)

$\mathcal{F} = (d\sigma/d\Omega_e)\mathcal{A}^2$ figure of merit (ex: 1% precision requires $\mathcal{F} \sim 10^{-38}\ \mathrm{cm}^2\ \mathrm{sr}^{-1}$)

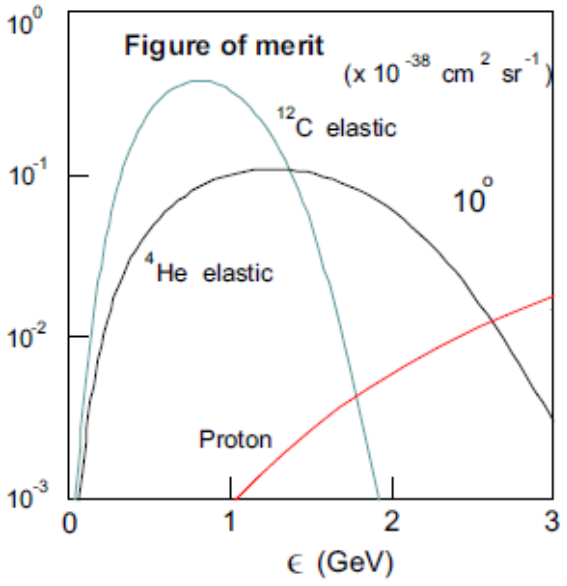

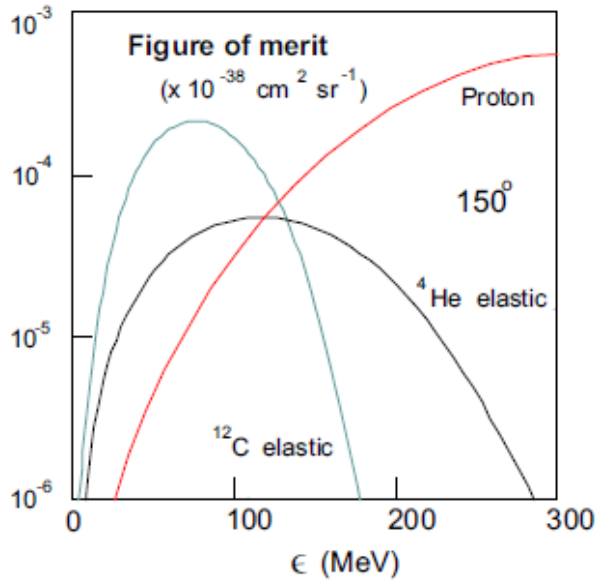

Elastic scattering: the coherence (~Z^2) helps

Inelastic nuclear transitions: F falls by several orders of magnitude

Favorable cases for sensitive studies are elastic and quasielastic

Experiments

SAMPLE (MIT/Bates): E_e~200 MeV, H and ^{2}H targets, large angles

HAPPEX (Jlab): E_e~3 GeV, H and ^{4}He targets, forward angles

PVA4 (MAMI/Mainz): various E_e , H and ^{2}H targets, backward angles

G0 (Jlab): E_e~3 GeV, H and ^{2}H targets, forward and backward angles

Q-weak (Jlab): H target, very low momentum transfer, test of SM

PVDIS (Jlab): deep inelastic scattering from ^{2}H, Q^2=1.1 and 1.9 GeV^2

PREX (Jlab): Lead Radius Exp't, measure of ^{208}Pb RMS neutron radius

PV Leptonic Tensor

$$\eta^{\rm PV}_{\mu\nu} = \overline{\sum_{\rm leptons} j^{\rm EM*}_\mu j^{\rm WNC}_\nu}$$

EM electron current

$$j^{\rm EM}_\mu(K',\lambda';K,\lambda) \sim \bar u(K',\lambda')\gamma_\mu u(K,\lambda)$$

WNC electron current

$$j^{\rm WNC}_\mu(K',\lambda';K,\lambda) \sim \bar u(K',\lambda')\left[a_V\gamma_\mu + a_A\gamma_\mu\gamma_5\right]u(K,\lambda)$$

$$\begin{aligned} a_V &= 4\sin^2\theta_W - 1 \cong -0.08 \\ a_A &= -1\,, \end{aligned}$$

PV leptonic tensor

$$\begin{aligned} \eta^{\rm PV}_{\mu\nu} &= \frac{1}{16m_e^2}\Big(a_V {\rm Tr}\left\{\gamma_\mu\left(\not K' + m_e\right)\gamma_\nu\left(1+\gamma_5\not S\right)\left(\not K + m_e\right)\right\} \\ &\quad + a_A {\rm Tr}\left\{\gamma_\mu\left(\not K' + m_e\right)\gamma_\nu\gamma_5\left(1+\gamma_5\not S\right)\left(\not K + m_e\right)\right\}\Big) \\ &\equiv \frac{1}{2}\left[a_V\eta_{\mu\nu} + a_A\tilde\eta_{\mu\nu}\right]\,. \end{aligned}$$

Longitudinally polarized electrons:

$$m_e S^\mu = h\epsilon(\beta,\vec u_L)$$

$$\beta = k/\epsilon = \sqrt{1-(m_e/\epsilon)^2}$$

EM case

EM-WNC interference

$$\tilde\eta_{\mu\nu} = \frac{1}{2}\left[\tilde\eta^{\rm unpol}_{\mu\nu} + \tilde\eta^{\rm pol}_{\mu\nu}\right]$$

$$\begin{aligned} \tilde\eta^{\rm unpol}_{\mu\nu} &\equiv -\frac{1}{2m_e^2}\left(i\epsilon_{\mu\nu\alpha\beta}K^\alpha K'^\beta\right) \quad \text{VA, AV, antisymmetric} \\ \tilde\eta^{\rm pol}_{\mu\nu} &\equiv \frac{1}{2m_e^2}\Big\{\left[K_\mu(m_eS_\nu) - K_\nu(m_eS_\mu)\right] \quad \text{VV, AA, symm} \\ &\quad + \left[K'_\mu(m_eS_\nu) + K'_\nu(m_eS_\mu) - g_{\mu\nu}K'\cdot(m_eS)\right]\Big\} \end{aligned}$$

The PV Leptonic Tensor in the ERL

In the Extreme Relativistic Limit $m_e << k$ $\boxed{\beta \to 1, \gamma \to \infty}$

$$\begin{aligned} K^\mu &\longrightarrow \epsilon(1, \vec{u}_L) \\ (m_e S^\mu)_L &\longrightarrow h\epsilon(1, \vec{u}_L) = hK^\mu \end{aligned}$$

$$\begin{aligned} 2m_e^2 \tilde{\eta}^{\rm unpol}_{\mu\nu} &\to -i\epsilon_{\mu\nu\alpha\beta} K^\alpha K'^\beta \equiv \tilde{\chi}^{\rm unpol}_{\mu\nu} \\ 2m_e^2 \tilde{\eta}^{\rm pol}_{\mu\nu} &\to h\left[K_\mu K'_\nu + K'_\mu K_\nu - g_{\mu\nu} K\cdot K'\right] \equiv \tilde{\chi}^{\rm pol}_{\mu\nu} \end{aligned}$$

h=±1 helicity of the polarized electron

$$2m_e^2 \eta^{\rm PV}_{\mu\nu} \to \chi^{\rm PV}_{\mu\nu} = \frac{1}{2}(a_V + h a_A)\left[\chi^{(1)}_{\mu\nu} + h\chi^{(2)}_{\mu\nu}\right]$$

symmetric

antisymmetric

$$\chi^{\rm PV,helicity-difference}_{\mu\nu} = a_A \chi^{(1)}_{\mu\nu} + a_V \chi^{(2)}_{\mu\nu} \,.$$

$$\begin{aligned} a_V &= 4\sin^2\theta_W - 1 \cong -0.08 \\ a_A &= -1\,, \end{aligned}$$

The Hadronic Tensor

$$W^{\mu\nu}_{\rm PV} = \overline{\sum}_{\rm hadrons} J^{\mu *}_{{\rm EM}fi} J^{\nu}_{{\rm WNC}fi}$$

Nucleon's WNC

$$\widetilde{J}^{\mu}_{WNC} = \overline{u}(\mathbf{p}) \left(\widetilde{F}_1 \gamma^{\mu} + \frac{i}{2m} \widetilde{F}_2 \sigma^{\mu\nu} Q_{\nu} + \widetilde{G}_A \gamma_5 \gamma^{\mu} \right) u(\mathbf{h})$$

General structure
(II rank Lorentz tensor)

$$\widetilde{W}^{\mu\nu}_{s} = \widetilde{X}_1 g^{\mu\nu} + \widetilde{X}_2 Q^{\mu} Q^{\nu} + \widetilde{X}_3 V_i^{\mu} V_i^{\nu} + \widetilde{X}_4 \left(Q^{\mu} V_i^{\nu} + V_i^{\mu} Q^{\nu} \right)$$ Symm.

$$\widetilde{W}^{\mu\nu}_{a} = i\widetilde{Y}_1 \left(Q^{\mu} V_i^{\nu} - V_i^{\mu} Q^{\nu} \right) + i\widetilde{Y}_2 \epsilon^{\mu\nu\alpha\beta} Q_{\alpha} V_{i\beta}$$ Antisymm.

CVC → $\widetilde{X}_1 + \widetilde{X}_2 Q^2 = 0$, $\widetilde{X}_4 = 0$; $\widetilde{Y}_1 = 0.$ → 3 independent structure functions

$$\widetilde{W}^{\mu\nu}_{s} = -\widetilde{W}_1 \left(g^{\mu\nu} - \frac{Q^{\mu} Q^{\nu}}{Q^2} \right) + \widetilde{W}_2 V_i^{\mu} V_i^{\nu}$$
$$\widetilde{W}^{\mu\nu}_{a} = i\widetilde{W}_3 \epsilon^{\mu\nu\alpha\beta} Q_{\alpha} V_{i\beta} \, .$$

$$V_i^{\mu} \equiv \frac{1}{M_i} \left\{ P_i^{\mu} - \left(\frac{Q \cdot P_i}{Q^2} \right) Q^{\mu} \right\}$$

$$Q \cdot V_i = 0.$$

Contracting the hadronic and leptonic tensors we get:

$$\chi^{(1)}_{\mu\nu} \widetilde{W}^{\mu\nu}_{s} \sim \widetilde{W}_2 + 2\widetilde{W}_1 \tan^2 \frac{\theta_e}{2}$$
$$\chi^{(2)}_{\mu\nu} \widetilde{W}^{\mu\nu}_{a} \sim 2\widetilde{W}_3 (\epsilon + \epsilon') \tan^2 \frac{\theta_e}{2} \, .$$

Helicity Asymmetry and Response Functions

Asymmetry

$$\mathcal{A} = \frac{d\sigma^{+1} - d\sigma^{-1}}{d\sigma^{+1} + d\sigma^{-1}} = \mathcal{A}_0 \times \frac{W^{\rm PV}}{W^{\rm PC}}$$

$$\mathcal{A}_0 \equiv \frac{G}{2\pi\alpha\sqrt{2}}\,|Q^2| \cong 3.25 \times 10^{-6}\,|Q^2({\rm fm}^{-2})|$$

The nuclear physics content of the problem is in the PV/PC hadronic tensors

$$W^{\rm PC} = v_L R^L + v_T R^T$$

electromagnetic

$$W^{\rm PV} = v_L R^L_{AV} + v_T R^T_{AV} + v_{T'} R^{T'}_{VA}$$

electromagnetic/weak interference
AV: axial lepton current, vector hadron current
VA: vector lepton current, axial hadron current

5 response functions in the Asymmetry

$$R^L_{AV} = (\widetilde{W}_2 - \rho\widetilde{W}_1)/\rho^2, \quad R^T_{AV} = 2\widetilde{W}_1, \quad R^{T'}_{VA} = 2q\widetilde{W}_3$$

PV (3)

$$R^L = (W_2 - \rho W_1)/\rho^2$$
$$R^T = 2W_1\,.$$

PC (2)

The responses depend only upon q and ω, not on θ_e: they can <u>in principle</u> be separated by varying the scattering angle

Kinematic factors

$$\rho \equiv -Q^2/q^2$$

$$v_L = \rho^2$$
$$v_T = \frac{1}{2}\rho + \tan^2\frac{\theta_e}{2}$$

$$v_{T'} \equiv \tan\frac{\theta_e}{2}\sqrt{\rho + \tan^2\frac{\theta_e}{2}}$$

PV elastic scattering off proton

The PV cross section from the proton involves 9 weak form factors

$$\widetilde{G}_E^{(p,n,s)}\ ,\ \widetilde{G}_M^{(p,n,s)}\ ,\ \widetilde{G}_A^{(p,n,s)}$$

The elastic e.m. squared form factor can be written as

$$W^{(\mathrm{PC})} \equiv F^2 = \frac{1}{(1+\tau)\mathcal{E}}\left[\mathcal{E}G_{E_p}^2 + \tau G_{M_p}^2\right]$$

$$\tau = \frac{Q^2}{4M_N^2}$$

$$\mathcal{E} \equiv \left[1 + 2(1+\tau)\tan^2\frac{\theta_e}{2}\right]^{-1}$$

Degree of longitudinal polarization of γ (represents the "virtualness" of the exchanged photon)

$\mathcal{E} \to 1(0)$ when $\theta_e \to 0°(180°)$

Similarly

$$W^{(\mathrm{PV})} = \frac{1}{(1+\tau)\mathcal{E}}\left[a_A\left\{\mathcal{E}G_{E_p}\tilde{G}_{E_p} + \tau G_{M_p}\tilde{G}_{M_p}\right\} + a_V\left\{\sqrt{1-\mathcal{E}^2}\sqrt{\tau(1+\tau)}\,G_{M_p}\tilde{G}_{A_p}\right\}\right]$$

$$a_V = 4\sin^2\theta_W - 1 \cong -0.08$$

$$a_A = -1$$

leptonic couplings (from Standard Model)

- The hadronic axial-vector contributions are inhibited by the leptonic coupling a_V (not so in neutrino scattering, where $a_V = a_A$)
- Forward angle (ε→1, τ→0) ⇒ Electric form factor
- Backward angle (ε→0) ⇒ Magnetic (and axial) form factor

The neutron's electric form factor

Ignoring strangeness

$$\begin{aligned} G_{E_p} &= (G_E^{(0)} + G_E^{(1)})/2 \\ \tilde{G}_{E_p} &= (\beta_V^{(0)} G_E^{(0)} + \beta_V^{(1)} G_E^{(1)})/2 \end{aligned}$$

$$\beta_V^{(0)} = -2\sin^2\theta_W, \quad \beta_V^{(1)} = 1 - 2\sin^2\theta_W$$

$$\beta_V^{(0)} \simeq -\beta_V^{(1)}$$

Isoscalar and isovector hadronic couplings (from Standard Model at tree level)

If G_{Ep} and $\hat{G}_{Ep}$ could be separetly measured, then the isoscalar and isovector charge ff's would be determined. As a consequence the charge form factor of the neutron (poorly known) could be determined:

$$\begin{aligned} G_{E_n} &= (G_E^{(0)} - G_E^{(1)})/2 \\ \tilde{G}_{E_n} &= (\beta_V^{(0)} G_E^{(0)} - \beta_V^{(1)} G_E^{(1)})/2 \end{aligned}$$

PC and PV scattering only on the proton allow to extract information on the neutron form factors!

Conversely: using PV electron scattering from the proton to test the SM at 1% level of precision will be extremely difficult, since the G_{En} effects are 10-20% of the asymmetry. Alternative means are necessary to measure G_{En} : polarized targets and complex nuclei.

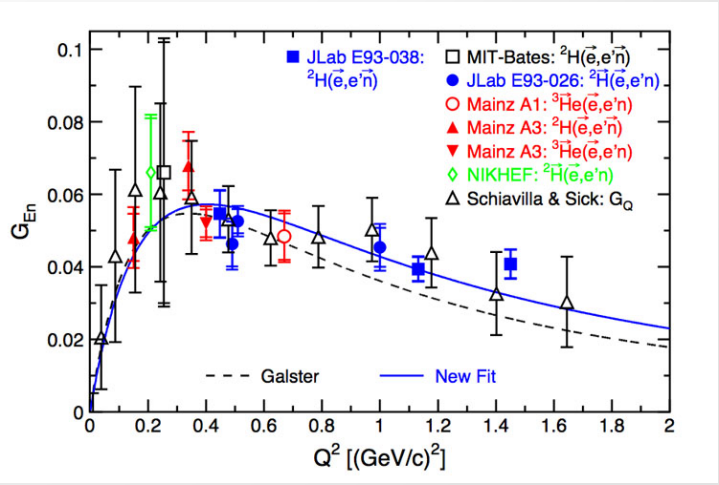

Strangeness

Possible strange content of the nucleon

$$\tilde{G}_{E_p} = \frac{1}{2}\left[\left(1-4\sin^2\theta_W\right)G_{E_p} - G_{E_n} - G_E^{(s)}\right]$$

$$\tilde{G}_{M_p} = \frac{1}{2}\left[\left(1-4\sin^2\theta_W\right)G_{M_p} - G_{M_n} - G_M^{(s)}\right]$$

$$\tilde{G}_{A_p} = \frac{1}{2}\left[G_{A_p} - G_{A_n} - G_A^{(s)}\right]$$

Inserting these in the asymmetry:

$$\mathcal{A}(\mathrm{p,elastic}) = \frac{\mathcal{A}_0}{2}\left[a_A X_{AV} + a_V X_{VA}\right]$$

$$X_{AV} = \left(1-4\sin^2\theta_W\right) - \frac{\mathcal{E}G_{E_p}\left(G_{E_n} + G_E^{(s)}\right) + \tau G_{M_p}\left(G_{M_n} + G_M^{(s)}\right)}{\mathcal{E}\left(G_{E_p}\right)^2 + \tau\left(G_{M_p}\right)^2}$$

$$X_{VA} = \frac{\sqrt{1-\mathcal{E}^2}\sqrt{\tau(1+\tau)}\,G_{M_p}\left(G_{A_p} - G_{A_n} - G_A^{(s)}\right)}{\mathcal{E}\left(G_{E_p}\right)^2 + \tau\left(G_{M_p}\right)^2}$$

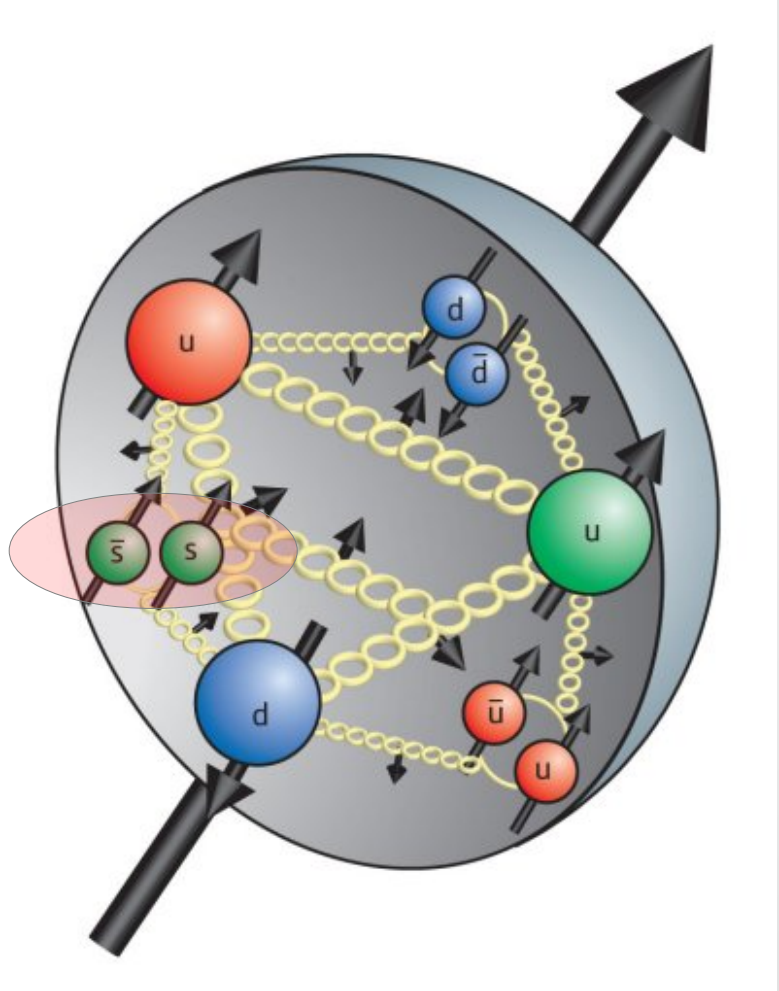

Extraction of strange form factors

$$\mathcal{E} \to 1(0) \text{ when } \theta_e \to 0^\circ(180^\circ)$$

Forward angles

$$X_{AV} = \left(1-4\sin^2\theta_W\right) - \frac{\mathcal{E}G_{E_p}\left(G_{E_n}+G_E^{(s)}\right)+\tau G_{M_p}\left(G_{M_n}+G_M^{(s)}\right)}{\mathcal{E}\left(G_{E_p}\right)^2+\tau\left(G_{M_p}\right)^2}$$

$$X_{VA} = \frac{\sqrt{1-\mathcal{E}^2}\sqrt{\tau(1+\tau)}\,G_{M_p}\left(G_{A_p}-G_{A_n}-G_A^{(s)}\right)}{\mathcal{E}\left(G_{E_p}\right)^2+\tau\left(G_{M_p}\right)^2}$$

Information on $G_E^{(s)}$ and $G_M^{(s)}$ can be extracted, the axial-vector form factors can be neglected

Backward angles

$$X_{AV} = \left(1-4\sin^2\theta_W\right) - \frac{\mathcal{E}G_{E_p}\left(G_{E_n}+G_E^{(s)}\right)+\tau G_{M_p}\left(G_{M_n}+G_M^{(s)}\right)}{\mathcal{E}\left(G_{E_p}\right)^2+\tau\left(G_{M_p}\right)^2}$$

$$X_{VA} = \frac{\sqrt{1-\mathcal{E}^2}\sqrt{\tau(1+\tau)}\,G_{M_p}\left(G_{A_p}-G_{A_n}-G_A^{(s)}\right)}{\mathcal{E}\left(G_{E_p}\right)^2+\tau\left(G_{M_p}\right)^2}$$

$G_M^{(s)}$ can be isolated, providing $G_A^{(1)}$ and $G_A^{(s)}$ are known from other sources

Strangeness: vector form factors <$s\gamma_\mu s$>

$$G_E^{(s)}(\tau) \equiv \tau \rho_s G_E^{(0)}(\tau)$$

$$G_M^{(s)}(\tau) \equiv \mu_s \left[G_{M_p}(\tau)/\mu_p \right]$$

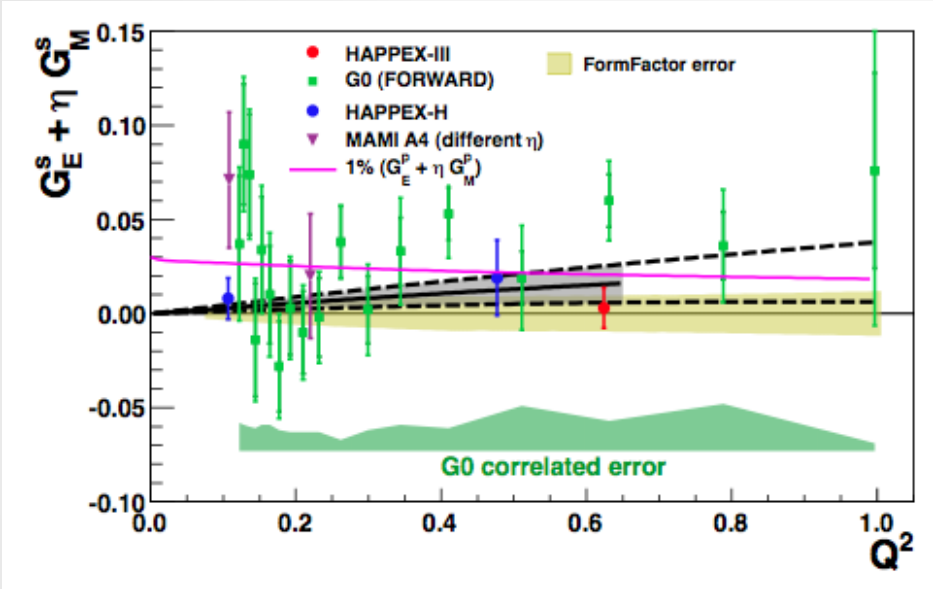

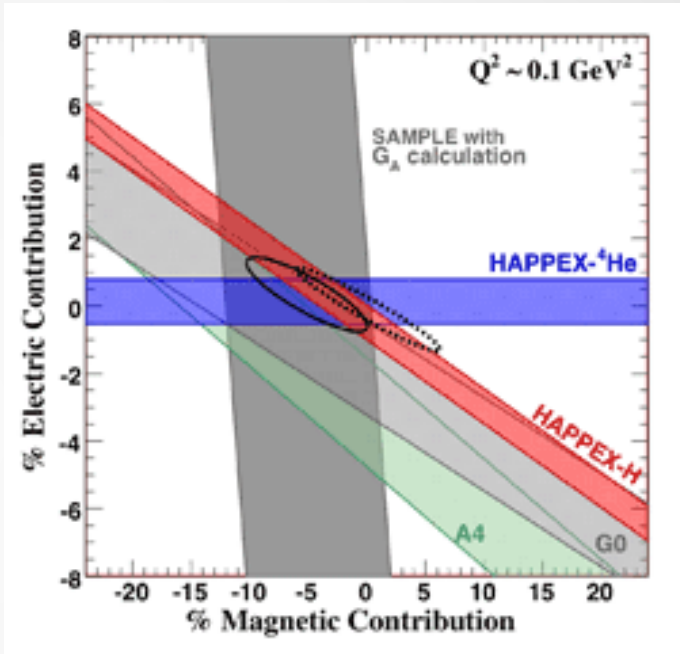

(2012)HAPPEX coll, PRL108, 102001

World data at low Q^2

$$\eta = \tau G_M^p / (\epsilon G_E^p)$$

<u>The s-quark contribution to electric and magnetic form factor is compatible with zero</u>
(consistent with lattice calculations)

Neutron skin in heavy nuclei

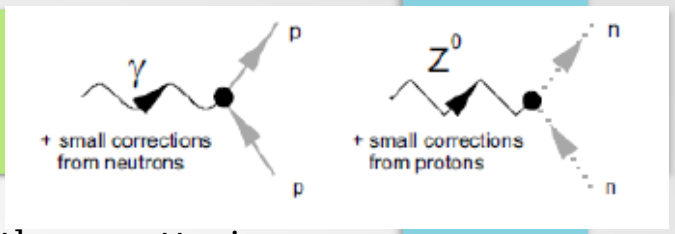

- Nuclear charge densities are measured very accurately with e- scattering
- Theoretical models based on RMF predict that the radius of neutron distribution in heavy nuclei is larger than the proton one (neutron skin)
- The thickness of neutron skin in heavy nuclei is usually measured using hadronic probes (p,π): large uncertainties in the interpretation of experimental data due to strong interaction
- PVES provides a measurement of neutron densities free from strong interaction uncertainties.

Measurement of the Neutron Radius of ^{208}Pb through Parity Violation in Electron Scattering

PREX experiment at JLab

$$A_{\mathrm{PV}} = \frac{\sigma_R - \sigma_L}{\sigma_R + \sigma_L} \approx \frac{G_F Q^2}{4\pi\alpha\sqrt{2}} \frac{F_W(Q^2)}{F_{\mathrm{ch}}(Q^2)},$$

$$A_{\mathrm{PV}} = 0.656 \pm 0.060(\mathrm{stat}) \pm 0.014(\mathrm{syst})\ \mathrm{ppm}$$

$$\langle Q^2 \rangle = 0.008\,80 \pm 0.000\,11\ \mathrm{GeV}^2$$

$$R_n - R_p = 0.33^{+0.16}_{-0.18}\ \mathrm{fm}$$

$$R_n = 5.78^{+0.16}_{-0.18}\ \mathrm{fm}$$

The result (PREXI) is compatible with most models' predictions. Next expt (PREXII, 2014) should be able to discriminate among models.

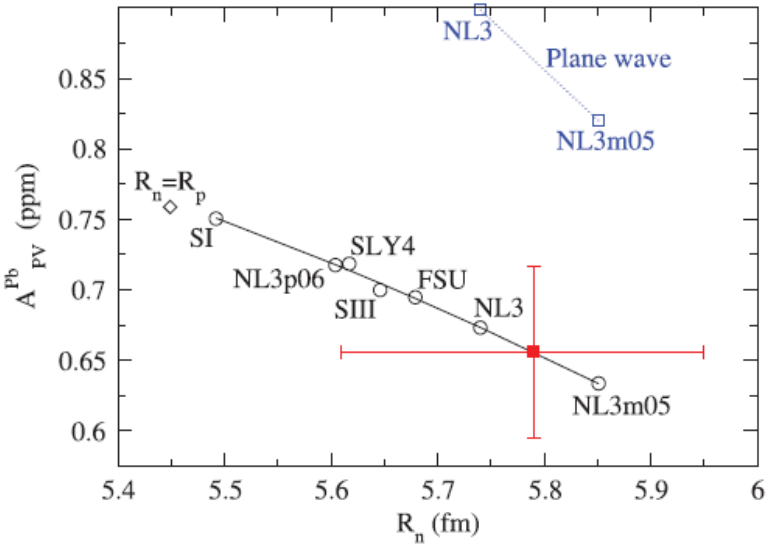

FIG. 1 (color). Result of this experiment (red square) vs neutron point radius R_n in 208Pb. Distorted-wave calculations for seven mean-field neutron densities are circles while the diamond marks the expectation for $R_n = R_p$[39]. References: NL3m05, NL3, and NL3p06 from [11], FSU from [12], SIII from [13], SLY4 from [14], SI from [15]. The blue squares show plane wave impulse approximation results. PRL **108,** 112502 (2012)

Nuclear Isospin Mixing Effects in PVES

For PV elastic electron scattering between $J^\pi = 0^+$ states the asymmetry is

$$\mathcal{A} = \frac{G}{2\pi\alpha\sqrt{2}}|Q^2|\frac{W^{PV}}{F^2}\,,$$

$$F^2(q) = v_L F_{C0}^2(q), \quad W^{PV} = v_L a_A F_{C0}(q)\tilde{F}_{C0}(q)\,,$$

$$\frac{W^{PV}}{F^2} = a_A \frac{\tilde{F}_{C0}(q)}{F_{C0}(q)}\,.$$

Monopole Coulomb ff 's

For N=Z nuclei, assuming they are in an exact isospin eigenstate T=0, only the isoscalar component contributes:

$$\tilde{F}_{C0}(q) = \beta_V^{(0)} F_{C0}(q)\,.$$

$$\mathcal{A} = \mathcal{A}^0 \equiv \left[\frac{G\,|Q^2|}{2\pi\alpha\sqrt{2}}\right] a_A \beta_V^{(0)} \cong 3.22 \times 10^{-6}|Q^2| \text{ (in fm}^{-2}),$$

The asymmetry is independent of the form factors: it can be used to test the Standard Model.

However, if isospin symmetry is violated at the nuclear level, this modifies to:

$$\mathcal{A} = \mathcal{A}^0(1+\Gamma)$$

$$\Gamma = \frac{1}{\beta_V^{(0)}}\frac{\tilde{F}_{C0}(q)}{F_{C0}(q)} - 1$$

Γ accounts for effects due to nuclear isospin mixing (and strangeness)

T. W. Donnelly, J. Dubach and I. Sick, Nucl. Phys. A 503 (1989) 589.

Nuclear Isospin Mixing Effects in PVES

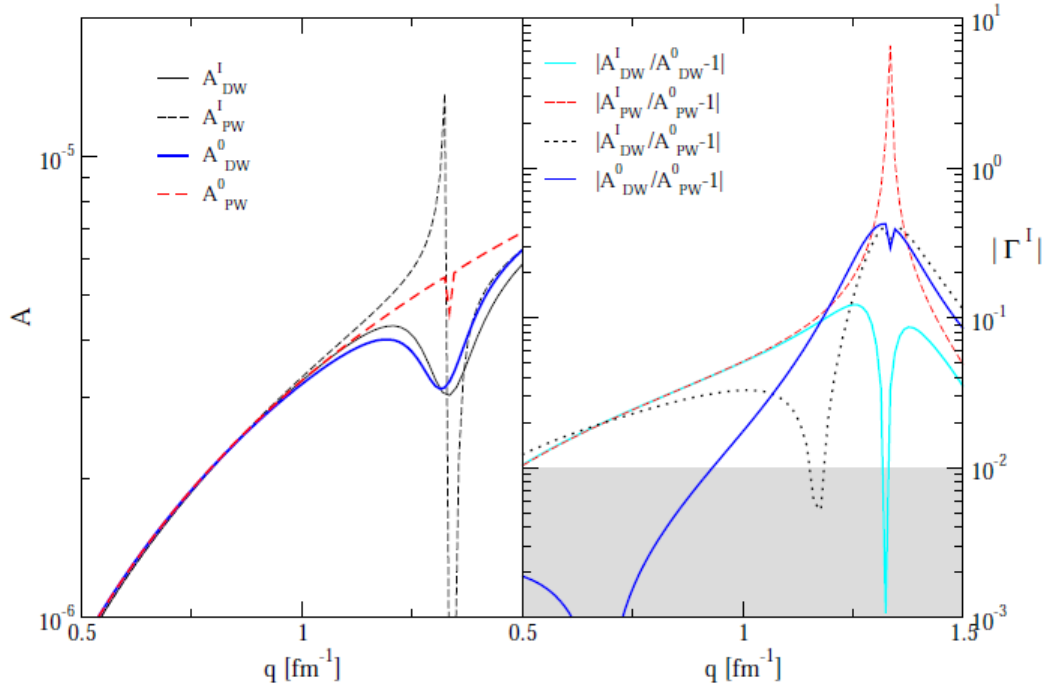

FIG. 2: (Color online) Left-hand panel: PV asymmetry for ^{28}Si allowing for nuclear isospin mixing in PWBA and in the fully distorted calculation (PW^I and DW^I) and in the non-isospin-mixing case by constraining $\rho^p = \rho^n$ (PW^0 and DW^0). Right-hand panel: Asymmetry deviations for ^{28}Si: due to pure isospin mixing effects in DW (solid line) and in PWBA (dashed line), due to isospin mixing and distortion effects together (dotted line) and due to distortion effects only (thick solid line).

O. Moreno et al., Nucl.Phys. A828 (2009)

Quasielastic PV electron scattering

- Why quasielastic?
- Complex nuclei complement experiments on proton
- QE cross sections (and hence the figure of merit) are large: σ~A
- The form factors are less rapidly decreasing with q than in elastic scattering
- New tool for studying nuclear dynamics?

- In the “static approximation” (ignore motion of nucleons in the nucleus):

$$\mathcal{A} = \mathcal{A}_0 \times \frac{W^{\mathrm{PV}}}{W^{\mathrm{PC}}}$$

$$W^{\mathrm{PC}} = v_L \left\{ \frac{q^2}{2|Q^2|} \left[Z G_{E_p}^2 + N G_{E_n}^2 \right] \right\} + v_T \left\{ \tau \left[Z G_{M_p}^2 + N G_{M_n}^2 \right] \right\}$$

$$W^{\mathrm{PV}} = a_A \left[v_L \left\{ \frac{q^2}{2|Q^2|} \left[Z G_{E_p} \tilde{G}_{E_p} + N G_{E_n} \tilde{G}_{E_n} \right] \right\} + v_T \left\{ \tau \left[Z G_{M_p} \tilde{G}_{M_p} + N G_{M_n} \tilde{G}_{M_n} \right] \right\} \right] + a_V \left[v_{T'} \left\{ \sqrt{\tau(1+\tau)} \left[Z G_{M_p} \tilde{G}_{A_p} + N G_{M_n} \tilde{G}_{A_n} \right] \right\} \right]$$

dominant
al large θ

Quasielastic PV electron scattering

The ff's $G_A^{(s)}$ and $G_M^{(s)}$ are multiplied by the combination $Z\,G_{Mp} + N\,G_{Mn}$ whereas $G_A^{(1)}$ is multiplied by the combination $Z\,G_{Mp} - N\,G_{Mn}$.
Comparing with the proton:

$$\frac{ZG_{M_p} + NG_{M_n}}{ZG_{M_p} - NG_{M_n}} = 1 \quad \text{for the proton}$$

$$= \frac{\mu_p + \mu_n}{\mu_p - \mu_n} \cong 0.187 \quad \text{for N = Z nuclei}$$

Effects of $G_A^{(s)}$ and $G_M^{(s)}$ suppressed in QE Scattering: they can be minimized by tuning N and Z.
Example: ^{183}W (Z=74, N=109)

$$N/Z \sim |\mu_p/\mu_n| \rightarrow \frac{ZG_{M_p} + NG_{M_n}}{ZG_{M_p} - NG_{M_n}} = -0.009$$

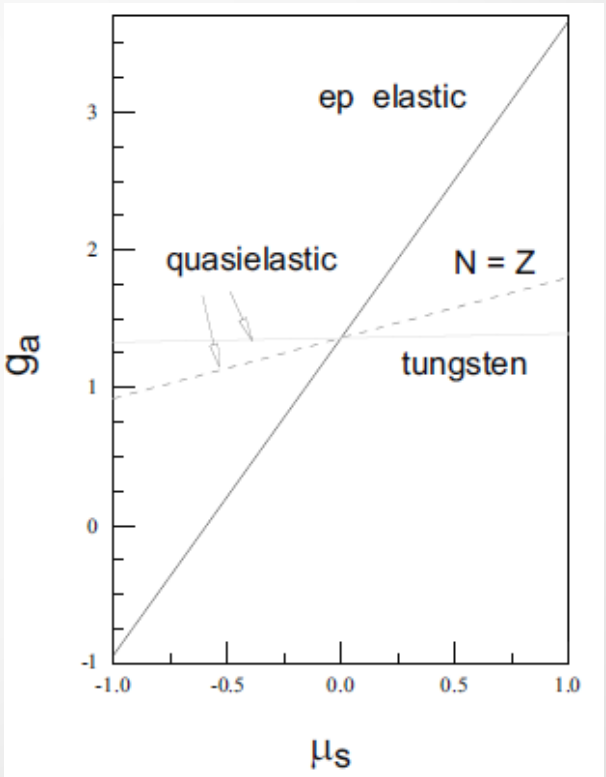

PV QES: free RFG

$$\mathcal{A} = \mathcal{A}_0 \frac{v_L \widetilde{R}^L(q,\omega) + v_T \widetilde{R}^T(q,\omega) + v'_T \widetilde{R}^{T'}(q,\omega)}{v_L R^L(q,\omega) + v_T R^T(q,\omega)}$$

$$\widetilde{R}^L(q,\omega) = \left(\frac{q^2}{Q^2}\right)^2 \left[\widetilde{W}^{00} - \frac{\omega}{q}(\widetilde{W}^{03} + \widetilde{W}^{30}) + \frac{\omega^2}{q^2}\widetilde{W}^{33}\right]$$

$$\widetilde{R}^T(q,\omega) = \widetilde{W}^{11} + \widetilde{W}^{22} \qquad \widetilde{R}^{T'}(q,\omega) = -i\widetilde{W}^{12}$$

$$\widetilde{W}^{\mu\nu} = \overline{\sum_i \sum_f} \langle f|\widetilde{J}^\mu|i\rangle^* \langle f|\hat{J}^\nu|i\rangle \delta(E_i + \omega - E_f)$$

Interference hadronic tensor

In the <u>free RFG model:</u>

$$\widetilde{W}^{\mu\nu} = \frac{3Z}{8\pi k_F^3 q} \int_{h_0}^{k_F} h dh (\omega + E_{\mathbf{h}}) \int_0^{2\pi} d\phi_h \times \sum_{s_p, s_h} 2\mathrm{Re}\left[\langle ph^{-1}|\widetilde{j}^\mu|F\rangle^* \langle ph^{-1}|j^\nu|F\rangle\right]$$

$$\widetilde{R}^{L,T,T'}(q,\omega) = R_0(q,\omega)\left[\widetilde{U}_p^{L,T,T'}(q,\omega) + \widetilde{U}_n^{L,T,T'}(q,\omega)\right]$$

$$R_0(q,\omega) = \frac{3\mathcal{N}\xi_F}{4m_N \kappa \eta_F^3}(1-\psi^2)$$

$$\widetilde{U}^L = \frac{\kappa^2}{\tau}\left\{\widetilde{G}_E G_E + \frac{\mathcal{D}(\kappa,\tau)}{1+\tau}\left[\widetilde{G}_E G_E + \tau \widetilde{G}_M G_M\right]\right\}$$

$$\widetilde{U}^T = 2\tau \widetilde{G}_M G_M + \frac{\mathcal{D}(\kappa,\tau)}{1+\tau}\left[\widetilde{G}_E G_E + \tau \widetilde{G}_M G_M\right]$$

$$\widetilde{U}^{T'} = 2\sqrt{\tau(1+\tau)}\widetilde{G}_A G_M (1 + \widetilde{\mathcal{D}}(\kappa,\tau))$$

$$\widetilde{\mathcal{D}}(\kappa,\tau) = \frac{1}{\varepsilon_F - \varepsilon_0}\int_{\varepsilon_0}^{\varepsilon_F}\left(\sqrt{1 + \frac{\eta_T^2}{1+\tau}} - 1\right) d\varepsilon$$

PV QES: Pionic Correlations

The PV longitudinal response of a free RFG is very small due to a cancellation between the isoscalar and isovector contributions. Equivalently, since the proton (neutron) couples strongly (weakly) to longitudinal photons, and viceversa for the Z^0, we have:

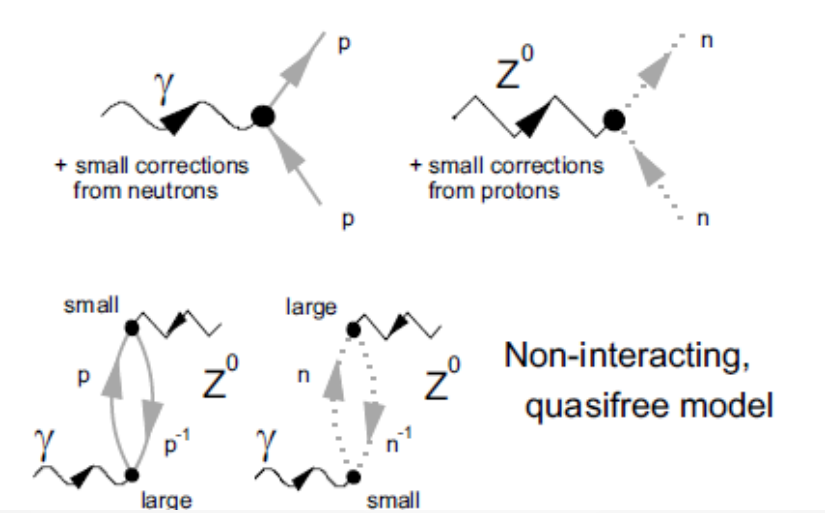

Dressing the nucleon lines (Hartree-Fock) does not change this mechanism. However, including correlations where a charged meson is exchanged between the p and h lines, the "large" vertices can both occur
→ no overall suppression of the PV L response

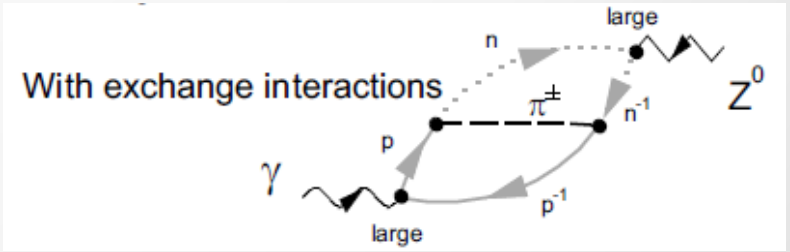

Such effects should be observable in the forward-angle asymmetry and could in principle provide a new tool to investigate the roles of specific classes of many-body correlations in nuclei.

Quasielastic asymmetry

^{12}C

free

correlated

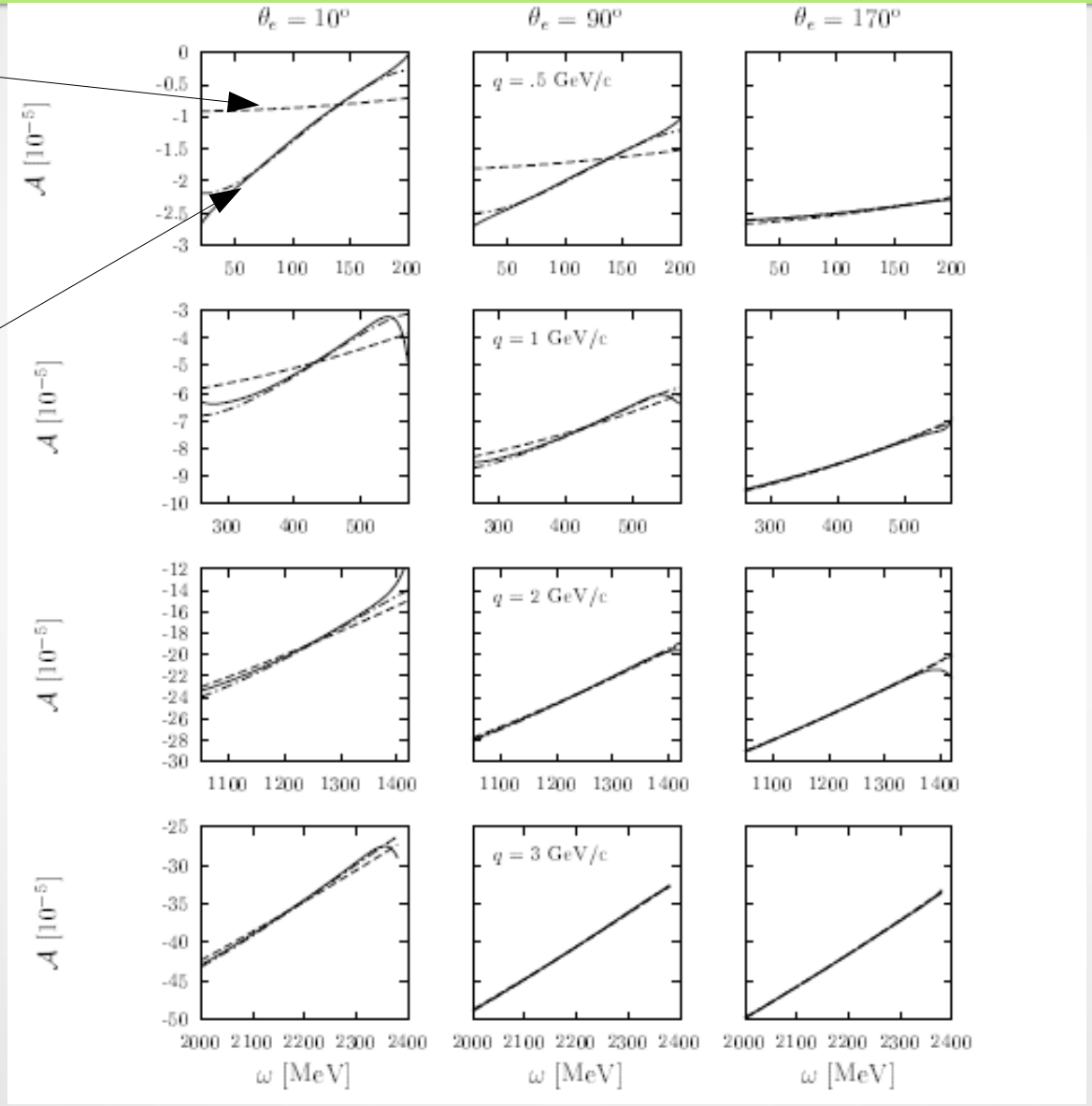

Amaro et al., Phys.Rept. 368 (2002)

A final remark

There are still many good reasons to work on electron scattering.

Motivations have changed and evolved since the first Raimondo Anni school on electroweak interactions in 2005:

- the interpretation of new generation neutrino experiments is strictly connected to our understanding of electron scattering

- new very interesting results from electron scattering both on the proton and on nuclei with electron and/or target polarization

- old open questions (ex: L/T separation, Coulomb Sum Rule) still wait to be clarified